UNCLASSIFIED

AD NUMBER
AD813007
LIMITATION CHANGES

TO:

Approved for public release; distribution is unlimited.

FROM:

Distribution authorized to U.S. Gov't. agencies and their contractors; Administrative/Operational Use; 02 FEB 1967. Other requests shall be referred to Air Force Technical Applications Center, Washington, DC 20333.

AUTHORITY

USAF ltr dtd 25 Jan 1972

THIS PAGE IS UNCLASSIFIED

TECHNICAL REPORT NO. 67-3

FINAL REPORT, PROJECT VT/5051
DEEP-WELL RESEARCH

GEOTECH

A TELEDYNE COMPANY

TECHNICAL REPORT NO. 67-3

FINAL REPORT, PROJECT VT/5051
DEEP-WELL RESEARCH

by

Richard M. Shappee
Eduard J. Douze

GEOTECH
A Teledyne Company
3401 Shiloh Road
Garland, Texas

2 February 1967

IDENTIFICATION

AFTAC Project No:	VELA T/5051
Project Title:	Deep-Well Research
ARPA Order No:	624
ARPA Project Code No:	8100
Contractor:	The Geotechnical Corporation
	Garland, Texas
Contract No:	AF 33(657)-13668
Date of Contract:	16 July 1964
Date of Supplemental Agreement No. 1:	27 August 1965
Date of Supplemental Agreement No. 2:	6 August 1965
Date of Supplemental Agreement No. 3:	29 October 1965
Date of Supplemental Agreement No. 4:	24 November 1965
Date of Supplemental Agreement No. 5:	1 March 1966
Date of Supplemental Agreement No. 6:	10 November 1966
Amount of Contract and Supplements:	$1,261,029.00
Contract Expiration Date:	28 February 1967
Program Manager:	Richard M. Shappee
	Garland, Texas
	BR 8-8102, Area Code 214

CONTENTS

TR 67-3

CONTENTS, Continued

ILLUSTRATIONS

ILLUSTRATIONS, Continued

-iv-

ILLUSTRATIONS, Continued

-v-

ILLUSTRATIONS, Continued

TR 67-3

TABLES

-viii-

ABSTRACT

A deep-hole array of six short-period seismometers was tested at the test
site near Grapevine, Texas (GV-TX). After a brief period of successful
operation, half the array was moved to the site near Apache, Oklahoma
(AP-OK), and the other half was moved to the site near Franklin, West
Virginia (FN-WV). Various techniques were employed to process the output
of these arrays. The deep-hole test site (GV-TX) was maintained for testing
applications requiring the use of a deep hole, including testing the triaxial
seismometer and testing to determine if a useful long-period response could
be obtained from the Model 11167 deep-hole seismometer. The results
indicated it would require a complex and unstable system to provide a long-
period response.

During the 29-month duration of this program, measurements were made
in deep holes in West Virginia, Texas, Utah, Oklahoma, and Pennsylvania.
Additionally, an off-shore measurement program was undertaken.

The information from wells and surface arrays was used to study short-period
(6.0-0.3 sec period) noise and signals. An attempt was made to show that
higher mode Rayleigh waves and body waves are present in the noise by com-
paring theoretical curves with experimental results. It was shown that
surface waves generally predominate at the longer periods while body waves
appear at the shorter periods at quiet sites. Not all data could be interpreted
to define the wave types present. The short-period signals were analyzed
both visually and digitally. Signal amplitudes at the surface were shown to
be at least twice as large as at depth. The impulse response of layered
media was used to compute inverse filters which changed the waveform
characteristics of the deep-hole signals into those of the surface signals.
Some preliminary work was done with the horizontal data obtained from the
triaxial seismographs.

A complete system, composed of four triaxial seismometers, a digital
processor, and associated equipment, was installed and operated at AP-OK.
Data obtained from this array were processed using optimum filtering
techniques. These techniques required the use of the inverse filters mentioned
above and filters derived from the Wiener least mean-square technique. Both
single-channel and multichannel processes were employed; however, the
results obtained to date indicated that a one-sided single-channel optimum
filter was the most effective processor.

FINAL REPORT, PROJECT VT/5051
DEEP-WELL RESEARCH

1. INTRODUCTION

This report discusses a project of research in deep-hole seismology. The work reported herein covers systems engineering and subsequent assembly, test, and operation of a six-element vertical array of seismometers; maintenance and operation of the Grapevine test site; measurement of signals and noise in shallow and deep wells; operation of a seismometer on the ocean bottom; specification of an on-line array signal processor, its installation in a recording van and its subsequent operation; assembly and operation of an array of triaxial short-period seismometers; and the analysis of signals and noise.

The purpose of this report is to present the technical findings and accomplishments of the project from 16 July 1964 through 31 December 1966. It is submitted in compliance with paragraph 2, **Reports**, of the Statement of Work to be Done, Project VT/5051. The project was under the technical direction of the Air Force Technical Applications Center (AFTAC) and under the overall direction of the Advanced Research Projects Agency (ARPA).

The main body of the report is generally presented in the same sequence as the tasks in the Statement of Work. A copy of the Statement of Work and subsequent additions are included as appendix 1. A list of reports submitted during the performance of the contract is given in table 1.

2. SYSTEMS ENGINEERING, SIX-ELEMENT ARRAY, TASK 1a

A deep-hole array of short-period seismometers was designed, constructed, and tested. A special report describing the array was submitted. A copy of the report (Technical Report 65-3) is included as appendix 4 to this report.

Subsequent to the date of the report, the array was routinely operated at the test site near Grapevine, Texas (GV-TX). Figure 1 shows an event recorded. After a brief period of operation, half the array was moved to the test site near Apache, Oklahoma (AP-OK) and the other half was moved to the site near Franklin, West Virginia (FN-WV). Figures 2 and 3 show events recorded at these sites. An additional seismometer was operated in the deep well and another was operated in the shallow well at both of these sites, in addition to a surface Benioff seismometer. The result of this was to provide two arrays, each comprised of five deep-well systems.

-1-

Table 1. Reports submitted in performance of Contract AF 33(657)-13668

Date of Report	Title	Report No.
15 January 1965	Design of a Deep-Hole Vertical Array	TR 65-3
15 February 1965	Semiannual Report No. 1, Project VT/5051, Deep-Well Research	TR 65-15
17 June 1965	Preliminary Evaluation of V_dXM Vector-Correlation Process	TR 65-57
15 July 1965	Deep-Hole Site Report, University of Texas "EE" No. 1 Pecos County, Texas	TR 65-104
15 July 1965	Deep-Hole Site Report, Long No. 1, Centre County, Pennsylvania	TR 65-105
28 July 1965	Off-Shore Measurements Program	Memo Report
24 August 1965	Semiannual Report No. 2, Project VT/5051, Deep-Well Research	TR 65-112
15 October 1965	Quarterly Report No. 1, Project VT/5051, Deep-Well Research	TR 65-119
15 January 1966	Quarterly Report No. 2, Project VT/5051, Deep-Well Research	TR 66-2
15 April 1966	Quarterly Report No. 3, Project VT/5051, Deep-Well Research	TR 66-46
22 June 1966	Deep-Hole Symmetrical Triaxial Seismometer, Model 22700	TR 66-67
15 July 1966	Quarterly Report No. 4, Project VT/5051, Deep-Well Research	TR 66-72
15 October 1966	Quarterly Report No. 5, Project VT/5051, Deep-Well Research	TR 66-96
28 February 1967	Final Report, Project VT/5051, Deep-Well Research	TR 67-3
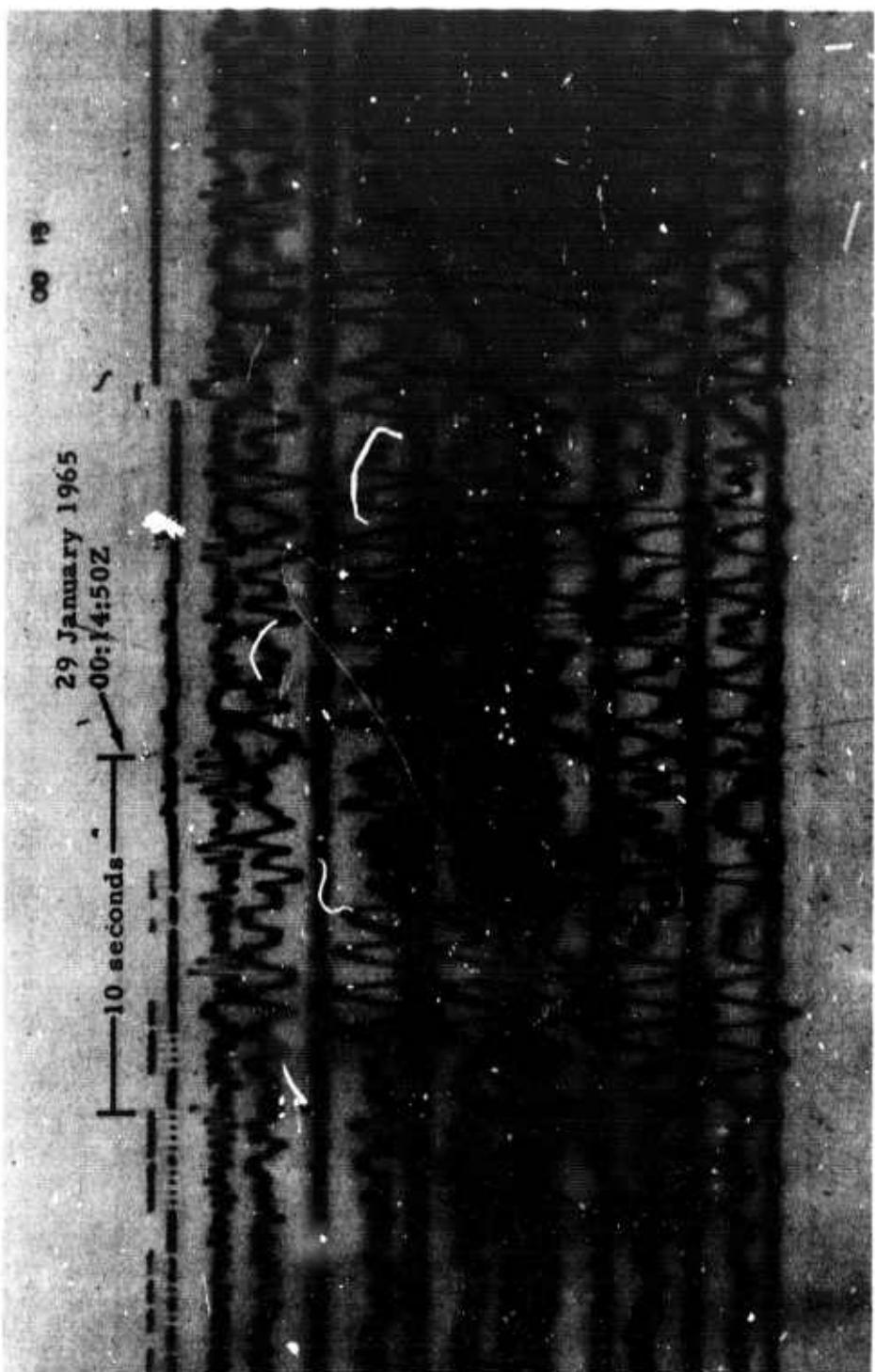
Figure 1. Recording of event by surface seismograph and deep-hole vertical array at Grapevine, Texas. Epicenter unknown. Magnification at 1 cps (X10 enlargement of 16 millimeter film). DHA-1 at 2900 m, DHA-2 at 2600 m, DHA-3 at 2300 m, DHA-4 at 2000 m, DHA-5 at 1700 m, DHA-6 at 1400 m

205

-3-

WWV

SPZ   265K

SPZ   27K

DH5   61K

DH5   61K

DH4   777K

DH4   78K

DH3   610K

DH3   61K

DH2   664K

DH2   67K

DH1   807K

DH1   81K

Anemometer
8 kmph = 1 mm

16 May 1965
22:53:00Z

22 53

10 seconds
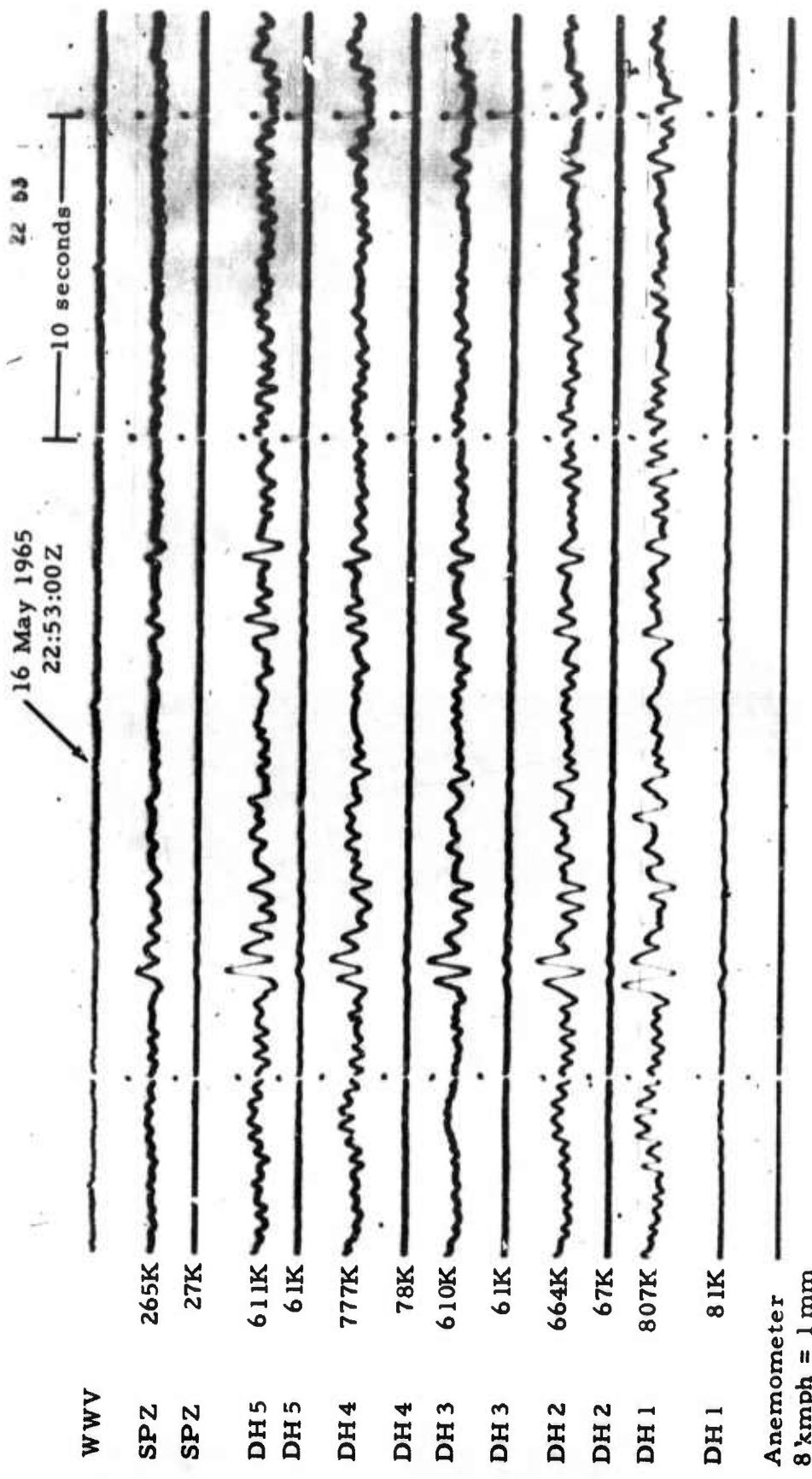
Figure 2. Recording of event by surface seismograph and deep-hole vertical array at Apache, Oklahoma. Epicenter unknown. Magnifications at 1 cps (X10 enlargement of 16 millimeter film). DHA-1 at 2880 m; DHA-2 at 2270 m; DHA-3 at 1970 m; DHA-4 at 1660 m; DHA-5 at 15 m.

224

-4-
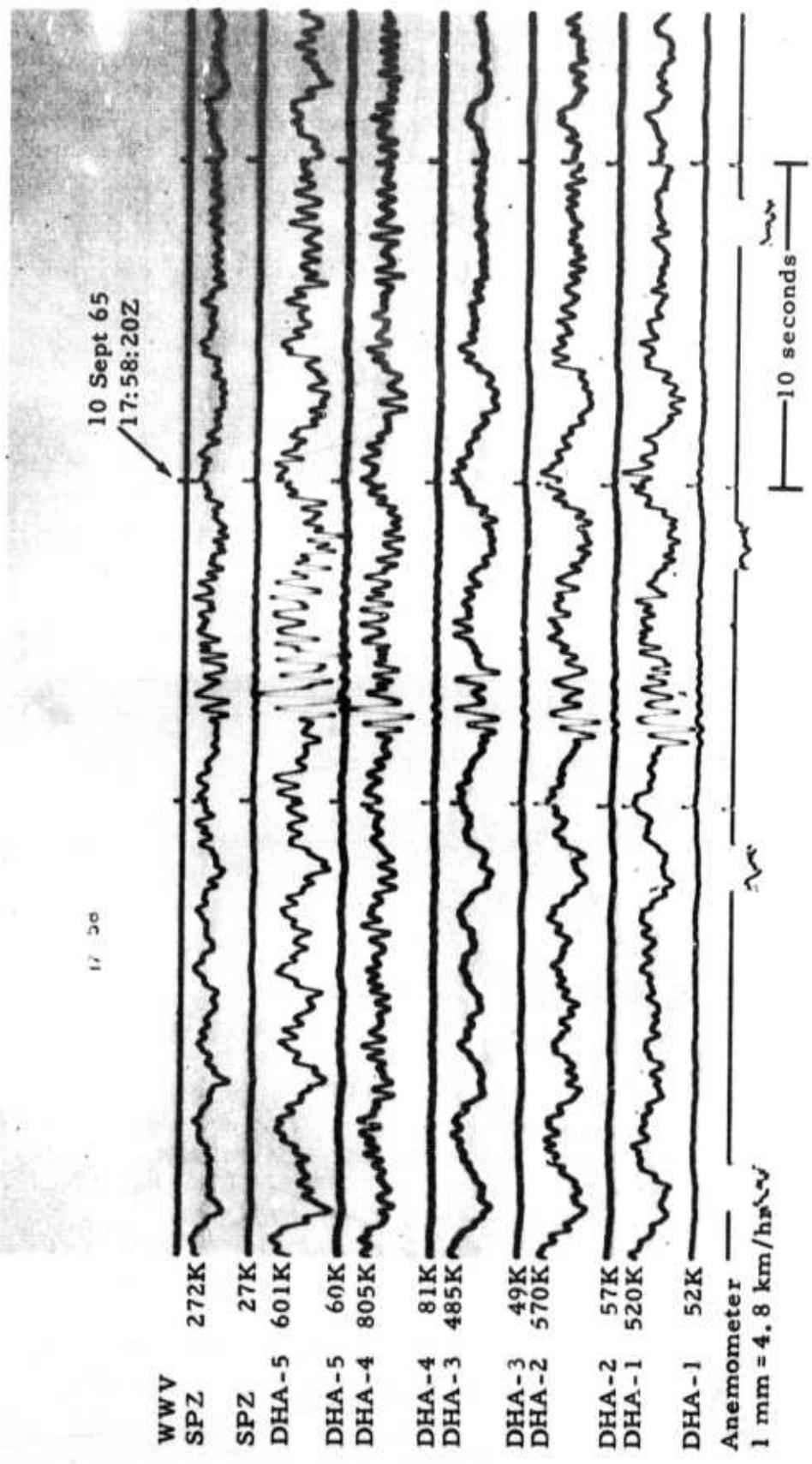
Figure 3. Recording of an event by surface seismograph and deep-hole vertical array at Franklin, West Virginia. Epicenter unknown. Magnifications at 1 cps (X10 enlargement of 16 millimeter film). DHA-1 at 3668 m, DHA-2 at 3062 m, DHA-3 at 2455 m, DHA-4 at 1830 m, DHA-5 at 15 m

237

-5-

TR 67-3

Figures 1, 2, and 3 clearly show the "step-out" of the signals as they travel up the well. In order to subtract the step-out and add the signals, a special recording head was constructed for use with the Ampex tape recorders used in the field. Figure 4 shows this unit. Figure 5 shows a summation module designed for the system. Our intention was to operate a system as shown in figure 6. The adjustable head was used at the AP-OK site, but the summed output was not obtained because the necessary playback amplifiers for the tape recorder were not available. Figure 7 shows a reproduction of an event made at our Garland laboratory and illustrates the results that we would have obtained in the field.

3. MAINTAIN TEST SITE, TASK 1b

The deep-hole test site (GV-TX) was maintained as a facility for evaluating new instruments, techniques, handling methods, and other applications requiring the use of a deep hole. The principle use of the site was for the development of the six-element array. Additionally, it was used to test the triaxial seismometer (described in section 6) and for tests to determine if a useful long-period response could be obtained using the Model 11167 deep-hole seismometer.

The deep-hole long-period system designed and operated under this task consisted of a deep-hole short-period seismometer, suitable long-period filters to shape the response, amplifiers, and normal calibration and recording provisions. The best performance of the system was obtained using a deep-hole seismometer that was specially constructed to eliminate, as far as possible, all sources of thermal-electromotive potentials.

Based upon earlier work, the long cable required in a deep-hole seismograph was thought to be the major source of long-period noise. However, it was found that with extreme care and attention to all electrical connections, an ordinary deep-hole system would perform reasonably well at long periods. The block diagram and response curve of such a system are shown in figure 8.

An event recorded by the system diagramed in figure 8 is shown in figure 9. Some long-term drift occurred although it is not evident in this example. This very long-period drift was never completely eliminated. The seismometer was at 152 m in the shallow hole at GV-TX. A comparison of this drift with a microbarograph did not yield significant correlation.

Some work was done in an attempt to obtain both a long-period and a short-period response from one seismometer. The results, though inconclusive, indicated that such a dual system would be too complex and unstable for routine field operation. Also, because of the extreme care necessary to

-6-
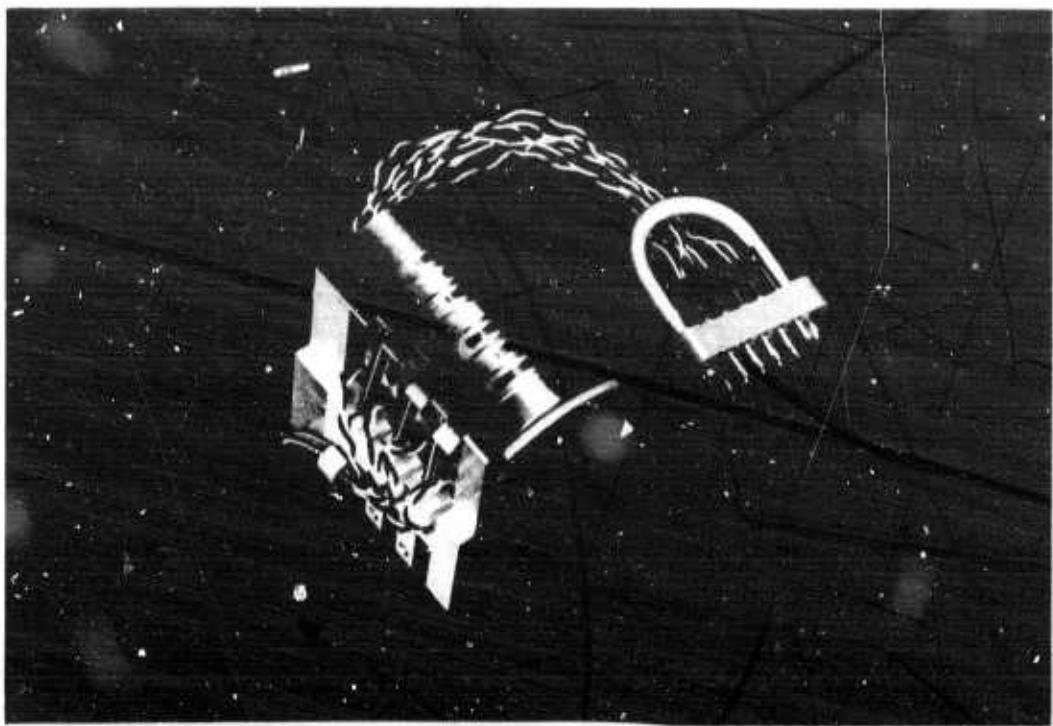
(a) Magnetic head stack
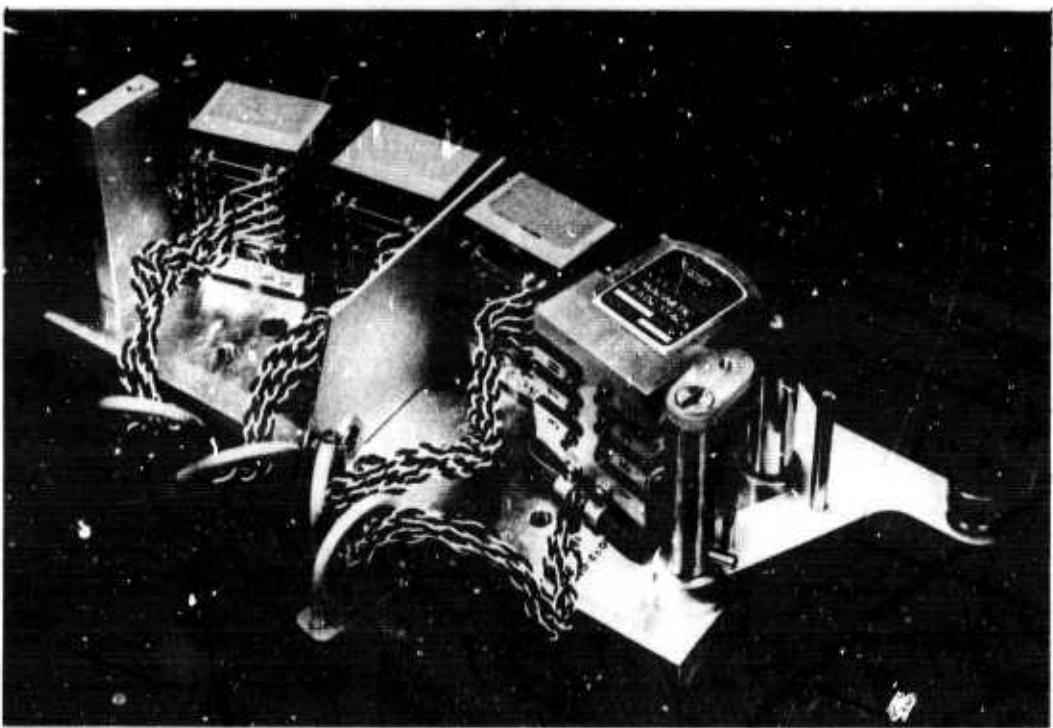
(b) Assembly for Ampex 300 recorder

Figure 4. Adjustable delay tape head

G 2212

-7-

TR 67-3
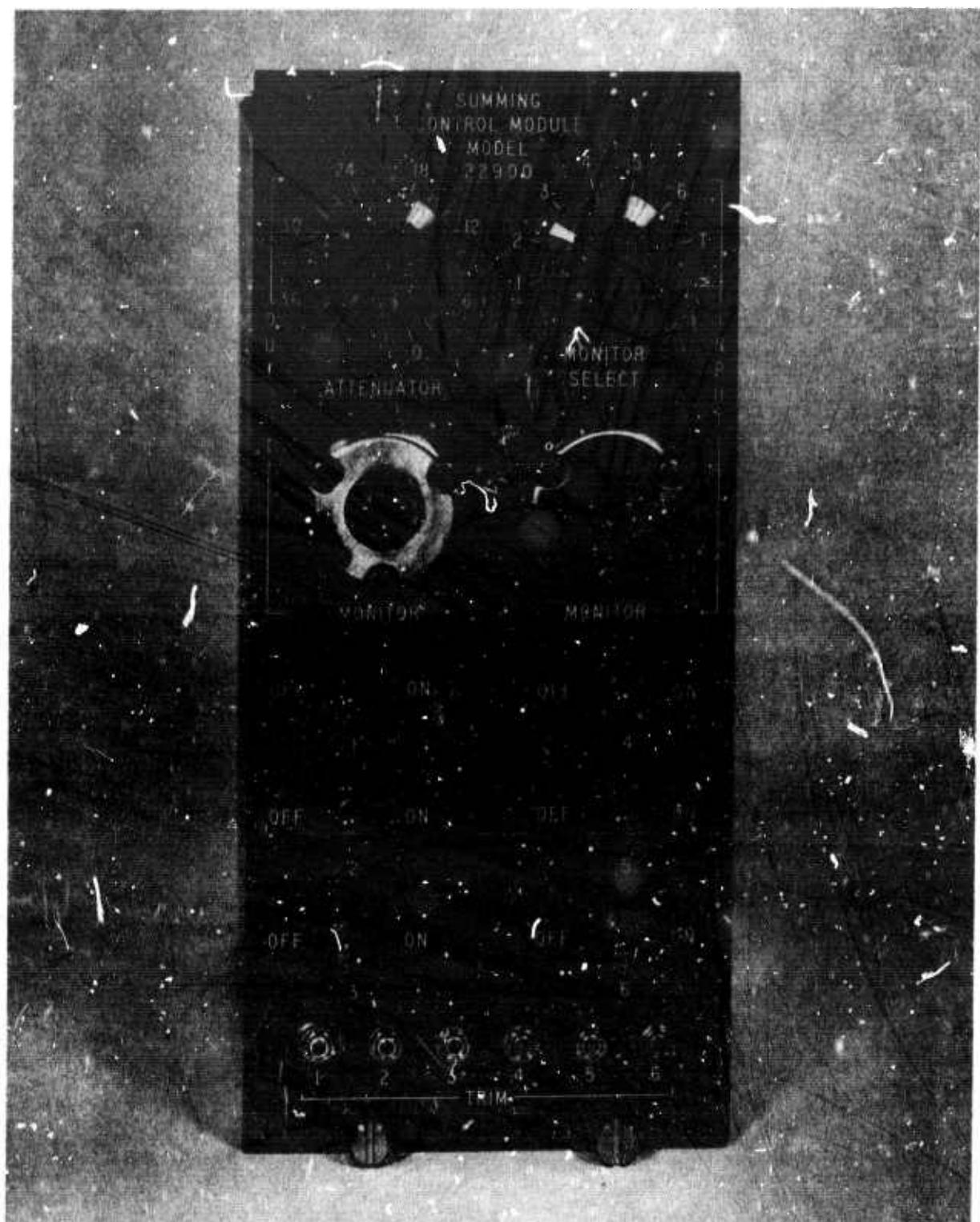
Figure 5. Summing Control Module, Model 22900

G 2213

Figure 6. Block diagram of on-line signal processing of the Deep-Hole Vertical Array, Model 22625
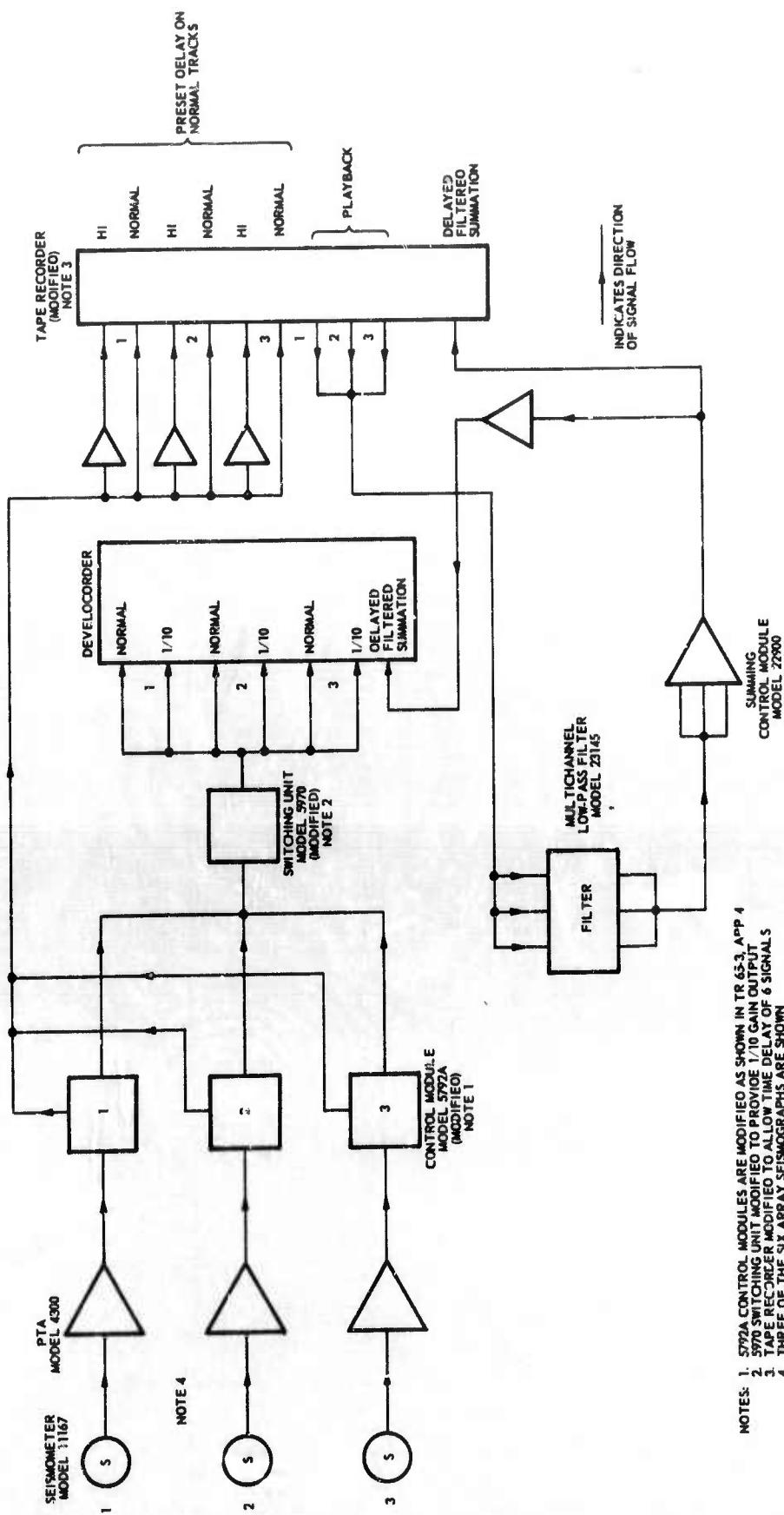
NOTES: 1. 5772A CONTROL MODULES ARE MODIFIED AS SHOWN IN TR 65-3, APP 4
2. 5970 SWITCHING UNIT MODIFIED TO PROVIDE 1/10 GAIN OUTPUT
3. TAPE RECORDER MODIFIED TO ALLOW TIME DELAY OF 6 SIGNALS
4. THREE OF THE SIX ARRAY SEISMOGRAPHS ARE SHOWN

-9-
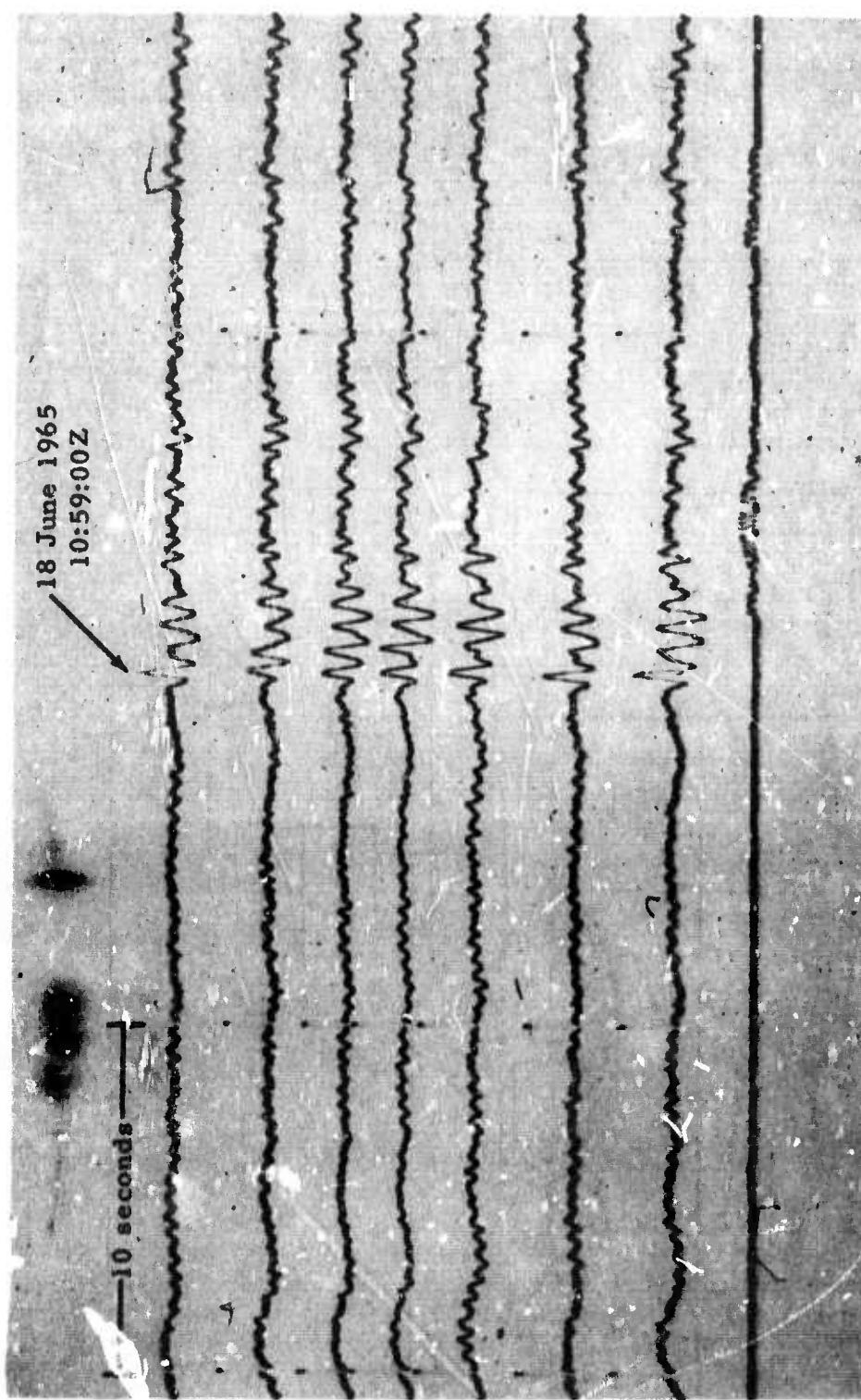
TR 67-3

Figure 7. Time-delayed summation of a signal received at AP-OK. Summation made off-line from signals delayed on-line by Model 23361 adjustable-delay tape head. DH1 at 2880 m, DH2 at 2270 m, DH3 at 1770 m, DH4 at 1660 m, and DH5 at 15 m.

234
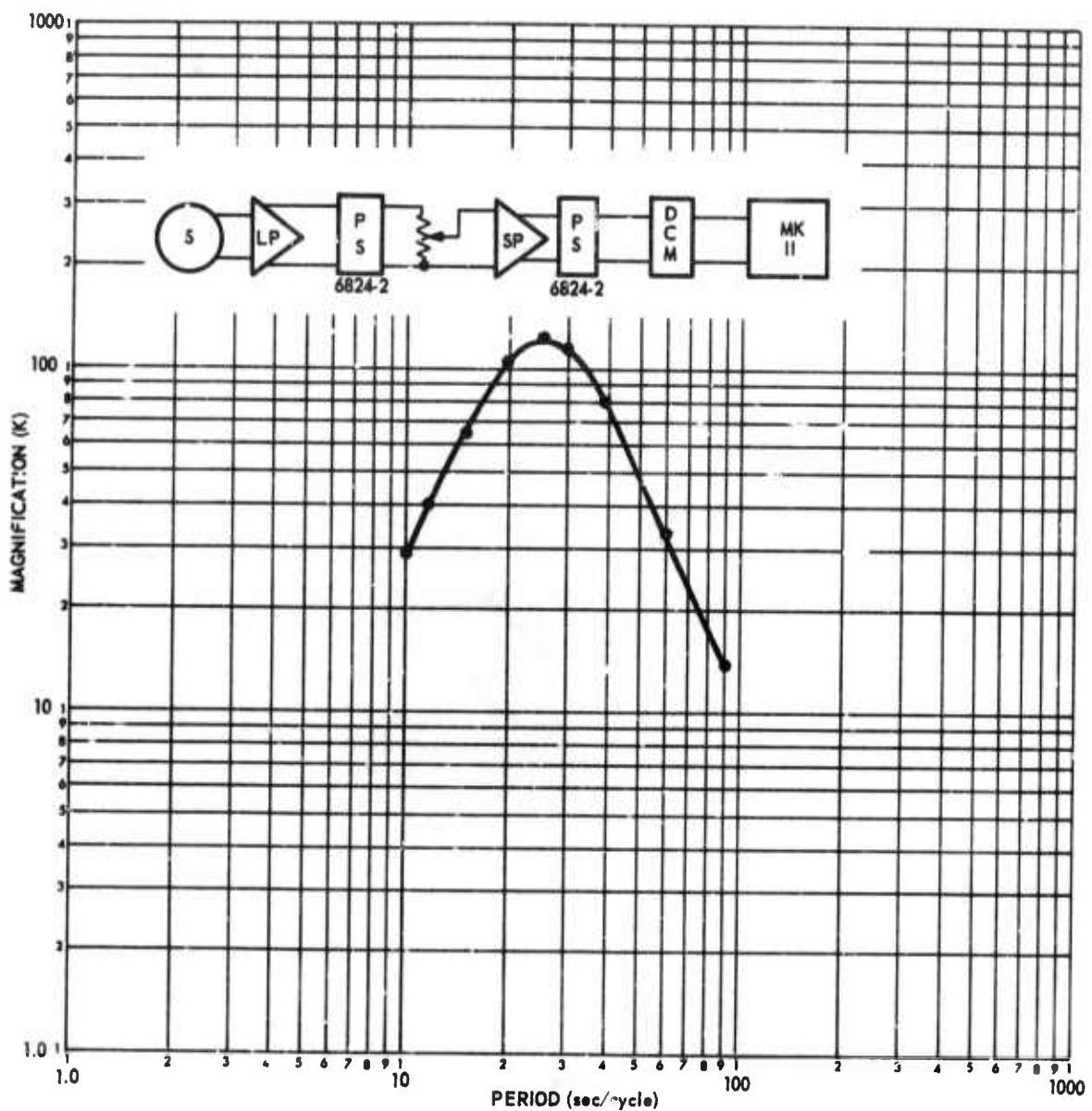
TR 67-3

Figure 8. Block diagram and response curve of a deep-hole
long-period system

G 2215

-11-
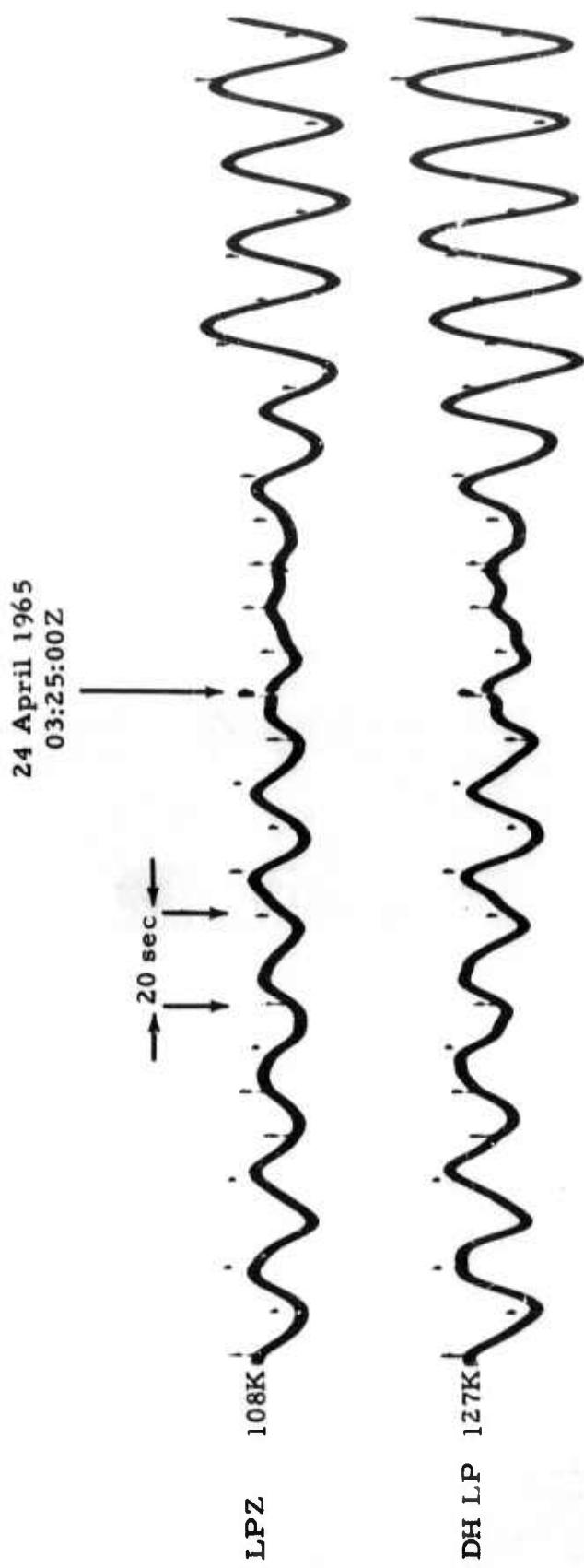
Figure 9. Recording of event by long-period surface vertical seismograph and a deep-hole long-period system. Deep hole at 152 m. Epicenter 7.3 N, 126.6 E. Phillippine Islands.

24 April 1965
03:25:00Z

20 sec

LPZ 108K

DH LP 127K

233

-12-

achieve satisfactory results, even the long-period response of the short period system is of questionable usefulness.

4. MEASURE SIGNALS AND NOISE IN SHALLOW AND DEEP HOLES, TASK 1c

During the 29-month duration of this program, measurements were made in deep holes in West Virginia, Texas, Utah, Oklahoma, and Pennsylvania. An off-shore measurement program was also undertaken. The results of routine measurements at two holes were reported in site reports: Technical Report (TR) 65-104 discussed the measurement program at the University of Texas "EE" No. 1, and TR 65-105 discussed the measurement program at the Long No. 1, Centre County, Pennsylvania.

Appendix 2 of this report discusses the off-shore measurement program. The measurement work at the Uinta Basin Seismological Observatory in Utah was done in cooperation with Project VT/1124 and the data were recorded using observatory equipment. Two deep-hole seismometers were operated in the hole.

An experiment was conducted in the shallow hole at the Wichita Mountains Seismological Observatory (WMSO) to obtain vertical strain measurements by subtracting the outputs of two matched deep-hole seismographs. This system is referred to as the "inertial strain" seismograph in this report. During the time that the inertial strain seismograph was operated at WMSO, the vertical strain seismograph was not in operation. Only the output of the crossed-horizontal strain seismographs was available. In theory, at the free surface the responses of the crossed horizontals and the vertical strain seismograph are identical. However, the vertical strain seismograph consists of a rod of finite length which measures the difference in displacement between two points. Under these conditions, a vertically incident P wave will be recorded by the vertical strain seismograph but not by the crossed-horizontal strain seismographs. Therefore, in practice, the outputs of the two types of instruments will not be identical.

The amplitude and phase responses of the two shallow-hole seismographs of the inertial strain (located at depths of 18 m and 37 m) were matched as closely as possible. A comparison between the inertial strain seismograph (obtained by subtraction) and the crossed-horizontal seismographs indicated that the two are quite similar for the first few cycles of an event; after the first few cycles, the differences become considerable. This behavior would be expected considering that the two types of instruments are measuring similar but not identical phenomena.

-13-

The inertial strain seismograph recorded P waves and noise approximately as predicted by theory. However, without a vertical strain seismograph for comparison, the extent of the differences and discrepancies could not be determined.

As mentioned in section 2, vertical arrays were operated at a site in Oklahoma and at a site in West Virginia. At West Virginia (FN WV) a high frequency response was operated part of the time in order to give a displacement response peaked at about 12 cps. Figure 10 shows a block diagram and the response of the system that was operated. Figure 11 shows a seismogram of an event recorded at GVTX during tests of the system. The data recorded with the high frequency systems were not used in the analysis work of this project.

5. ANALYZE DATA, PERFORM DETAILED ANALYSES, TASK 1d

5.1 SHORT-PERIOD SEISMIC NOISE

5.1.1 Introduction

Previous studies of short-period seismic noise have often assumed that only surface waves were present in short-period noise. However, the experimental results obtained to date cannot, in general, be explained in this fashion. The presence of random body-wave noise must also be taken into consideration. Recently, several reports have been published (Roden, 1965, Seriff, et al, 1965) in which the problem of body waves in the noise is discussed.

Seismometers placed at depth below the surface allow examination of the amplitude-depth relationships of the waves. If only surface waves, fundamental and higher modes, are present in the noise, the amplitude-depth relationships provide definite identification of the modes present. It is only necessary that the number of seismometers operating at depth be equal to the number of modes present (further explained under deep-hole theory). When body waves are present in the noise, the identification of wave types is no longer as simple, because all the possible angles of incidence of the random body waves must be taken into account.

In general, the amplitude-depth relationships obtained from deep-hole seismographs are not sufficient to differentiate between body waves and surface waves. As an example, the amplitude-depth relationships of the vertical component of the first higher mode and of P waves at close to vertical incidence are very similar for periods around 3.0 sec. Therefore, additional information must be obtained to differentiate between the possibilities. In this report, the information was obtained by measuring phase velocities at the

-14-
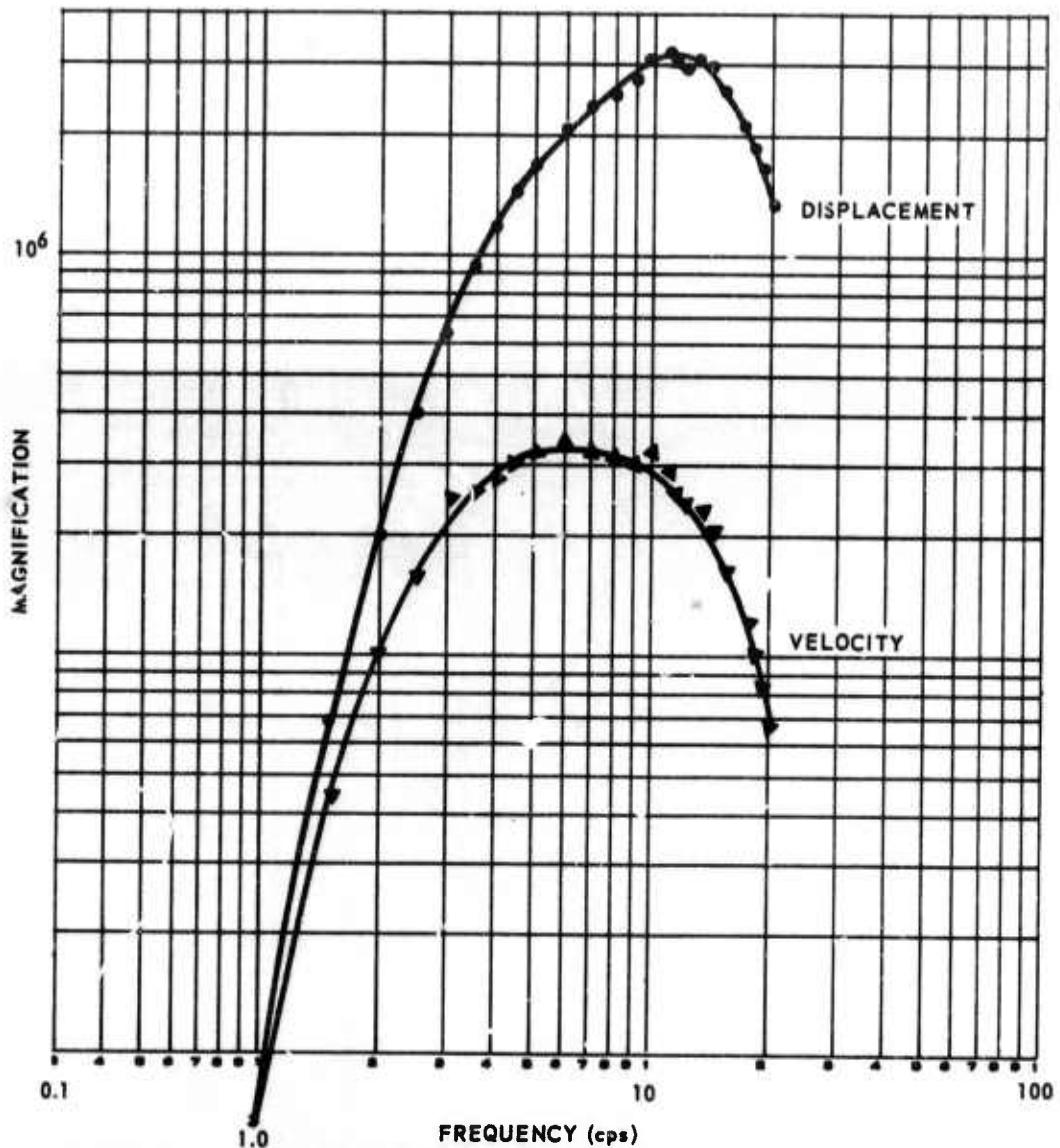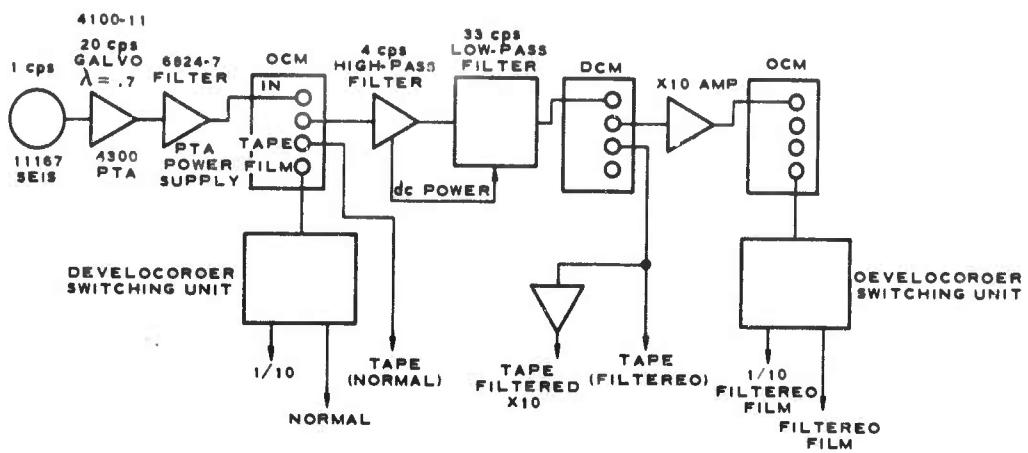
Figure 10. Displacement and velocity response of special
purpose deep-hole seismograph at GV-TX

G 2216

-15-
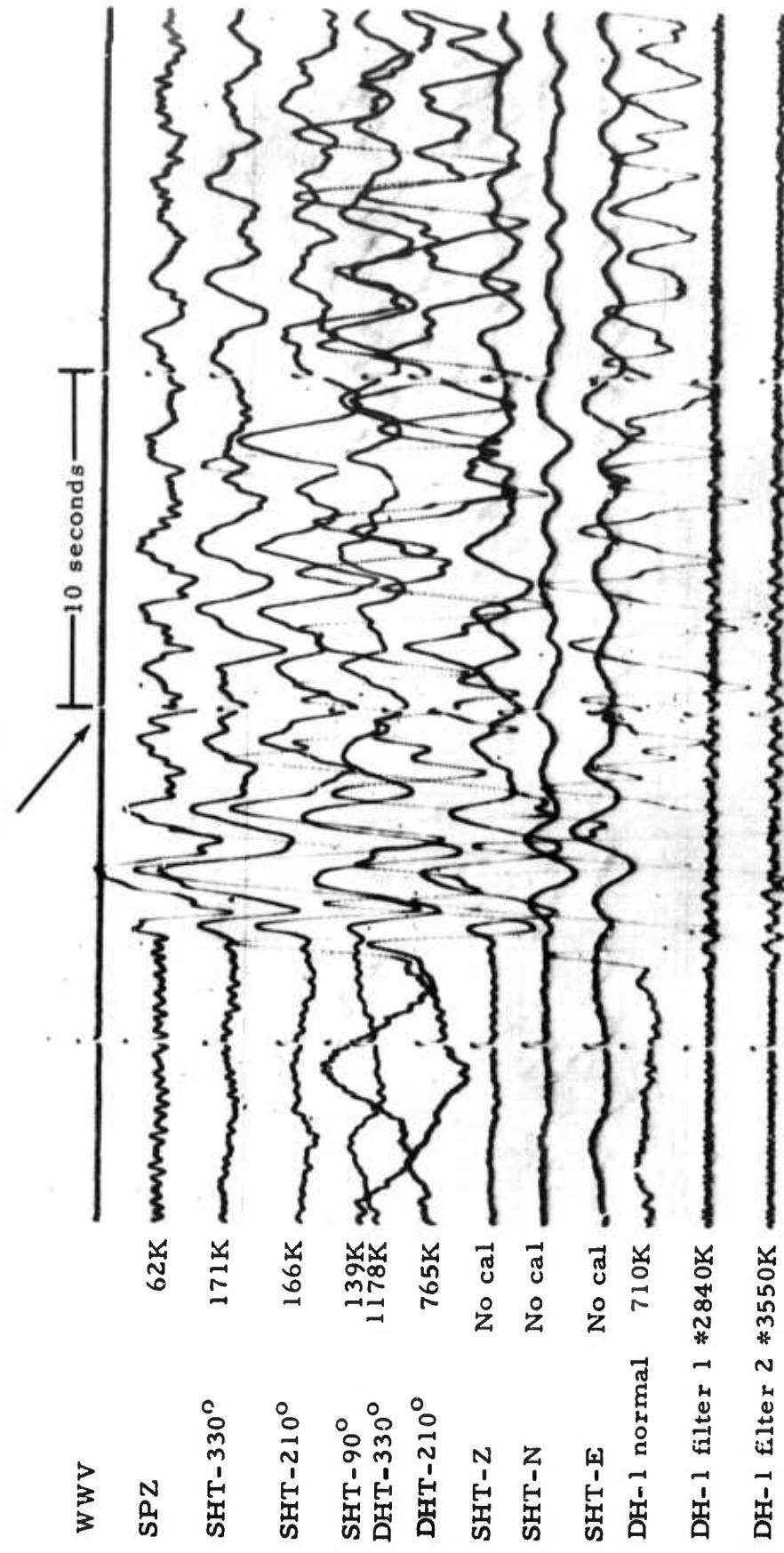
Figure 11. Recording of an event by a surface vertical seismograph (SPZ), deep-hole vertical seismograph (DH-1), shallow-hole triaxial seismograph (SHT), and deep-hole triaxial seismograph (DHT), at Grapevine, Texas. Epicenter unknown. Magnifications at 1 cps except those marked *, at 10 cps. (X10 enlargement of 16 mm film.) Shallow-hole triaxial at 153 m, deep-hole triaxial at 2135 m and deep-hole vertical at 2901 m. SHT-Z, SHT-N, and SHT-E are coordinate transformed outputs of SHT-330°, SHT-210°, and SHT-90°.

250

-16-

Wichita Mountains Seismological Observatory. In addition, the cross-correlation of surface and deep-hole noise was used to prove the presence of body-wave noise. Using all these data, a reasonably comprehensive understanding of the types of waves present was obtained. The results could only be interpreted qualitatively and not quantitatively. Despite the large amount of data available, the types of waves present could not always be identified. A possible explanation of the experimental results is given, while sufficient data are presented so that the reader can draw his own conclusion.

The results described were obtained with a deep-hole vertical-motion seismometer developed under Project VT/1139. The seismograph system has an amplitude and phase response similar to the short-period vertical Benioff seismograph (Benioff, 1932). The only surface waves considered are Rayleigh waves since all measurements were made with vertical seismometers. The period range discussed extends from the 6.0 sec microseisms to noise of 0.3 sec period.

The theoretical Rayleigh wave group velocities, phase velocities, and amplitude-depth relationships were obtained from the Seismic Data Laboratory in Alexandria, Virginia. Data from both deep-hole arrays and surface arrays were used in this study.

A brief description of the sites is given in table 2. A complete description of the sites can be found elsewhere (Geotechnical Corporation, 1964).

The following sites are of particular interest: (a) Fort Stockton, Texas, (FO-TX), because of the great depth (5790 m) of the deep hole; (b) Eureka, Nevada (EK-NV), because of the very low noise level; (c) Apache, Oklahoma (AP-OK) because the velocity section is a close approximation of a half space and because it is close (20 km) to the Wichita Mountains Seismological Observatory (WMSO) where phase velocities were measured. The site at Apache was of additional interest because the noise spectrum was similar to that at WMSO. Therefore, both the phase velocities and amplitude-depth relationship can be used.

It must be noted that all the information presented was obtained from sites at some distance from the coast. Sites close to the coast typically exhibit large amplitudes at periods around 1.0 sec (Douze, 1964). There are not sufficient experimental results available to determine the waves responsible.

5.1.2 Theory

This section derives the theory necessary to interpret the experimental results. The theory for both body waves and Rayleigh waves will be presented. For the deep-hole measurements, the amplitude-depth relationships need to be considered, while for the surface array measurements, the

-17-

Table 2. Site descriptions

Site	Location	Depth (m)	Geologic section
Apache, Oklahoma	34°49'59"N 98°26'09"W	2917	Consists of 1500 m of high-velocity limestones (6000 m/sec) overlying volcanics of somewhat lower velocities (5500 m/sec).
Eureka, Nevada	39°12'32"N 115°42'37"W	3130	The top 1100 m is made up of sandstones, shales, thinly bedded limestones, and dolomites overlying higher-velocity limestones and dolomites.
Fort Stockton, Texas	30°54'06"N 102°41'52"W	5792	Upper 3700 m consists of low-velocity shales, sand and limestones overlying higher-velocity limestones and dolomites.
Franklin, W. Virginia	38°33'02"N 79°30'47"W	3815	The upper 3060 m consists of high-velocity limestones and dolomites; below a major thrust fault at 3060 m, the section has lower velocities although the formations are repeated.
Grapevine, Texas	32°53'09"N 96°59'54"W	3118	The top section consists of shales. The hole bottoms in a limestone; velocity increases steadily with depth.
Pinedale, Wyoming	42°27'24"N 109°33'04"W	3022	Consists entirely of sandy shales; velocity increases slowly with depth.
Wichita Mountains Seismological Observatory	34°43'05"N 98°35'21"W		Located on the same volcanics as encountered in the Apache deep hole. Measured surface velocities vary between 3000 and 4000 m/sec.

-18-

TR 67-3

phase velocities are of interest. In both cases, the phase angles and coherences yield valuable information.

The main tool in the interpretation are the spectra and cross spectra of the noise detected by different seismometers placed in either a horizontal or vertical plane. Therefore, the theory will be concerned with the results obtained by spectral analysis techniques. The theory of the behavior of body waves in the deep hole and across surface arrays is, in general, confined to the results that would be obtained in a half space. For the case of a layered media, the amplitude-depth relationships for P waves at vertical incidence has been solved (Gupta, 1965). The reason for not extending the theory to the layered case is that the convenient matrix method does not appear to be applicable when each term is an integral, as in the case when spectra are considered. In the case of fundamental and higher mode Rayleigh waves recorded by the deep-hole seismometer, the azimuth of approach is not important because the amplitude-depth relationships are the values measured. However, in the case of body waves, the angle of incidence must be considered.

First, the theoretical amplitude-depth relationships that will be obtained from a mixture of Rayleigh modes are discussed. Then, the theory of body-wave noise at random angles of incidence is discussed in relation to the results that would be obtained from deep-hole measurements. The assumption of no P- to S-wave conversion at the free surface is made to show the mathematical procedure followed; the solution can, in this case, be obtained in closed form. Then, the formulas (not in closed form) that include P- to S-wave conversion at the free surface are derived. Next shown are the results that would be obtained in the deep hole if a mixture of Rayleigh waves were present.

The results obtained from cross spectra of the vertical seismometers of a surface array are discussed for the case of surface waves and body waves.

5.1.2.1 Rayleigh waves

The theory of higher Rayleigh modes has been extensively discussed in the literature (Ewing, et al., 1957), and the presence of higher Rayleigh modes in earthquake surface waves has been established (Oliver and Ewing, 1958). It has been previously suggested that Rayleigh waves, both fundamental and higher modes, are responsible for seismic noise (Gutenberg, 1958).

The data used in calculating the theoretical change in amplitude with depth of the different Rayleigh modes were obtained as follows. The compressional-wave velocities were obtained from sonic logs; the shear-wave velocities were calculated from the compressional-wave velocities by assuming an appropriate Poisson's ratio (usually around 0.27); and densities were used appropriate to the lithologies encountered in the hole.

-19-

No attempt was made to model the whole crust, but the velocities were increased with depth (on the model of an average crust) sufficiently o obtain the higher modes in the desired period ranges.

The oscillatory nature of the higher mode group velocities in a basic property of even simple structures, but is accentuated when a low-velocity channel, such as a sedimentary section, is present. The maxima and minima of the group velocity curves are of interest, because they produce large amplitude arrivals from earthquakes and may be associated with peaks in the noise spectra (Gutenberg, 1958).

An example of the results obtained for the change with depth of the displacements of the different Rayleigh modes (at FO-TX) is shown in figure 12. The fundamental mode displacement decreases monotonically with depth with only slight inflections at discontinuities. Large displacements are present at depth when a lobe of a higher mode occurs in a low-velocity zone which traps a large percentage of the total energy of the wave. Low-velocity zones are present at all the holes studied. At all the sites, except AP-OK, the low-velocity zone is caused by the sediments, and at AP-OK, by the volcanics below the high-velocity limestone.

5.1.2.2 Deep-Hole Theory

If the noise is assumed to consist of a mixture of uncorrelated Rayleigh modes the results of spectral analyses can be explained in the following manner. Subscript 1 will refer to the surface and subscript 2 to the deep hole.

$$X_1(t) = \sum_{n=1}^{N} X_n(t)$$

where N is the number of Rayleigh modes present in the noise. The spectrum is obtained by first autocorrelating and then taking the Fourier transform of the autocorrelation. The result is

$$\varphi_{11}(\omega) = \sum_{n=1}^{N} \varphi_n(\omega). \tag{1}$$

The spectrum of the noise recorded by the deep-hole seismograph is related to the surface noise by a transfer function $H_n(\omega) \exp(i\delta_n)$,

$$\varphi_{22}(\omega) = \sum_{n=1}^{N} |H_n(\omega)|^2 \varphi_n(\omega) \tag{2}$$

-20-
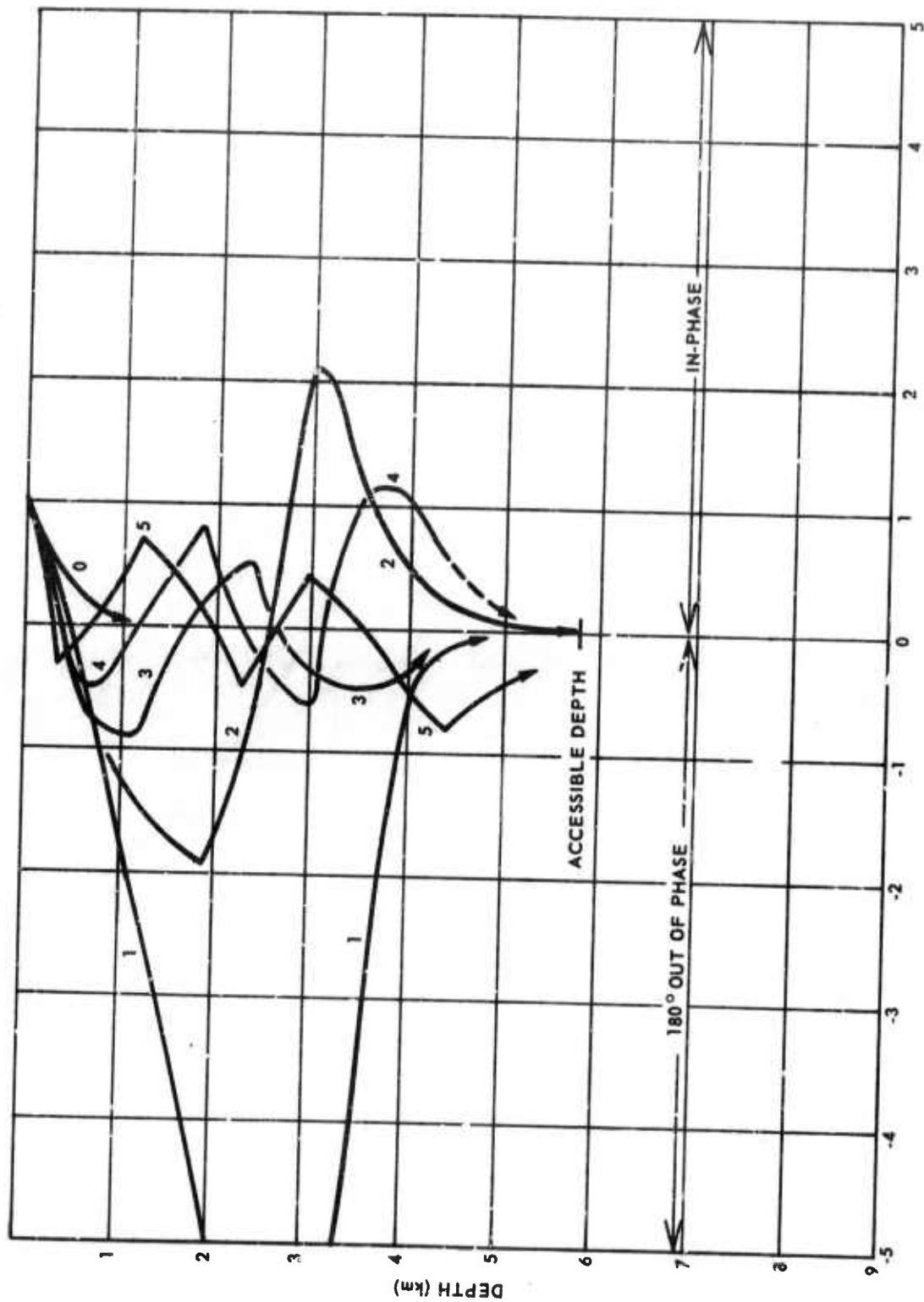
Figure 12. Rayleigh and higher-mode amplitude (normalized to amplitude at earth's surface) as a function of depth at FO-TX. Period = 0.5 sec

G 2217

-21-

The transfer function is the theoretical change of the displacements of the Rayleigh modes with depth. According to theory, the angle δ is always 0 or 180 deg (see figure 12); therefore, the absolute value signs are not strictly necessary in the equation.

The cross spectrum between a surface and a deep-hole noise sample is given by

$$\varphi_{12}(\omega) = \sum_{n=1}^{N} H_n(\omega) \, e^{i\delta_n} \, \varphi_n(\omega) \, .$$

(3)

Equation 3 indicates that the cross spectrum will be a real quantity if only Rayleigh waves are present because the angle δ_n is either 0 or 180 deg. A negative cross spectrum indicates that the "power" in the Rayleigh modes, 180 deg out-of-phase at depth, is larger than the power of the Rayleigh modes in phase at depth. The coherence is defined as

$$Coh = \frac{\left|\varphi_{12}\right|^2}{\varphi_{11} \cdot \varphi_{22}} \, .$$

The equations indicate that the coherence is unity at all depths if only one Rayleigh mode is present, and will always be less than unity for a mixture of modes. The coherence will be zero when equal amounts of power are in phase and 180 deg out-of-phase.

The behavior of seismic noise in the frequency range between 0.5 and 5.0 cps as a function of depth suggests the possibility of body-wave noise at random angles of incidence. First, the equations for body waves at random angles of incidence are solved under somewhat restrictive assumptions that allow a solution in closed form to be obtained. The more general solution can only be solved by numerical integration.

The following assumptions are made:

      a. P-wave noise arriving independently from all angles of incidence with equal energy content:

      b. No conversion from P to S waves at the free surface;

      c. An isotropic, homogeneous half space.

The equations are derived for the noise as it would be detected by a vertical-motion seismograph. The solutions are derived in some detail to indicate

-22-

the methods used. The particle displacement at the surface is taken to be

$$X_1(t) = \sum_{n=1}^{N} f_n(t) \cos \theta_n$$

where θ is the angle of incidence measured from the vertical. The auto-correlation of each independent time series $f_n(t)$ is denoted by $\frac{1}{N} \psi(\tau)$.

The autocorrelation of $X_1(t)$ then becomes

$$\psi_{11}(\tau) = \frac{1}{N} \sum_{n=1}^{N} \psi_n(\tau) \cos^2 \theta_n.$$

By taking the Fourier transform, the power spectrum is obtained

$$\varphi_{11}(\omega) = \frac{1}{N} \sum_{n=1}^{N} \varphi_n(\omega) \cos^2 \theta_n$$

Now let $N \to \infty$, the power spectrum of the surface noise becomes

$$\ddot{\psi}_{11}(\omega) = \frac{1}{\pi} \int_{-\pi/2}^{\pi/2} \cos^2 \theta \, d\theta = \frac{\varphi(\omega)}{2} \tag{4}$$

The spectrum of the noise at any depth is obtained as follows:

$$X_2(t) = \sum_{n=1}^{N} \left\{ \left[\frac{1}{2} f_n \left(t - \frac{\alpha}{2} \cos \theta_n \right) \right] + \left[\frac{1}{2} f_n \left(t + \frac{\alpha}{2} \cos \theta_n \right) \right] \right\} \cos \theta_n$$

where $\frac{\alpha}{2}$ is the vertical uphole time.

Going through the same procedure as for the surface we obtain the spectrum at depth

$$\varphi_{22}(\omega) = \varphi(\omega) \frac{1}{2\pi} \int_{-\pi/2}^{\pi/2} \left\{ \cos^2 \theta + \cos (\omega\alpha \cos \theta) \cos^2 \theta \right\} d\theta$$

$$= \varphi(\omega) \left\{ \frac{1}{4} + \frac{J_0(\alpha \omega)}{2} - \frac{J_1(\alpha \omega)}{2\alpha\omega} \right\} \tag{5}$$

-23-

Note that the expression in brackets approaches $\frac{1}{2}$ as $\omega \to 0$ because $\frac{J_1(\alpha\omega)}{\alpha\omega} \to 0.5$. The ratio of the deep-hole spectrum divided by the surface spectrum often used in the interpretation then becomes

$$R = \frac{1}{2} + J_0(\omega\alpha) - J_1(\omega\alpha)/(\alpha\omega)$$

which, as expected, approaches unity for very low frequencies.

The cross spectra between the surface and the deep-hole spectra are obtained in the same way

$$\varphi_{12}(\omega) = \varphi(\omega)\left\{ J_0\left(\frac{\alpha\omega}{2}\right) \frac{J_1(\frac{\alpha\omega}{2})}{\frac{\alpha\omega}{2}} \right\} \tag{6}$$

Notice that the cross spectrum is either positive or negative, but does not have an imaginary component, indicating that the phase changes from 0 to 180 deg. The coherence between the surface and the deep-hole noise becomes

$$Coh = \frac{\left| J_0\left(\frac{\alpha\omega}{2}\right) - \frac{J_1(\frac{\alpha\omega}{2})}{\alpha\omega/2} \right|^2}{\frac{1}{8} + \frac{J_0(\alpha\omega)}{4} - \frac{J_1(\alpha\omega)}{4\,\alpha\omega}}$$

which approaches unity as $\omega \to 0$.

The theory for S waves at random angles of incidence is similar. Define $\frac{\beta}{2}$ as the uphole time for S waves.

The equations become:

$$\varphi_{11}(\omega) = \frac{1}{2}\,\varphi(\omega)$$

$$\varphi_{22}(\omega) = \varphi(\omega)\left\{ \frac{1}{4} + \frac{J_1(\beta\omega)}{2\,\beta\omega} \right\}$$

$$\varphi_{12}(\omega) = \varphi(\omega)\,\frac{J_1(\frac{\beta\omega}{2})}{\frac{\beta\omega}{2}}$$

TR 67-3

In the previous example, the conversion of P to S waves at the free surface was neglected. Taking the conversions into account and keeping the rest of the assumptions made before, a more realistic solution can be obtained; however, the solution could not be obtained in closed form and numerical integration of the integrals is necessary.

In this case, the time series at the surface and at depth become

$$X_1(t) = \sum_{n=1}^{N} f_n(t) \cos \theta_n + b(\theta) f_n(t) \cos \theta_n + c(\theta) f_n(t) \sin \zeta_n$$

$$X_2(t) = \sum_{n=1}^{N} f_n(t-\alpha \cos \theta_n) \cos \theta_n + b(\theta) f_n(f + \alpha \cos \theta_n) \cos \theta_n$$
$$+ c(\theta) f_n(t + \beta \cos \xi_n) \sin \xi_n$$

where b and c are reflection coefficients for P and S waves from an incoming P wave. These coefficients are functions of the angle of incidence and can be found in the literature (Ewing, et al., 1957). S waves are reflected at an angle ξ, which is connected with θ by Snell's Law.

The procedure followed in obtaining the required integrals is the same as that employed previously. Because of the large number of terms involved in the derivation, only the resulting integrals will be given.

$$\varphi_{11}(\omega) = \varphi(\omega) \frac{1}{2\theta} \int_{-\theta}^{\theta} \left[\cos^2\theta + b^2 \cos^2\theta + c^2 \sin^2\xi \right.$$
$$\left. + 2b \cos^2\theta + 2c \cos\theta \sin\xi + 2bc \cos\theta \sin\xi \right] d\theta \qquad (7)$$

$$\varphi_{22}(\omega) = \varphi(\omega) \frac{1}{2\theta} \int_{-\theta}^{\theta} \left[\cos^2\theta + b \cos^2\theta + c^2 \sin^2\xi \right.$$
$$+ 2b \cos(\omega\alpha \cos\theta) \cos^2\theta$$
$$+ 2c \cos\omega(\frac{\alpha}{2}\cos\theta + \frac{3}{2}\cos\xi) \cos\theta \sin\xi \qquad (8)$$
$$\left. + 2 bc \cos\omega(\frac{3}{2}\cos\xi - \frac{\alpha}{2}\cos\theta) \cos\theta \sin\xi \right] d\theta$$

-25-

$$\omega_{12}(\omega) = \omega(\omega) \frac{1}{2\theta} \int_{-\theta}^{\theta} \left[\cos\left(\omega\frac{\alpha}{2}\cos\theta\right)\cos^2\theta + b^2\cos\left(\omega\frac{\alpha}{2}\cos\theta\right)\cos^2\theta \right.$$

$$+ c^2\cos\left(\omega\frac{\cdot}{2}\cos\xi\right)\sin^2\xi + 2b\cos\left(\omega\frac{\alpha}{2}\cos\theta\right)\cos^2\theta$$

$$+ i\,c\left\{\sin\left(\omega\frac{\alpha}{2}\cos\theta\right) - \sin\left(\omega\frac{\beta}{2}\cos\xi\right)\right\}\cos\theta\,\sin\xi$$

$$\left. + i\,bc\left\{\sin\left(\omega\frac{\alpha}{2}\cos\theta\right) + \sin\left(\omega\frac{\beta}{2}\cos\xi\right)\right\}\cos\theta\sin\xi\right]d\theta \qquad (9)$$

These formulas indicate that if the numerical integration is carried out between even limits, a number of the terms disappear because they are odd functions.

It will be noted that while the spectra are real quantities, as expected, the cross spectrum is a complex quantity, so that the phase is no longer either 0 or 180 deg but attains intermediate values. In cases of practical interest, the phase angles are so close to 0 or 180 deg that spectral analyses are not sufficiently accurate to detect the difference. Numerical integration of the integrals was carried out on a CDC 160-A computer.

Rayleigh waves and body waves at vertical incidence result in standing wave patterns because of the interference effects of incident and surface-reflected waves. Consequently, the phase angle at depth can only be either 0 or 180 deg as compared with the surface. The cross spectra given in equation (9) indicates that this is no longer the case for body waves at angles of incidence other than the vertical. The cross spectrum has an imaginary component indicating that a standing wave pattern is not set up with depth. The same conclusion has been reached by Felix Nagel (unpublished manuscript) from the amplitude-depth relationships obtained when plane waves arrive at the free surface at some arbitrary angle of incidence. The amplitude-depth relationships are a function of time and standing waves are not obtained. The position of the zero amplitude value changes only slightly with time; there-fore, a low value resembling a nodal point will be obtained at depth (for a particular frequency) if the wave motion is averaged over some time.

In general, over a narrow band of frequencies, the amplitude-depth relation-ship of P waves at close to vertical incidence are often similar to one of the Rayleigh-mode amplitude-depth relationships. For example, the third higher Rayleigh mode and P waves at close to vertical incidence are almost identical for a frequency of 2 cps at AP-OK.

Narrow band-pass filtering together with cross-correlation offers the possibility of distinguishing between surface waves and body waves.

-26-

If surface waves are present in the noise, the cross-correlation between surface and deep-hole noise samples will have a maximum at zero lag. The maximum will be positive or negative, depending on whether the surface waves at depth are in phase or 180 deg out-of-phase with the surface. In the case of body waves, the maximum in the cross-correlation will be at a lag time equal to the up-hole travel time of the body waves.

It must be recognized that if any one frequency acts like a plane wave, P waves at vertical incidence will set up a standing wave pattern and cross-correlation results will look as if surface waves are present. Therefore, some caution is necessary in interpreting the results. If very narrow-band filtering were employed, that is, examining essentially one frequency, it would be possible to interpret the results quantitatively. However, the cross-correlations over a finite bandwidth used here can only be interpreted qualititatively to distinguish between surface waves and body waves.

5.1.2.3 Surface Array Theory

In the case of surface waves arriving at the array from a given direction (or a given direction and angle of incidence in the case of body waves), the equations can be obtained easily. The spectrum of the noise at two seismometers (a and b) will be the same (ignoring seismometer-to-ground coupling problems).

$$\varphi_{aa} = \varphi_{bb} = \sum_{n=1}^{N} \varphi_n(\omega)$$

The cross spectra will be:

$$\varphi_{ab} = \sum_{n=1}^{N} \varphi_n(\omega) \, e^{-i\,\omega\left(\frac{\Delta x}{v_n}\cos\beta\right)} \tag{10}$$

where

N = number of wave types present in the noise

Δx = distance between the seismometers

v = phase velocity of the waves

β = angle between the direction connecting the seismometers and the direction of arrival.

-27-

The cross spectra between two seismometers give only apparent phase velocities, and two cross spectra are necessary to obtain the real phase velocities and directions of arrival.

The theoretical results indicate that coherence will be unity if only one wave type is present, and less than unity in all other cases.

Experimental data from arrays usually indicate that the noise often appears to be omnidirectional (isotropic), that is, arriving with approximately equal energy content from all directions. For the case of surface waves, the solution that would be obtained has been solved by Backus, et, al., (1964). The spectrum of each seismometer is the same, $\varphi(\omega)$, and the cross spectra become

$$\varphi_{ab}(\omega) = \varphi(\omega) \, J_0 \left(\frac{\omega \Delta x}{v} \right) \tag{11}$$

where the Δx and v are, respectively, separation between seismometers and phase velocity.

This solution can easily be extended to more than one wave type and results in the sum of Bessel functions equal to the number of wave types present.

Because of the possible presence of body-wave noise, it is necessary to also consider the case of body waves from random directions and random angles of incidence.

For P waves arriving at the surface seismometers with equal energy content from random directions and all angles of incidence, the time series for a vertical-motion seismometer a is

$$X_a(t) = \sum_{n=1}^{N} f_n(t) \cos \theta_n \; .$$

At seismometer b, the time series becomes

$$X_b(t) = \sum_{n=1}^{N} f_n \left(t - \frac{\Delta x}{v} \sin \theta_n \cos \beta_n \right) \cos \theta_n$$

where θ refers to the angle of incidence and β to the direction of the waves. Proceeding in exactly the same fashion as described in the previous section, the spectrum of each seismometer becomes

-28-

$$\omega_{aa}(\omega) = \omega_{bb}(\omega) = \frac{1}{2}\omega(\omega)$$

and the cross spectrum becomes

$$\omega_{ab}(\omega) = \omega(\omega) \cdot \frac{1}{2\pi} \cdot \frac{1}{\pi} \int_{0}^{2\pi} \int_{-\pi/2}^{\pi/2} e^{-i\omega(\frac{\Delta x}{v}\sin\theta\cos\beta)} \cos^2\theta \cdot d\beta d\theta \cdot$$

By performing the last integration, the expression reduces to

$$\varphi_{ab}(\omega) = \omega(\omega) \frac{1}{2\pi} \int_{0}^{2\pi} \frac{J_1(\frac{\omega\Delta x}{v}\cos\beta)}{\frac{\omega\Delta x}{v}\cos\beta} \cdot d\beta. \tag{12}$$

This equation must be solved by numerical methods of integration.

Notice that under the assumptions made, both formulas (11) and (12) have no imaginary parts and the phase angle is either 0 or 180 deg. Therefore, velocities can only be obtained from the coherence values.

5.1.3 Experimental Results

The methods used in spectral analysis are briefly discussed in order to acquaint the reader with the reliability of the results. In order to facilitate discussion of the experimental results, the passband of the short-period Benioff was divided somewhat arbitrarily into three period ranges: 5.0 to 2.0 sec, 2.0 to 0.8 sec, and 0.8 to 0.3 sec. These divisions were chosen partly for convenience, and partly because somewhat different wave types appear to predominate in the different period ranges.

The 6.0 sec microseisms are not discussed here, because the analyses indicated clearly that, as measured by a vertical-motion seismometer, the fundamental mode Rayleigh wave is the only wave type present. This conclusion has been previously reached by a number of authors (see for example, Gutenberg, 1958).

It must be noted that the examples of noise analyses discussed in this section are only a small part of the large amount of information that lead the author to the stated conclusions.

5.1.3.1 Spectral Analysis

The principal tool used in the interpretation of the data consisted of obtaining spectra and cross spectra, and the associated auto- and cross-correlations of long noise samples. The techniques used to obtain spectra, and the accuracy and resolution that is obtained have been extensively discussed in the literature (for example, Blackman and Tukey, 1958) and need not be discussed here.

The length of the noise sample used varied between 180 and 450 sec. As a compromise between accuracy and resolution, a lag of 8 percent of the sample was usually used; however, either smaller or greater lags were sometimes employed to increase either the accuracy or the resolution of the results. A hanning smoothing function was used in all cases. In this section of the report, each figure will give the length of sample and the lag used, to allow the reader to determine the reliability of the results. The sampling rate used (usually 25 samples/sec) ensured that the folding frequency was well outside of the frequency range of interest.

Theoretical studies on the accuracy of cross spectra have been published in the literature (for example, Amos, et. al., 1963). The results indicate that the experimental coherences are a complex function of the actual coherence, the smoothing function, and the lag window and that considerable errors are to be expected when actual coherences are close to zero.

The magnifications at 1 cps were used to calibrate the power spectrum; therefore, only the values at 1 cps are correct ground motion values. Because of the identical responses of the seismographs used, the deep-hole-divided-by surface ratios used in the interpretation are correct at all frequencies. The ratios are obtained by dividing the deep-hole noise spectrum by the surface spectrum, and will be called power ratios in the body of the report. The square root of the power ratio will be referred to as the amplitude ratio.

5.1.3.2 Microseisms, 5.0 to 2.0 Sec

The ratio of deep-hole-divided-by-surface-noise spectra at all sites investigated indicates that fundamental mode Rayleigh waves is not the only wave present in the period range between 5.0 and 2.0 sec.

Figure 13 shows the experimental power ratio, and figure 14 shows the phase angle and coherence obtained from noise samples when the deep-hole seismometer was located at a depth of 5200 m at FO-TX. The theoretical curves for the first three Rayleigh modes and for P waves at vertical incidence are also shown. These analyses were made at a time when a storm in the Atlantic was the cause of large microseisms in the period range of 2.0 to 6.0 sec. The lowest value of the power ratio occurs at a period of 4.0 sec; however, the coherence is not zero until a period of 3.4 sec is reached. This behavior

-30-
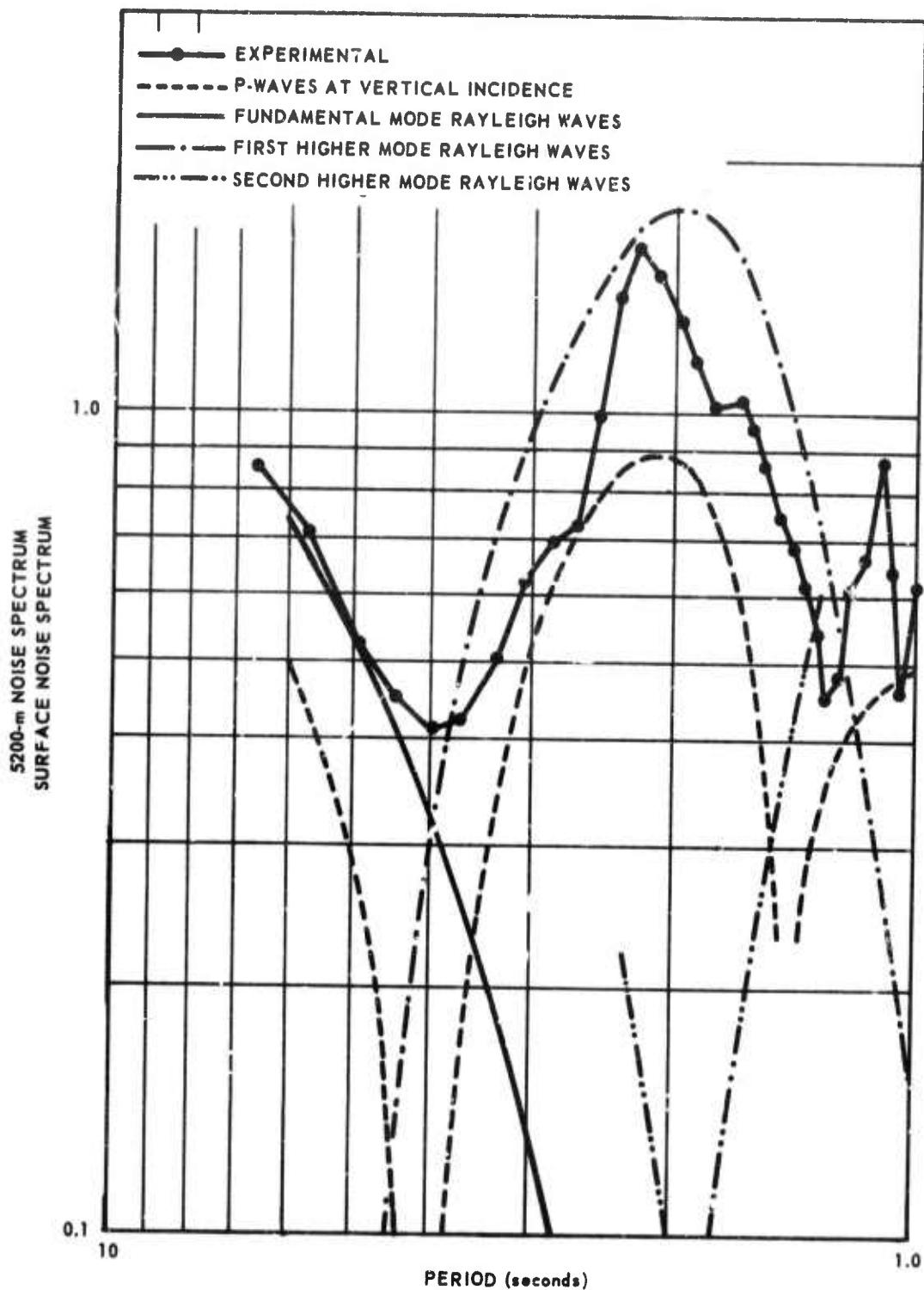
Figure 13. Deep-hole (5200 m) vertical noise spectrum divided by surface
noise spectrum. Theoretical amplitudes are included. FO-TX
300 sec sample, 10 samples/sec, 5 percent lags

G 2218

-31-
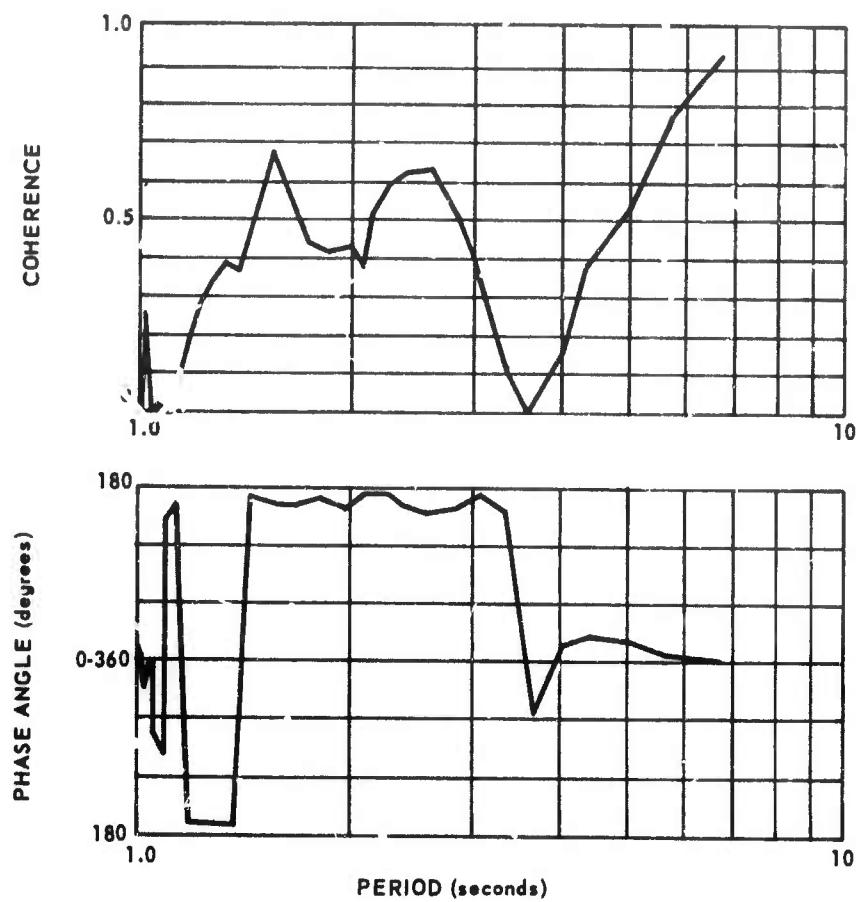
Figure 14. Phase angle and coherence of the noise between the surface and 5200 m, FO-TX. 300 sec sample, 10 samples/sec, 5 percent lags

G 2219

-32-

indicates that between 3.4 and 4.9 sec most of the power was in phase as is also shown by the phase angle (figure 14); therefore, the fundamental mode, which is the only wave in phase, predominated at these periods. To explain the power ratio, the rest of the energy must be in the first higher mode.

Examination of the figures (13 and 14) indicates that for periods less than 3.4 sec, only a small amount of fundamental mode Rayleigh waves can be present in the noise. The experimental values lie between the theoretical first higher Rayleigh mode and P-wave curves. The experimental data can be explained by either mixtures of fundamental and first higher mode Rayleigh waves, or P waves and first higher mode Rayleigh waves.

The deep-hole results at FO-TX indicated that either P waves or first higher mode Rayleigh waves predominated in the noise but the results could not be used to conclusively distinguish between the two waves. In an attempt to distinguish between these two possibilities, information from WMSO was used from the same time as the FO-TX analyses. Cross spectra between noise samples from three seismometers located in a 3 km tripartite were obtained. The cross spectra of the noise from two seismometers are sufficient to specify an apparent velocity. Two pairs of seismometers are sufficient to specify phase velocity and angle of arrival. The cross spectra between the noise samples from all three noise samples were used to check if consistent results were obtained from all combinations of pairs. The results obtained are given in table 3.

As indicated in the theoretical results, if the noise field is isotropic, the phase angle is 0 or 180 deg. The phase angles obtained from the experimental results indicated clearly that part of the noise at periods greater than 2.0 sec was directional. The directions obtained indicated that the storm in the Atlantic was responsible for the directional part of the noise.

Examinations of combinations of directional and nondirectional noise (from equation 10, 11, and 12) indicate that the phase velocity obtained for periods greater than approximately 2.0 sec by these measurements is too large. This behavior is caused by the isotropic noise staying either in phase or 180 deg out of phase. In the period range under examination here, this causes the phase angle from the cross spectra to be intermediate between the actual value for the directional noise and 0 deg value of the omnidirectional noise. As an example, assume 50-percent isotropic 3.0 sec period waves at 4 km/sec and 50-percent directional waves at 4 km/sec arriving along the line connecting two seismometers 3 km apart; in this case, the phase angle will be 64 deg. If only the unidirectional waves were present, the phase angle would be 88 deg. The above presented argument indicates that the real phase velocities of the directional noise are less than those obtained from the cross spectra. Therefore, the phase velocities in table 3 indicate that body waves are excluded for anything except every shallow angles of emergence.

-33-

The choice, therefore, lies between fundamental and first higher mode Rayleigh waves; however, results from FO-TX during the same time indicate that only small amounts of fundamental mode Rayleigh waves were present in the noise at these periods. Therefore, the first higher mode Rayleigh waves must predominate.

Table 3. Phase velocity measurements from cross spectra, WMSO

Period (sec)	Azimuth (deg)	Velocity (km/sec)	Average (coherence)^2	Spectral amplitude (m μ^2/cps)
6.667	213	2.85	0.88	51.0
5.714	215	3.16	0.88	91.1
5.000	219	3.49	0.86	92.2
4.444	226	3.68	0.83	67.0
4.000	229	3.63	0.76	39.8
3.636	228	3.83	0.70	26.3
3.333	228	4.26	0.69	22.4
3.077	229	4.33	0.64	23.6
2.857	226	4.41	0.54	21.8
2.667	226	4.24	0.46	18.5
2.500	228	4.51	0.46	16.1
2.353	229	4.87	0.41	15.1
2.222	231	4.23	0.22	13.2
2.105	237	4.69	0.23	10.6
2.000	235	5.70	0.25	9.12

The arguments given above are meant to show the existence of the first higher Rayleigh mode, and are not intended to prove that this mode predominates at all times and at all locations. However, phase angles from all deep-hole measurements always show the same behavior; the phase angle changes from 0 to 180 deg at a period that can be explained by P waves or higher modes. The fundamental mode never predominates at periods less than approximately 4.0 sec. It is of interest that when the first higher mode can be shown to predominate, a small high in the spectra usually appears at 3.0 sec (see table 3).

Particle motion diagrams of the 3.0 sec microseisms produced ambiguous results; almost all sizes and shapes of ellipses were obtained. This failure was possible caused by the presence of different wave types in closely adjacent period ranges. The possible presence of Love waves in the noise could also contribute to the failure to obtain reproducible results.

TR 67-3

At the sites where thick sections of low-velocity rock are present (usually shales), the results obtained are more difficult to interpret than at the sites where predominantly high-velocity rocks are present. Figure 15 shows an example of the results obtained at the Pinedale, Wyoming, site. The section at this location is composed entirely of shales. The results can probably be best explained by a combination of P waves and fundamental Rayleigh waves if the location of the nodal point is taken as the main criteria for interpretation. However, there is some doubt as to the validity of this interpretation. Figure 15 also shows the results obtained from spectral analysis of a surface wave of an earthquake from Baja California. The group velocity of these waves was about 3.2 km/sec, indicating that they are surface waves, probably higher mode Rayleigh waves as recorded by the vertical-motion seismographs. It is noticeable from the figure that the behavior of the amplitude-depth relationships of the noise and these surface waves is very similar, especially in regard to the location of the nodal point. This behavior suggests that the theoretical Rayleigh wave curves may be in error. The theoretical Rayleigh wave computer program used does not take into account the well known velocity anisotropy of shales. Preliminary results from an anisotropic Rayleigh wave program suggest that the discrepancies between theoretical and experimental results can be explained in this way.

It is, of course, entirely possible that the noise does consist of fundamental mode Rayleigh waves and P waves, and that the first higher mode was not present at the time of the experiments. With the limited depth of the hole and with no surface array information, the problem cannot be solved. With holes of the usual depth of approximately 3000 m, it is not possible to distinguish between the two possibilities of P waves or first higher mode Rayleigh waves. Figure 16 shows the amplitude-depth relationship of the 2.0 sec noise at AP-OK. Either theoretical curve will explain the experimental data.

5.1.3.3 Noise in the Period Range of 2.0 and 0.8 Sec

The noise in this period range predominates in the spectra at sites close to the coast; at quiet sites distant from the coast, the noise at these periods has usually been attenuated to very small values.

Considerable difficulty has been encountered in interpreting the data at these periods. The amplitude-depth relationships agree quite well with the theoretically predicted P-wave amplitude-depth relationships. As an example, figure 17 shows the power ratio obtained at AP-OK from the noise at the surface and 2917 m. The theoretically predicted amplitude-depth relationship for P wave at random angles of incidence between -45 and +45 deg from the vertical, and the experimental and theoretical phase angles and coherences are also shown in the same figure. The agreement between theory and experiment is quite good, and could be improved even further by assuming the presence of some S-wave noise. Figure 16 shows the amplitude-depth relationships for the 1.0 sec noise as measured at AP-OK; the theoretical

-35-
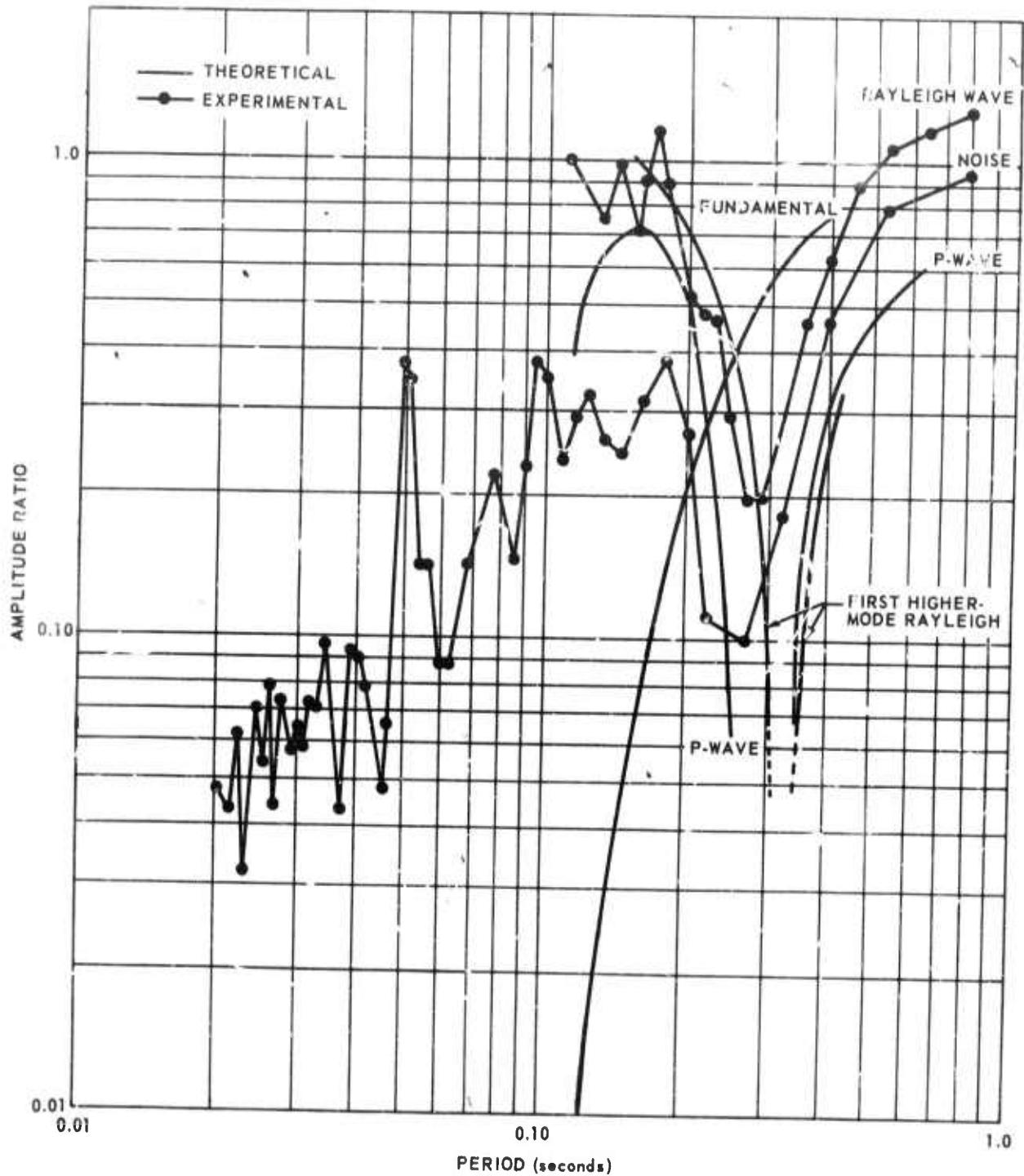
Figure 15. Amplitude ratio of the noise and a Rayleigh mode from Baja
California, as recorded at 3060 m at Pinedale, Wyoming. Theoretical
curves for P waves and Rayleigh waves are included.

G 2220

-36-
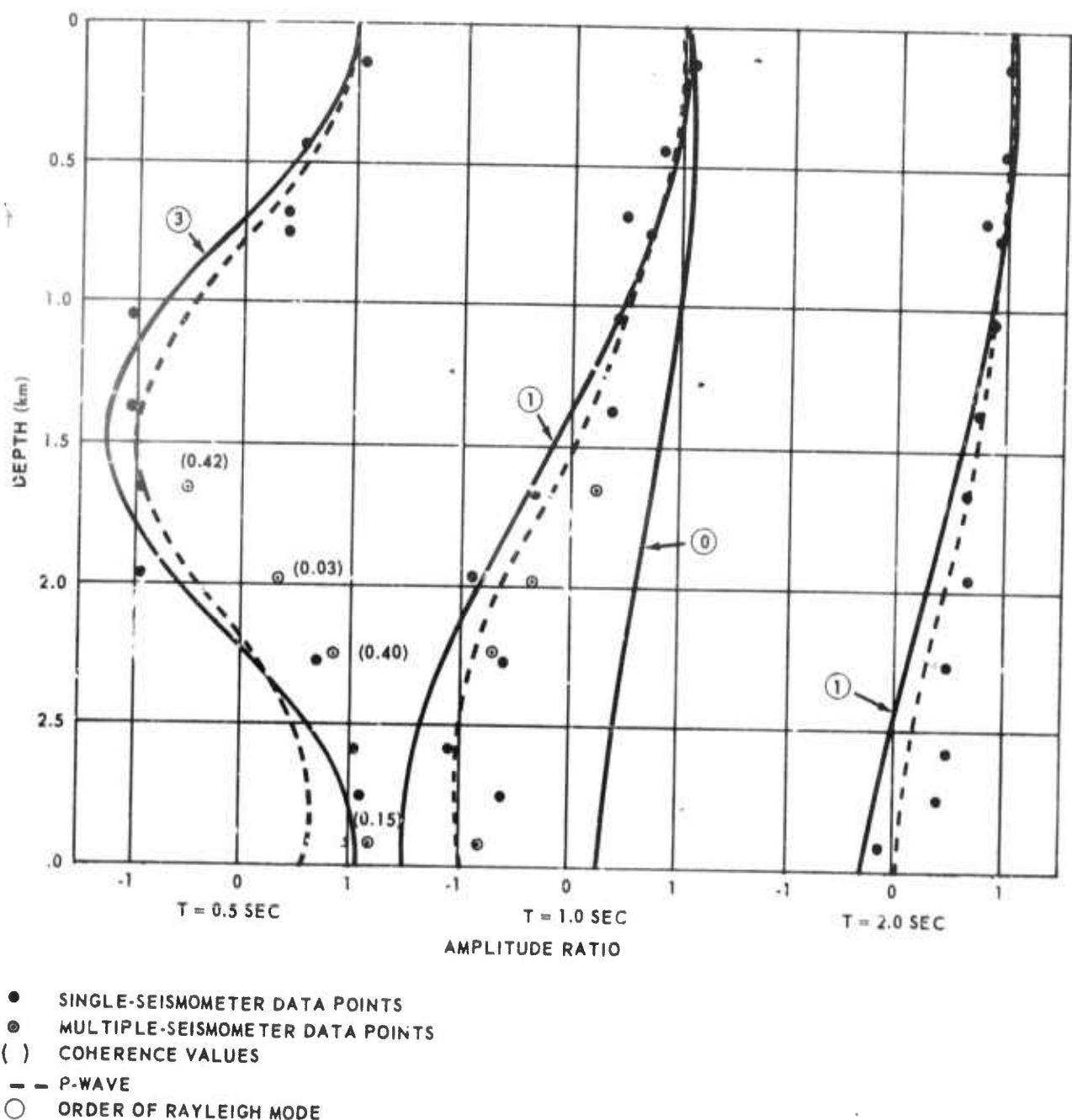
Figure 16. Observed and theoretical amplitude ratio with depth for periods of 0.5, 1.0, and 2.0 sec. 180 sec sample, 25 sample/sec, 5 percent lags

G 2221

TR 67-3
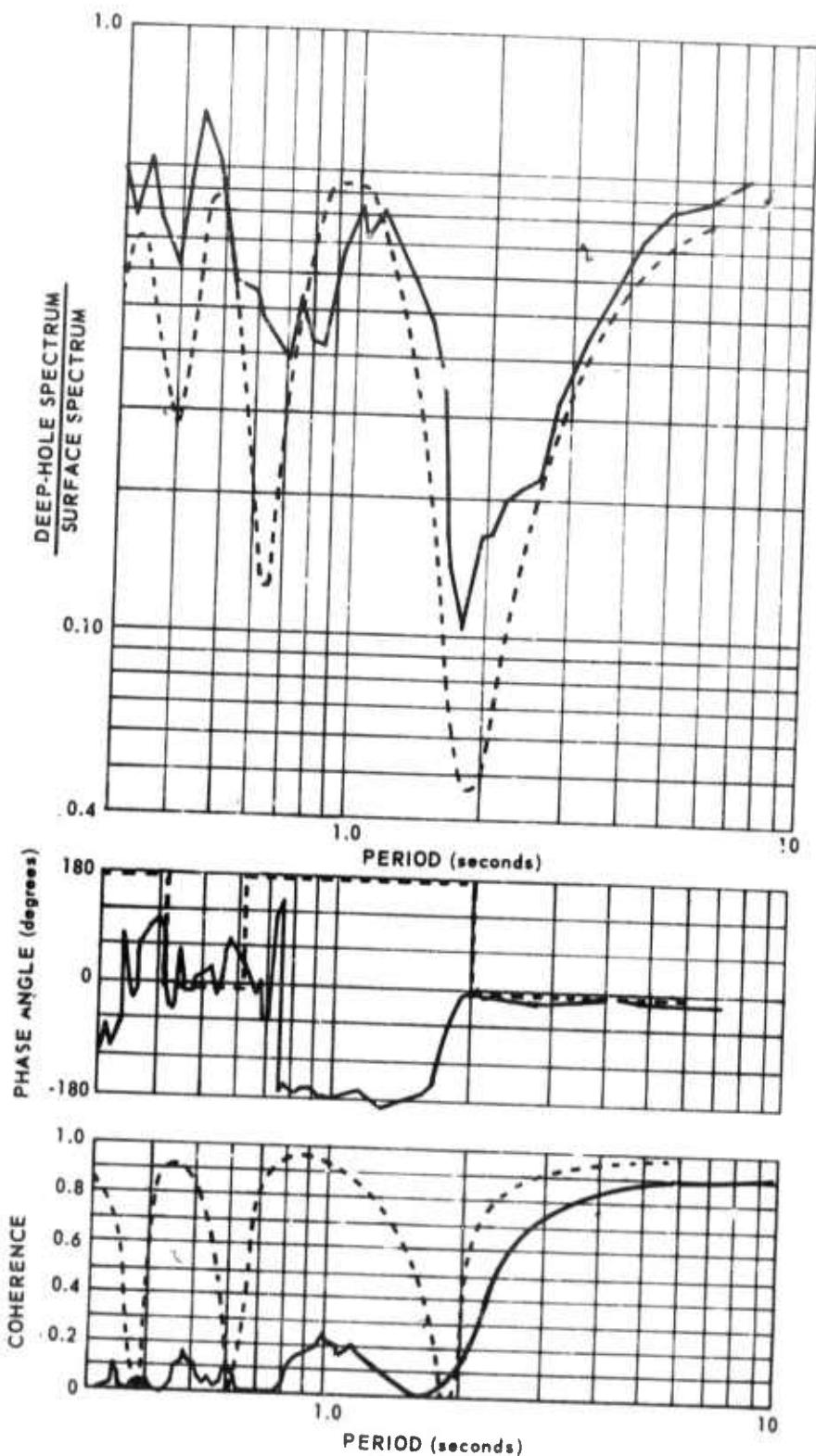
Figure 17. Theoretical and experimental power ratios, phase angles, and coherences theory for P waves arriving randomly -45 to +45 deg from the vertical. Uphole 0.5 sec. 180 sec sample, 25 sample/sec 9 percent lags

G 2222

-38-

curve for P waves at vertical incidence fits the experimental data quite well. However, the first higher mode theory is also quite close to the experimental data. There exists some doubt that P waves are the correct explanation of the noise at these periods. In an attempt to distinguish between the two possibilities (surface or body waves), cross-correlations were obtained after digital filtering. The digital filters had extremely sharp cut-offs, and only noise in the period range of interest passed through. Figure 18 shows the results obtained in the period ranges of 2.5 to 1.5 sec and 1.5 to 0.8 sec.

The experimental evidence shown in figure 18 indicates that surface waves are responsible for the noise in these two period ranges. As mentioned in the section on deep-hole theory, P waves at close to vertical incidence can set up a standing wave pattern that will result in cross-correlations of the type shown in figure 18. However, it appears unlikely that noise, the statistics of which indicate that it is a completely random phenomenon, will act in this fashion. It must be noted at this time that the cross-correlation of signals will result in the highest value at a lag equal to the uphole time. Furthermore, as will be shown in the next section, random P waves, when present, will give maximum in the cross-correlation at a lag other than zero.

Figure 19 shows the coherence between noise samples from seismometers 3 km apart at WMSO. The high coherences at periods greater than 2.0 sec were caused by directional noise. For periods between 1.0 and 2.0 sec, the phase angles indicated the presence of essentially isotropic noise. The experimental results can best be explained by wave traveling at velocities of 3.0 to 4.0 km/sec.

The most probable solution is that the noise consists of a mixture of Rayleigh modes, possibly on the basis of equipartition of energy as proposed by Sax and Hartenberger (1964). Some evidence for the presence of the second higher mode is obtained from figure 13, where at a period of 1.1 sec, the experimental data can only be explained by the presence of the second higher mode. However, this peak in the power ratio did not appear at all times; therefore, while it may be present, the second higher mode does not always predominate. It is apparent from the results that the fundamental mode Rayleigh wave does not exist with appreciable energy content at the quiet sites. Close to the coast, however, a considerable percentage of the noise must consist of the fundamental mode to explain results obtained during previously reported experiments (Douze, 1964).

5.1.3.4 Noise in the Period Range of 0.8 to 0.3 Sec

The noise amplitudes in the period range between 0.8 and 0.3 sec varies considerably from site to site. The sites with large noise amplitudes are close to centers of population, and the noise is usually connected with cultural activity.

-39-
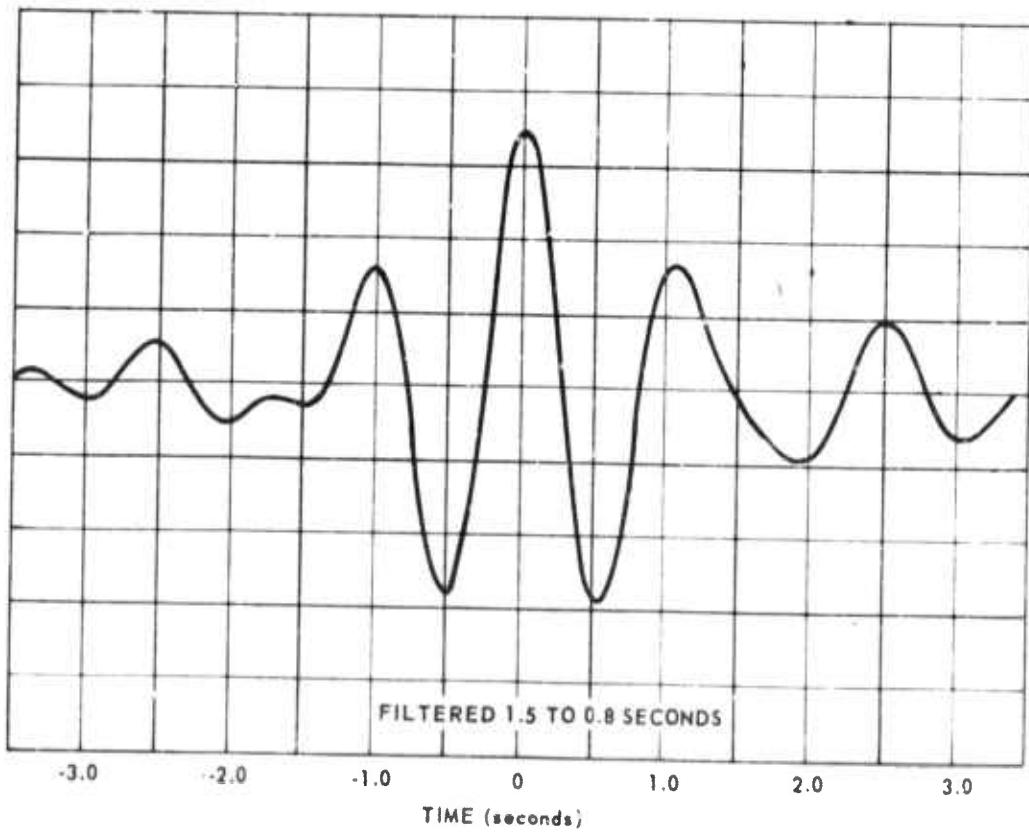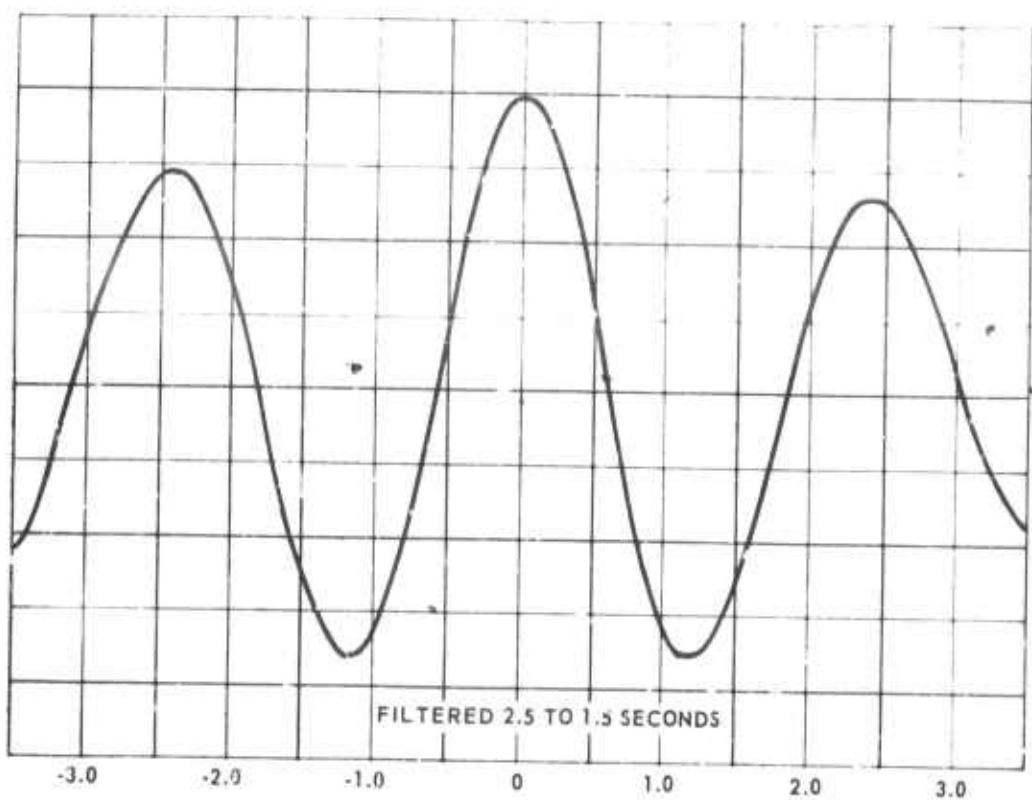
Figure 18. Cross-correlations of noise from seismometers at depths of 1970 and 2880 m, AP-OK

G 2223
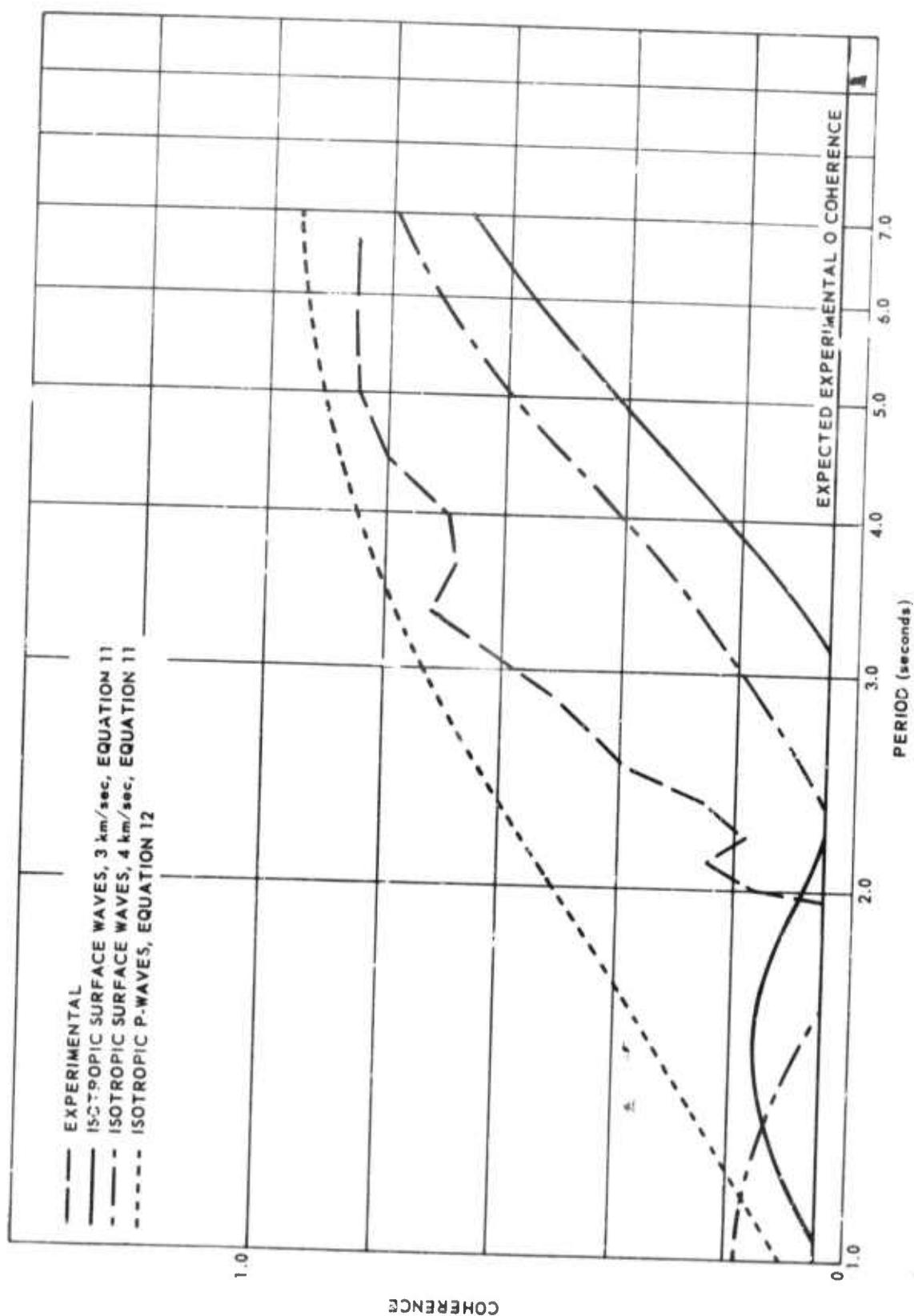
TR 67-3

Figure 19. Experimental and theoretical coherences of noise from seismometers 3 km apart, WMSO. 180 sec sample, 25 samples/sec, 8 percent lags

G 2224

-41-

The noise at this period range can logically be divided into three parts: the cultural noise, the sharp spectral peaks, and the residual noise when the other two noise types are not present. Each of the three parts is characterized by different wave types.

Figure 20 shows the spectra of the noise at the surface, at 1370 and 2890 m at GV-TX. Because of the close proximity of the site to Dallas, Texas, the cultural noise background is extremely large at the surface. The spectra in figure 20 indicate clearly that the amplitude (on the average) of the noise decreased very rapidly from the surface down to 1370 m and that the level only decreased slowly below this depth.

The only wave type that decreases in amplitude with depth with sufficient rapidity to account for experimental results is the fundamental mode Rayleigh wave. Figure 21 shows the experimental power ratio between the 668 m depth and the surface, together with the theoretical fundamental mode, first higher mode, and P waves. The results clearly indicate, with minor discrepancies, that the fundamental mode accounts for the rapid decrease in noise amplitudes in the first 668 m.

At depths where the amplitude of the fundamental mode has become negligible, the amplitude-depth relationships can be explained by either a combination of higher-mode Rayleigh waves, by body waves, or by a mixture of both. The power ratio in figure 21 shows lows at both the nodal points of the first higher mode and the P waves indicating the possible presence of these waves. In an attempt to distinguish between the possibilities, the noise from seismometers at depths of 2570 and 2890 m were cross-correlated after narrow-band analog filtering (low pass and high pass at 3 cps, 24 dB/octave. The result (figure 22) shows that the cross-correlation peaks at 0.1 sec, indicating that the noise consists of body waves and not of surface waves. If only P waves were present, the measured uphole time would indicate that the average angle of incidence is 45 deg from the vertical. However, it is likely that S waves also contributed to the average uphole time measured. Cross-correlation between deep-hole noise samples from EK-NV, a very quiet site, showed that the noise at approximately 3.0 cps also consisted of body waves.

The coherences were typically high at all sites where multiple seismometers were placed in close proximity (<600 m). The coherence was a complex function of the distance between seismometers. Figure 23 shows the coherence and phase angle of the noise from seismometers at depths of 1370 and 1980 m. Notice that the phase angle departs from 0 deg at 0.5 sec period; as will be discussed later, the peak at this period probably consists of another wave type.

All sites investigated, with the exception of Eureka, Nevada, showed the presence of a sharp peak at 0.49 sec period. Often it was hidden by cultural

-42-
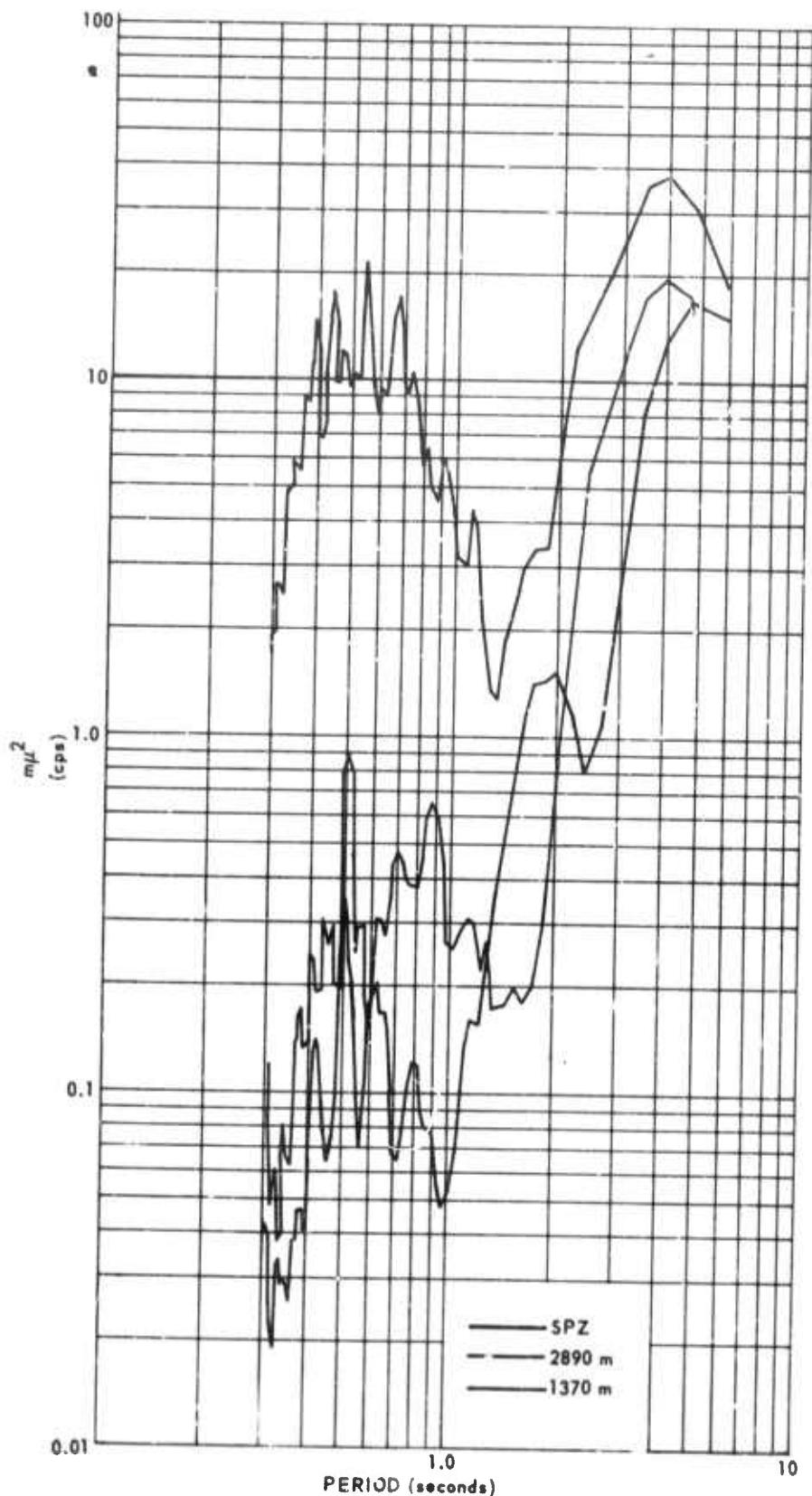
Figure 20. Spectra of the noise at the surface, and at 1370 and 2890 m,
GV-TX. 180 sec sample, 25 samples/sec, 8 percent lags G 2225

-43-

TR 67-3
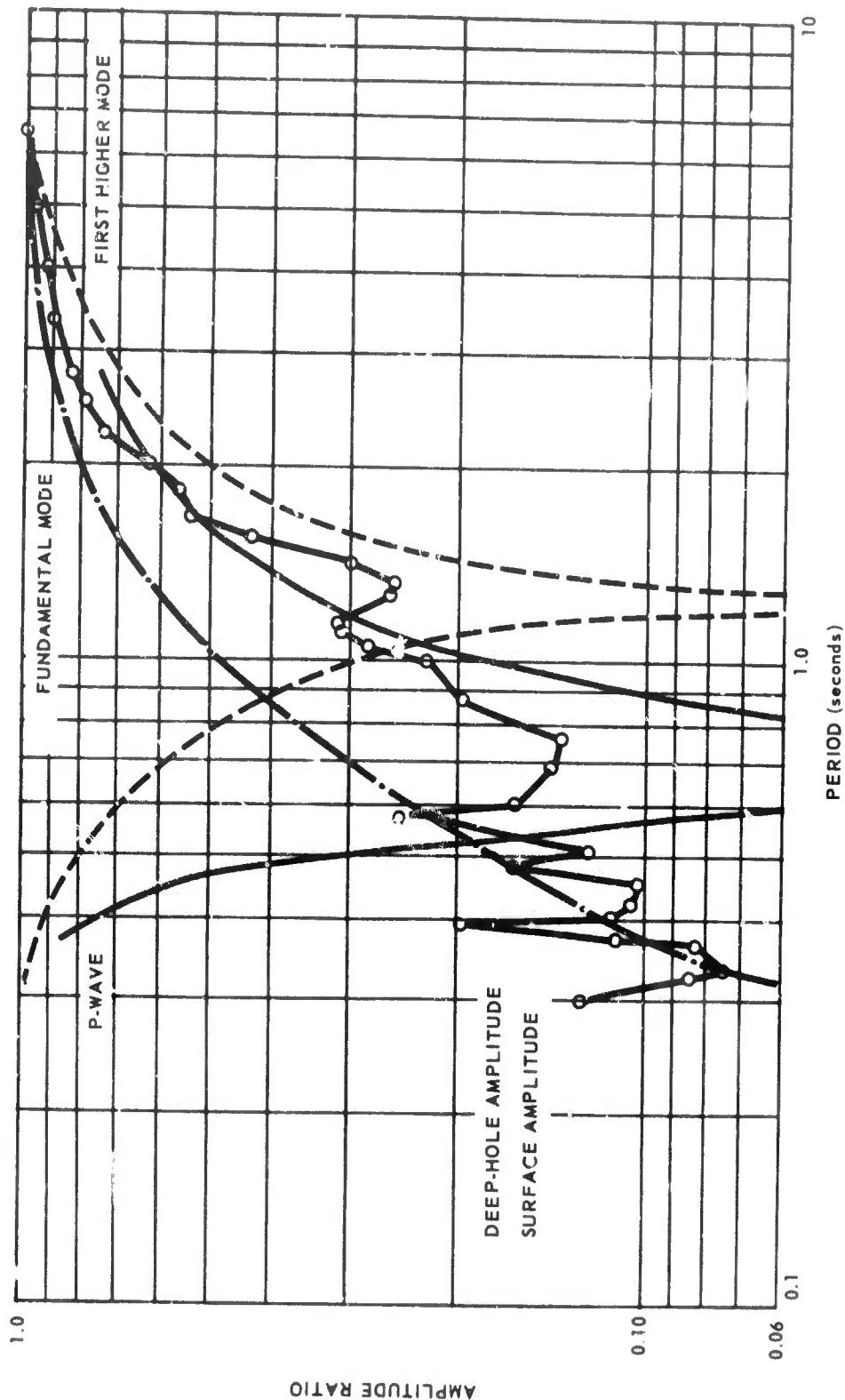
Figure 21. Amplitude ratio of deep-hole noise amplitude to surface noise amplitude as a function of period. Also shown are the theoretical fundamental and first higher Rayleigh modes and the theoretical P-wave amplitudes. Depth 668 m, GV-TX

G 2226

-44-
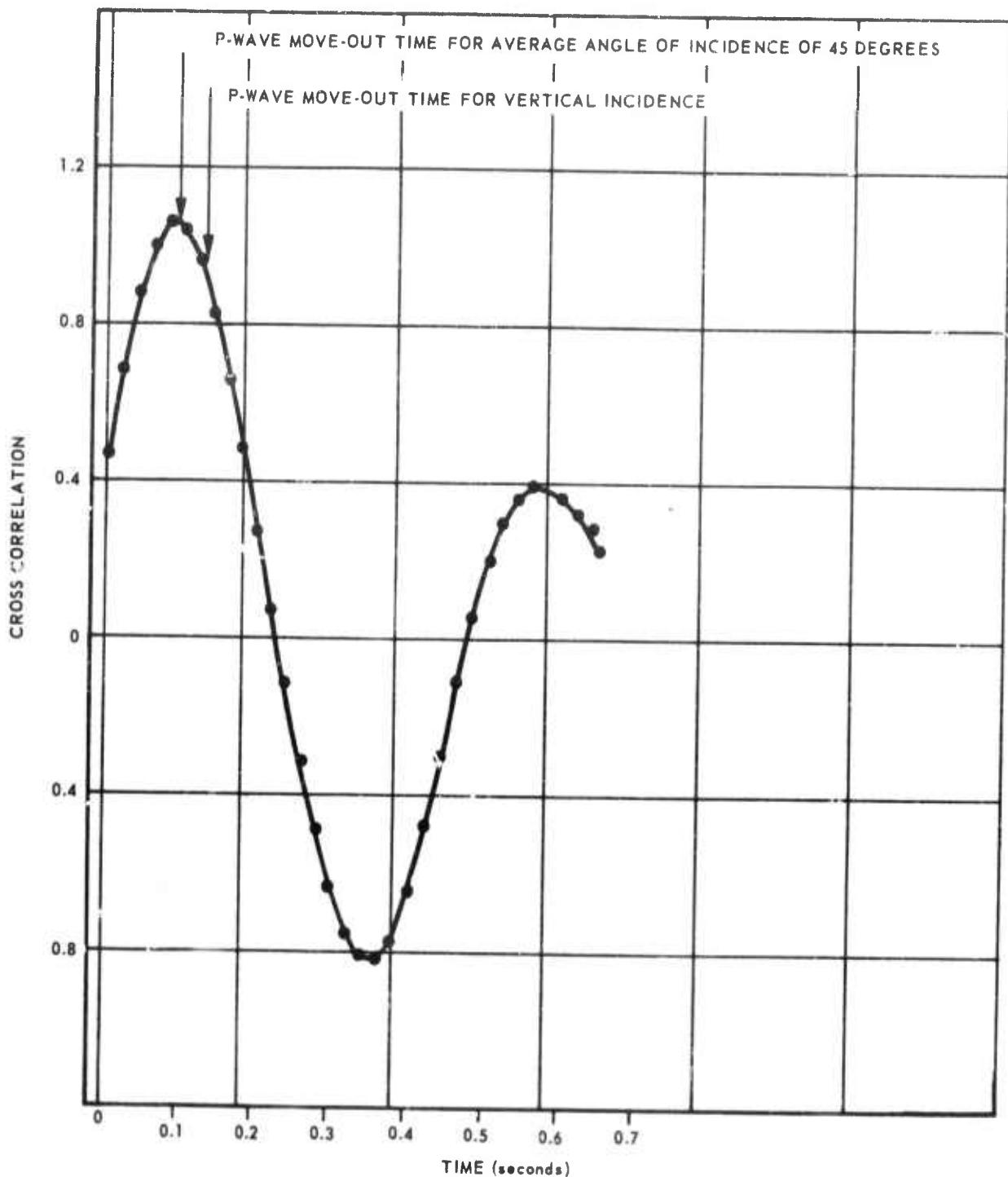
Figure 22.   Cross-correlation between seismometers at depths of
2890 and 2570 m at GV-TX

G 2227

-45-
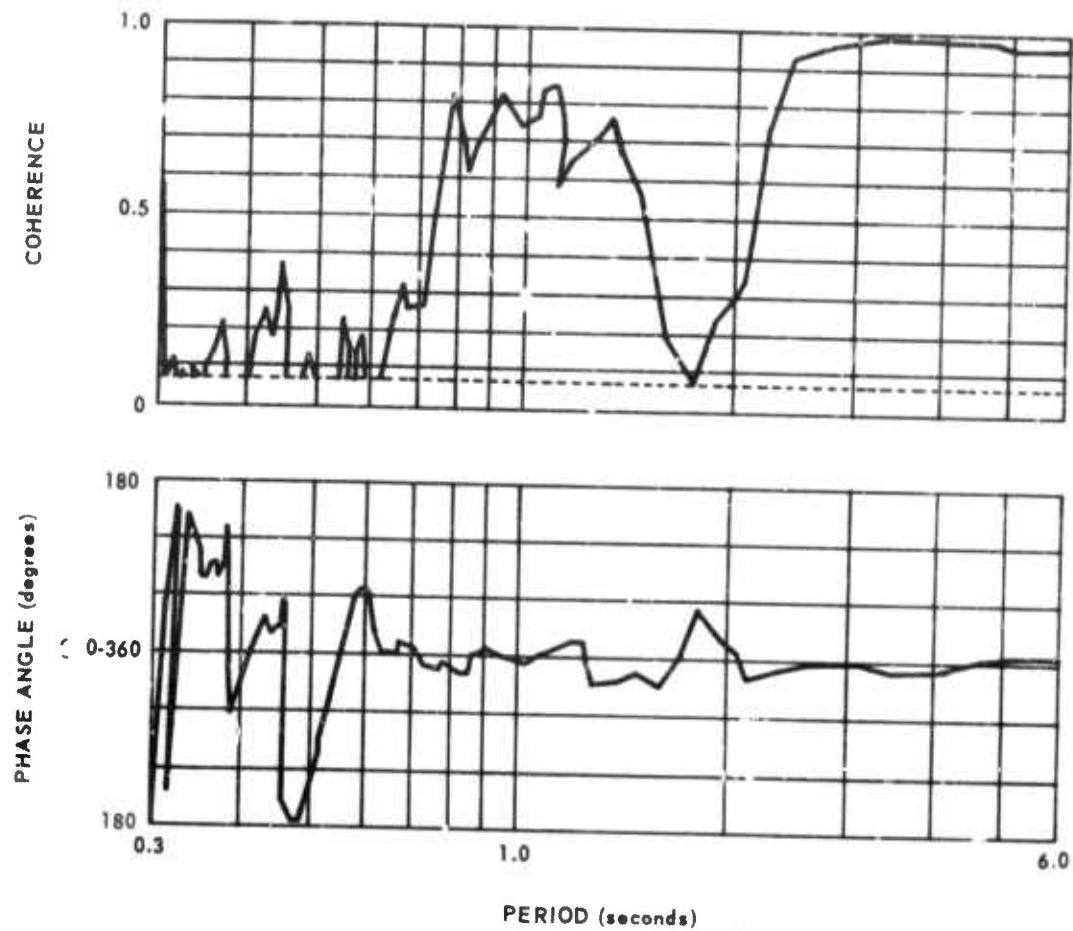
Figure 23. Coherence and phase angle of noise samples from
seismometers at depths of 1980 and 1370 m, GV-TX.
180 sec sample, 25 samples/sec, 8 percent lags

G 673

-46-

noise at the surface; however, at depth it was always clearly visible in the spectra.

In discussing the 0.49 sec peak, the data will be used from AP-OK, FO-TX, and WMSO, where the peak is very prominent.

In a previous publication (Douze, 1964), the 0.49 sec noise was attributed to the presence of the third higher Rayleigh mode. Figure 24 shows the spectra of the noise at the surface, 3048, and 5486 m at FO-TX. The sharp peak at 0.49 sec was still present at the bottom of the hole; comparison with the theoretical amplitude-depth relationships (figure 12) indicates that the third higher mode cannot be the cause of the peak at this period unless the theoretical results are greatly in error. Theoretical investigations indicated that the amplitude-depth relationships can also be explained by P waves arriving at close to vertical incidence. Figure 16 shows the results obtained with a single seismometer in the deep hole and an array of four deep-hole seismometers at AP-OK. The data from the array does not fit either of the theoretical curves closely. The experimental second nodal point appears to occur at a shallower depth than indicated by either theory suggesting the presence of an even higher Rayleigh mode. However, the amplitude-depth relationships of the Rayleigh modes depend on the assumptions made on the velocity section below the hole, and the third mode could probably be made to fit by changing the velocities. It must be noted that the P-wave theory does not depend on the velocity section below the hole.

Surface and body waves can, in theory, be identified by their phase velocities. The phase velocity of the 0.49 sec noise is approximately 3.0 km/sec as measured by WMSO personnel (personal communication, George Gray). Figure 25 shows the cross spectrum between seismometers 1 km apart at the observatory. In general, the noise is isotropic as indicated by the tendency of the phase angle to remain at either 0 or 180 deg. If the 0.49 sec noise is assumed to be isotropic, the coherence (0.29) and the theoretical results (formulas (11) and (12)) indicate that the phase velocity is 3.2 km/sec. This velocity indicated that the noise consists of surface waves.

However, several features of the experimental data are difficult to explain by the presence of one higher Rayleigh mode alone. Despite numerous attempts to locate a seismometer at a nodal point, no such depth could be found. The presence of mixture of wave types could explain this behavior. High resolution spectra often indicate the presence of another peak at approximately 0.51 sec period. If these two adjacent peaks were caused by different wave types, the results from spectral analysis can be expected to be inconclusive because of lack of resolution.

The coherences (see figure 16) gave values that would be expected if the 0.49 sec peak had very high coherence and the noise at the same period apart from the peak was incoherent like the noise at adjacent periods. The

-47-
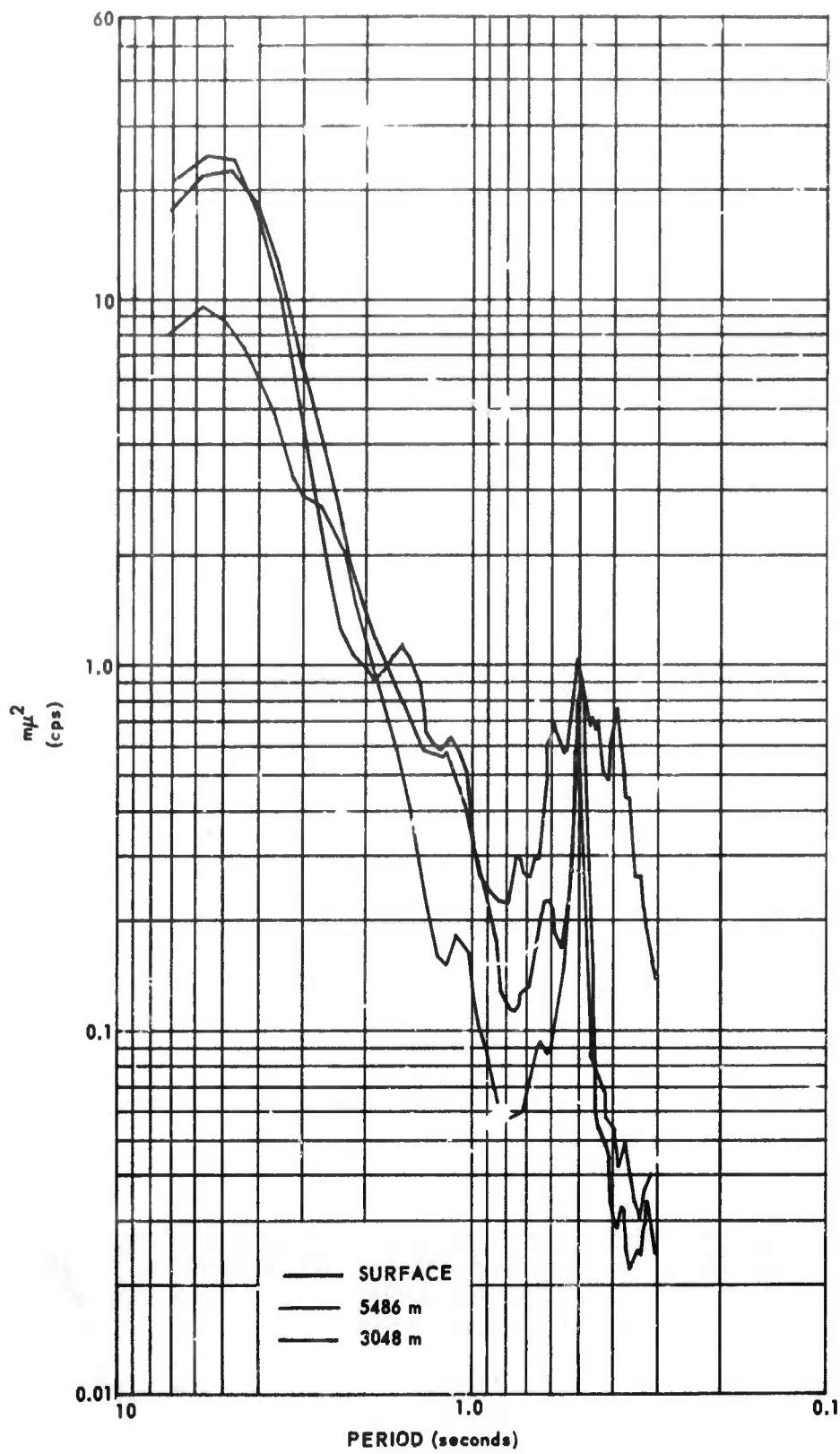
Figure 24. Spectra of the noise at the surface, and at 3048 and 5486 m, FO-TX, 180 sec sample, 10 samples/sec, 8 percent lags   G 2226

-48-

TR 67-3
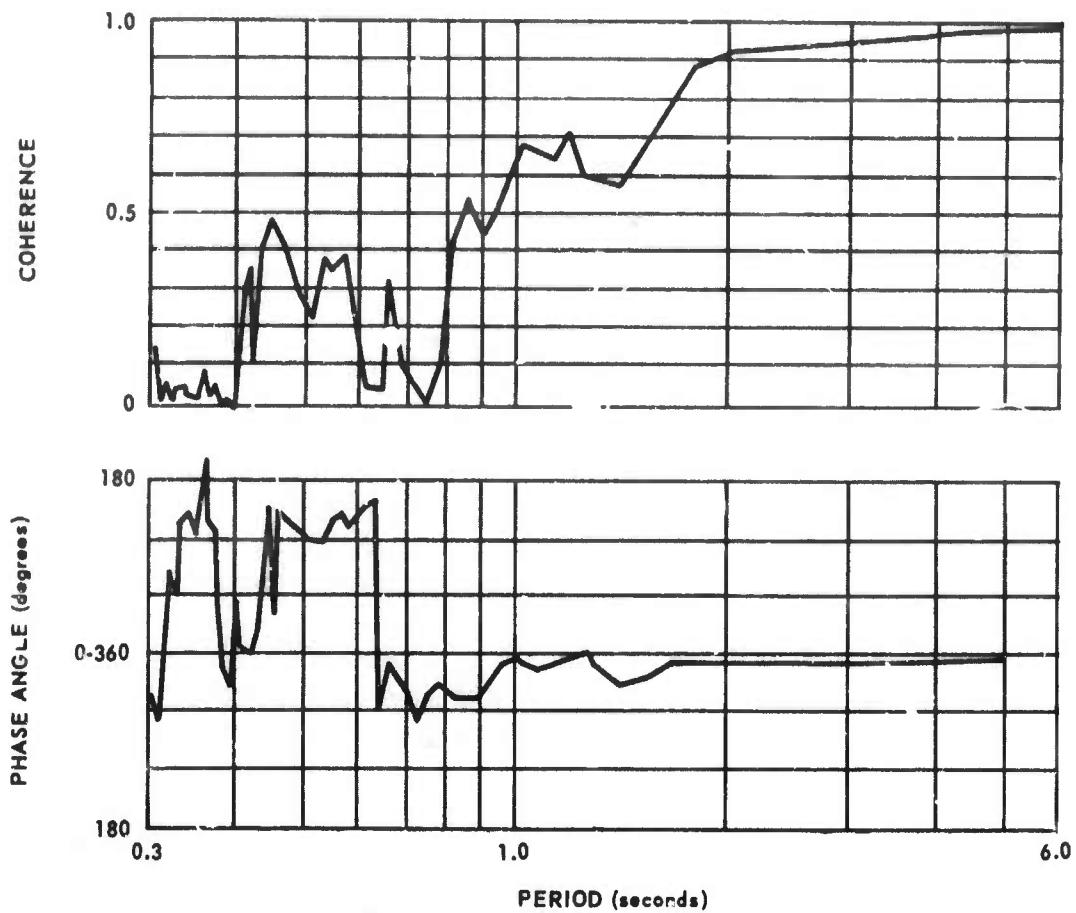
Figure 25. Phase angle and coherence of noise from seismometers 1 km apart, WMSO. 180 sec sample 25 samples/sec 8 percent lags

G 674

-49-

low coherence at 1950 m is typical of results close to theoretical nodal points, indicating the presence of approximately equal power in and out of phase.

In conclusion, the experimental results do not indicate which type of wave is responsible for 0.49 sec noise.

A discussion of the 0.49 sec noise is incomplete without a discussion of the reason for the existence of the sharp peak. Either there exists a very wide-spread source of this peak, or the earth in some fashion acts as a filter. Despite considerable effort, no common surface source has been found that can explain the sharp peak at this period. If the waves are body waves, some subsurface source must be hypothesized; earthquake records show that the earth does not act as a filter which preferentially passes 0.49 sec noise for body waves. If the waves are surface waves, some filtering mechanism presently not understood must exist. It is quite possible that further investigation of this phenomenon will result in some fundamental discovery on wave transmission in the crust.

5.1.4 Conclusions

Some of the waves present in the noise have been identified. The evidence presented shows that, apart from the fundamental mode, the first higher mode is present in the noise at periods around 3.0 sec. Because of the similarity between body waves and surface waves, it could not be established that the first higher Rayleigh mode always predominates at periods between 4.0 and 2.0 sec. However, it has been established that, at sites some distance from the coast, the fundamental Rayleigh mode is not present with appreciable amplitudes.

In the period range of 2.0 to 0.8 sec, the experimental data were not conclusive. The amplitude-depth relationships can be explained by either a mixture of higher modes or by a predominance of P waves. Both cross-correlations and coherences across surface arrays indicated that surface waves are the preferred interpretation.

In the period range of 0.8 to 0.3 sec, the cultural noise has been shown to consist principally of fundamental mode Rayleigh waves. At depths where the fundamental mode has decreased to negligible values, the remainder of the noise consists of random body waves. The sharp peak commonly present at 0.49 sec consists of Rayleigh mode or modes of order higher than third or of body waves.

5.1.5 Deep-Hole Horizontal Seismograph Noise

The theoretical amplitude-depth relationships for Love waves have been computed. In order to obtain accurate results at the higher frequencies, the original computer program was modified. In the original program, a loss of

-50-

accuracy occurred because of the large number of matrices that are multiplied together. This accuracy was improved by changing the mathematical development so that fewer matrix multiplications need to be carried out.

Table 4 gives the velocity section used in the computations; the velocities and densities in the hole are known (except for the S-velocity) from well-logs. Below the depth of the hole a reasonable estimate of the velocities in the crust was used. Figures 26 and 27 show the amplitude-depth relationships of the first three Love modes at periods of 1.0 and 3.0 sec. Because only small changes of velocity exist in the section, no large amplitudes occur at depth. The only surprising feature is the increase of amplitude of the fundamental Love mode at 1.0 sec in the first 1.5 km. No explanation is available for this behavior.

Table 4. Model parameters (AP-OK)

Layer thickness	P-velocity	S-velocity	Density
1.09400	6.10000	3.39000	2.70000
0.13700	5.64000	3.30000	2.60000
0.12200	4.70000	2.76000	2.60000
0.03900	5.55000	3.26000	2.60000
0.04600	5.09000	2.99000	2.80000
0.21600	5.55000	3.26000	2.60000
0.08000	4.70000	2.76000	2.60000
0.12200	5.55000	3.36000	2.60000
0.07600	5.10000	2.99000	2.60000
0.56400	5.55000	3.26000	2.80000
0.03000	5.10000	2.99000	2.80000
5.00000	6.00000	3.51000	2.80000
6.00000	6.20000	3.63000	2.80000
4.00000	6.50000	3.80000	2.80000
3.00000	6.60000	3.88000	2.80000
7.00000	7.24000	4.25000	2.80000
0.00000	8.20000	4.65000	3.30000

Figure 28 shows the spectrum of the noise of the horizontal directed north at the surface, and figure 29, shows the ratio of the deep-hole (2880 m) horizontal divided by the surface horizontal. Both triaxial-seismometer outputs were coordinate-transformed to produce horizontal information in the N-S and E-W directions. The necessary angles of rotation were obtained by measuring the angles between the recorded amplitudes of a large teleseism and the known direction of approach. This one example does not allow any valid interpretations to be made; however, it is noticeable that no
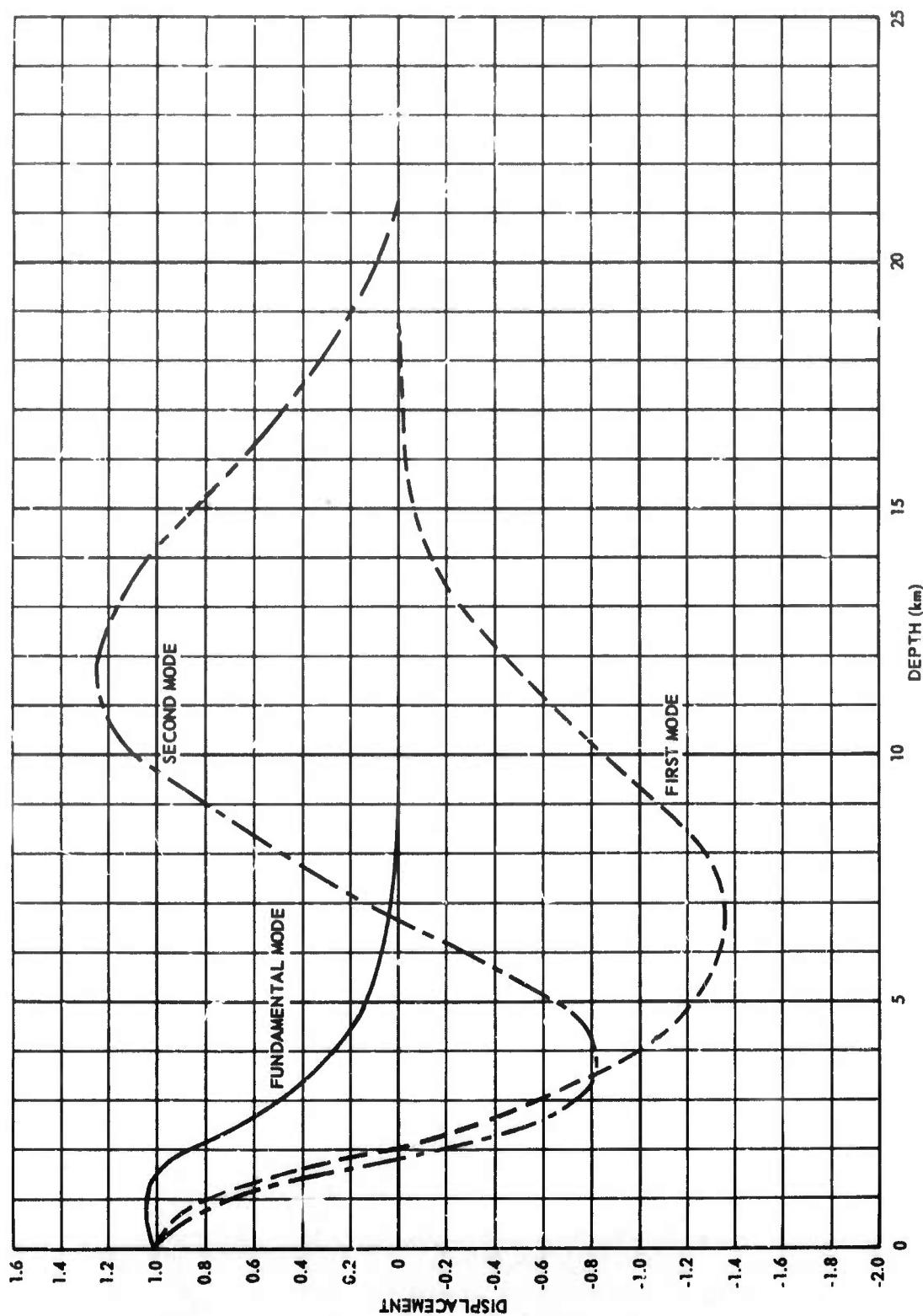
Figure 26. Amplitude-depth relationships of the first three Love modes at a period of 1.0 sec (AP-OK)

G 1874

-52-
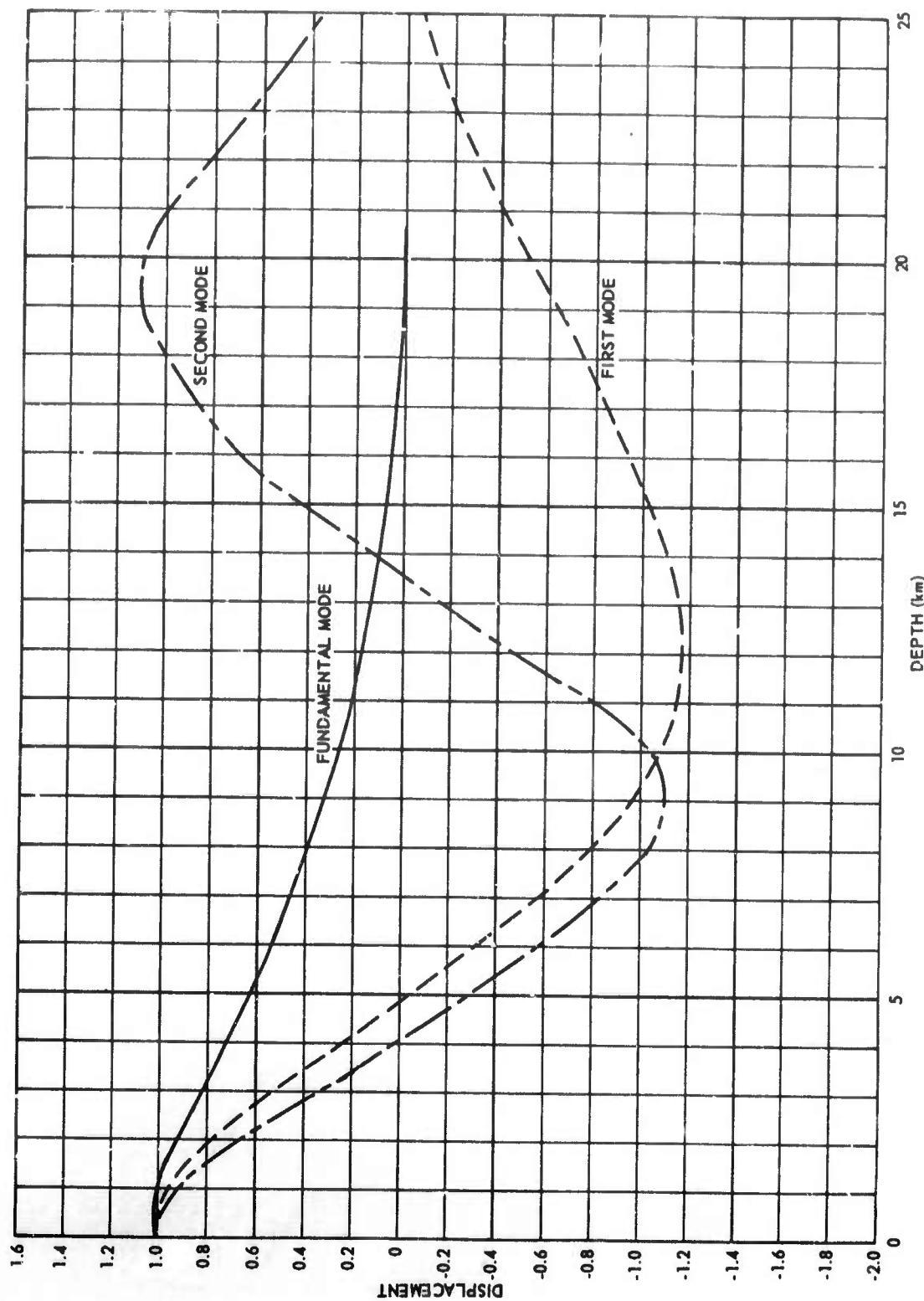
Figure 27. Amplitude-depth relationships of the first three Love modes at a period of 3.0 sec (AP-OK)

-53-
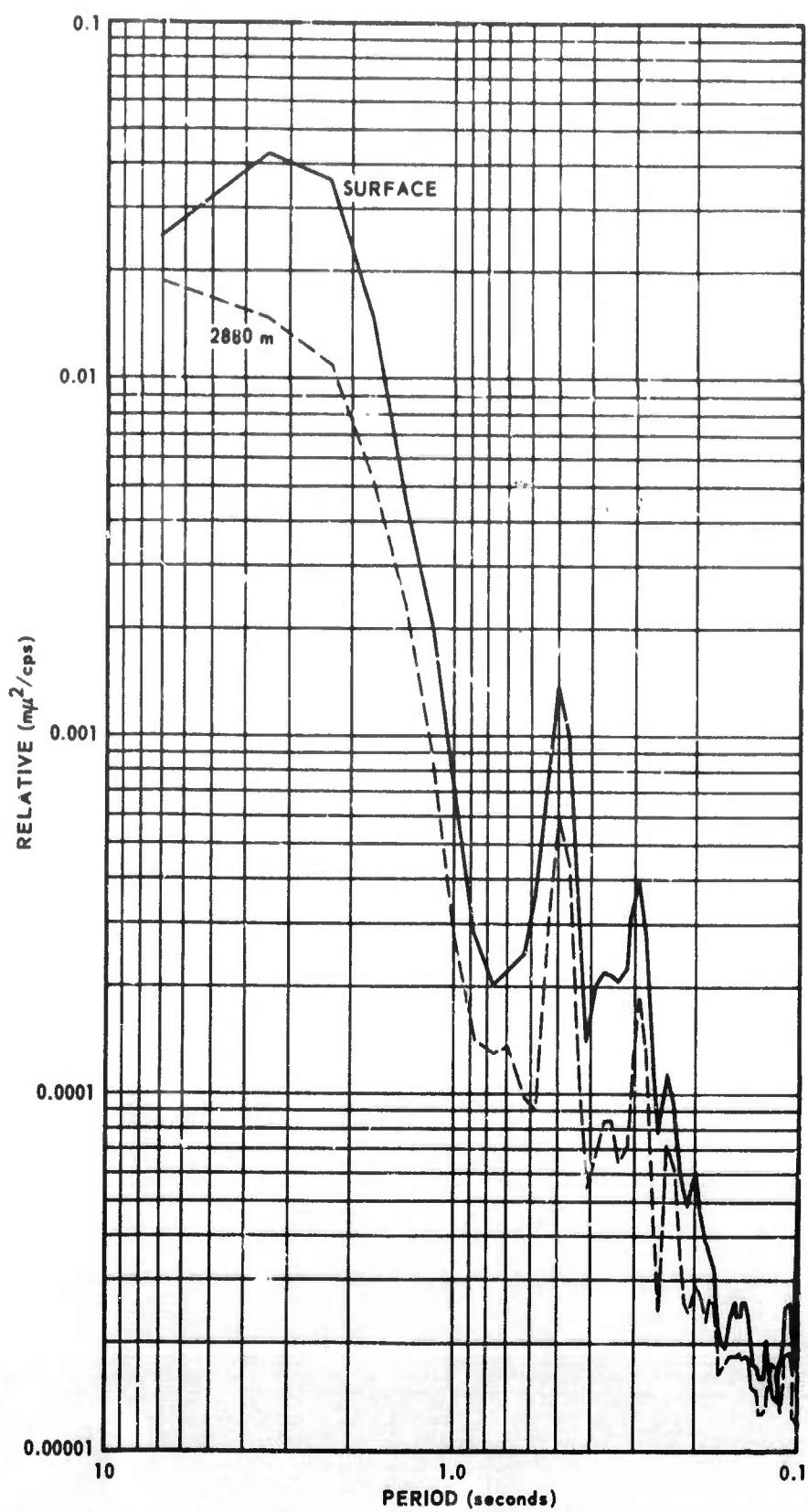
Figure 28. Spectra of the surface and deep-hole horizontal (N component) noise

G 1876

minimum in the ratio denoting a nodal point such as shown by the deep-hole vertical seismographs can be observed.

In order to show that the method used in computing the orientation of the triaxial seismometers gives the correct results, a teleseism was oriented using the same direction cosines as were used for the noise. Figure 30 shows the results obtained; as expected, the radial component detected P-wave motion while the transverse component showed no motion.

5.2 SHORT-PERIOD SEISMIC SIGNALS

Short-period seismic signals were analyzed both visually and digitally. Because the surface-reflected wave interferes with the incoming wave a short time after the first arrival, only the first breaks of large teleseisms were used to obtain visual amplitude measurements.
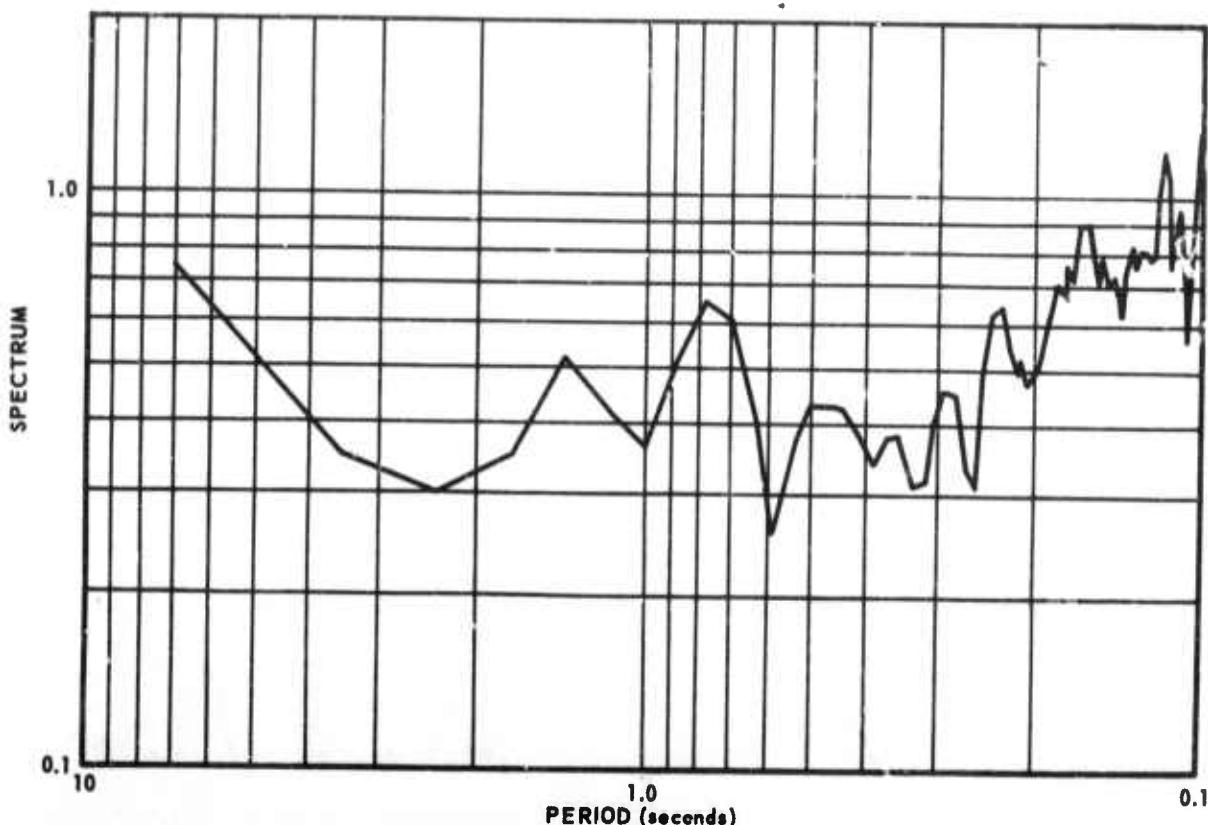
Figure 29. Deep-hole (2800 m) noise spectrum (N component) divided by surface noise spectrum

G 1877

-55-
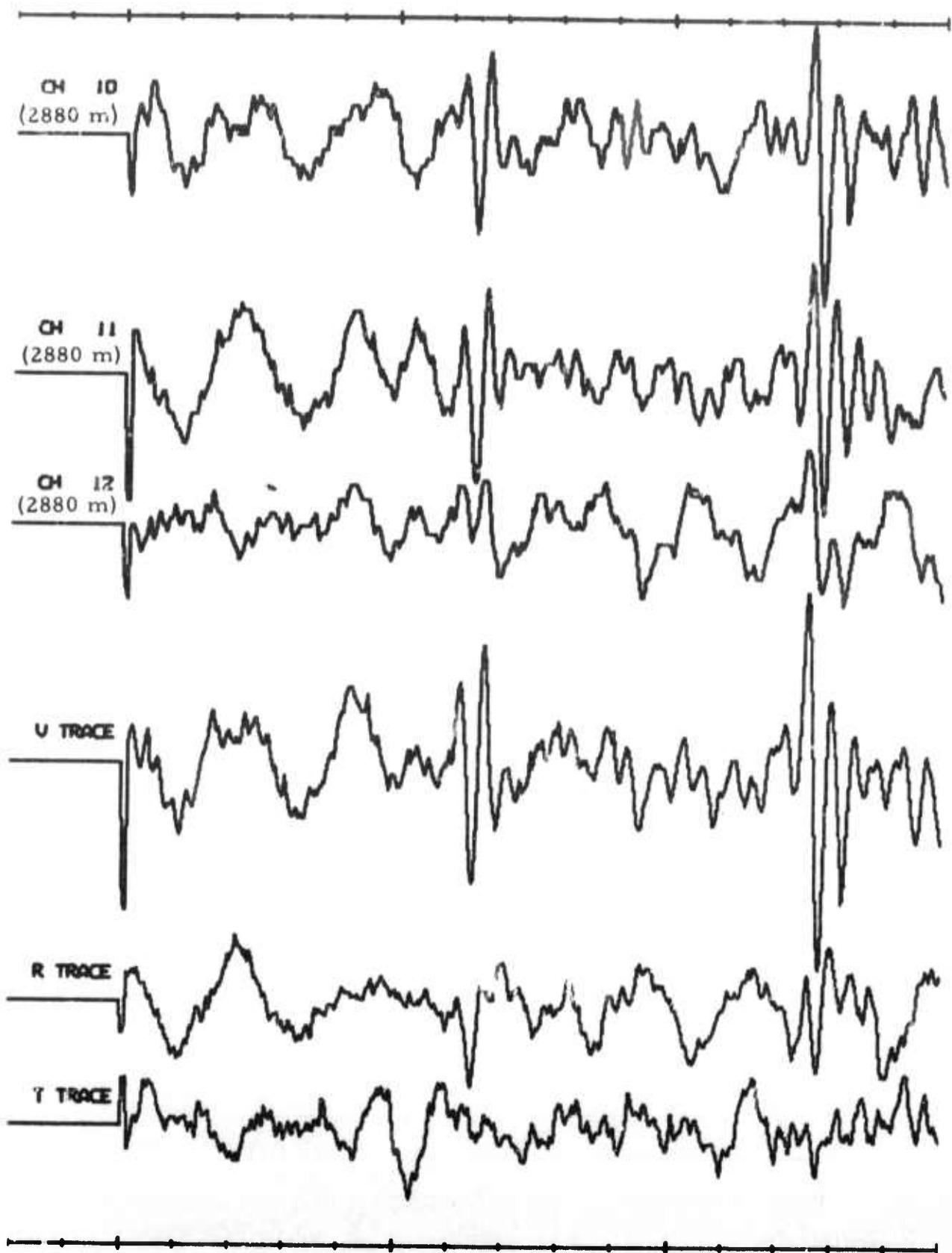
Figure 30. Triaxial and coordinate-transformed teleseismig signal

G 2229

-56-

5.2.1 Visual Measurement

Figure 31 shows the decrease in amplitude, with depth, of the first breaks of teleseismic P-wave signals. As predicted by the theory, the amplitudes at the surface are at least twice as large as at depth; this behavior is caused by the addition of the incoming and reflected waves. At sites where there is only a small change of velocity with depth (for example, AP-OK, FN-WV), the above discussed relationship holds almost exactly. For sites such as PI-WY where the velocity at depth is appreciably greater than at the surface, the amplitudes at depth are less than 0.5 times the surface value. In general, this behavior can be explained in terms of seismic impedance. The energy in an elastic wave is directly proportional to the square of the amplitude and inversely proportional to the velocity. Thus, a wave traveling up the hole through lower-velocity layers will increase in amplitude. This simple explanation ignores the reflections and refractions caused by the layering; however, it does explain the results obtained. For more detailed examination of the behavior, it is necessary to examine the behavior of the waves in the frequency domain.

Visual analysis of shear waves was attempted; however, the results obtained were not very meaningful when only vertical seismographs were being used.

Measured velocities were close to those expected if a Poisson's Ratio between 0.27 and 3.0 was assumed. Amplitude-depth relationship measurements scattered widely, probably because the first breaks could not be measured accurately in the presence of the P waves.

5.2.2 Computer Analysis

At only one site (AP-OK) have the P-wave signals been analyzed in detail in the frequency domain by using digital Fourier transform methods. In general, the results showed that P waves behave exactly as predicted by the theory.

The theoretical behavior of the amplitude-depth relationships in the frequency domain can most easily be calculated by the matrix formulation method (Haskell, 1963) which takes account of all the reflections and refractions and performs the calculations entirely in the frequency domain. For reasons that will become apparent in section 7 (inverse filters), the approach used was different. First the impulse response of the layered media which composes the section of the hole was computed and then the Fourier transform of the impulse response was calculated to obtain the amplitude-depth relationships in the frequency domain.

For vertical angles of incidence, a computer program is available to compute the impulse response; however, for angles of incidence other than the vertical, the computer program would have to be very elaborate. Therefore, computations were carried out on a hand calculator; considering the limited number
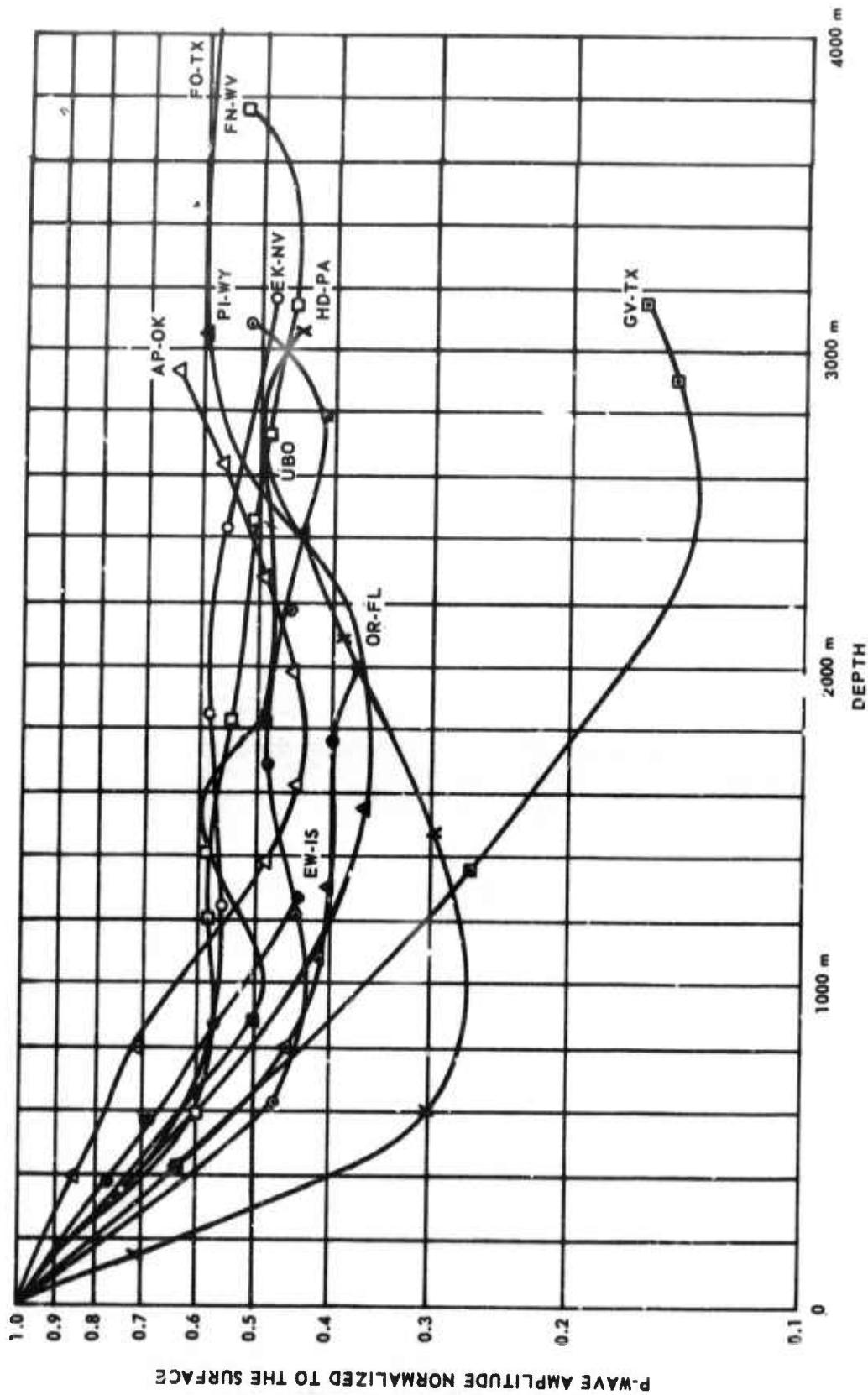
Figure 31. P-wave amplitude decrease with depth obtained from visual measurements of first breaks

G 2230

-58-

of sites which are to be used in the measurement program, this approach is by far the most efficient. The fact that the impulse responses computed in this fashion are correct is demonstrated by the fact that the inverse filters (section 7) computed from them did change the deep-hole signal into the surface signal.

As will be mentioned in section 7, the inverse filters work exactly as intended for only the first few cycles. While no definite conclusions have been reached about the types of waves that are responsible for this behavior, it was found that the amplitude-depth relationships change later in the signal.

To obtain the amplitude-depth relationships discussed above, several signals were analyzed as follows. Overlapping 5 sec segments of the signal were taken at the surface and at depth. The Fourier transform of each segment was calculated and the ratio of deep-hole signal-to-surface signal and the phase angle difference between them were recorded. Each segment was passed through a cosine window before the Fourier transform was taken to minimize the edge effects.

Figure 32 shows the results from two of these segments; the first segment covered the first 5 sec of the signal and the second covered the next 5.0 sec. It is apparent that there is an appreciable difference between them. The amplitude ratio of the first 5.0 sec is in excellent agreement with the theory for incident P waves. The next 5.0 sec is not in agreement indicating the presence of other wave types.

6. TRIAXIAL ARRAY, TASK 1e

The evaluation of deep-hole instruments that was called for in Task 1b resulted in a determination that the existing short-period triaxial seis-mometer (developed under Project VT/072) was inadequate for routine deep-well use. Extensive design modifications were made, resulting in an instrument suitable for field use. TR 66-67 was prepared which described the instrument in detail and the tests performed on it in the laboratory. A complete system, composed of four triaxial seismometers, amplifiers, cables, winches, control equipment, and associated standard equipment was assembled and made ready for field measurement program.

An installation was made at AP-OK and operated in conjunction with the digital recording system discussed in section 8 of this report. Figure 33 shows an outline drawing of the seismometer; figure 34 shows one module of the seismometer; figure 35 shows the array controller designed for the array; and figure 36 shows a block diagram of the system.

-59-
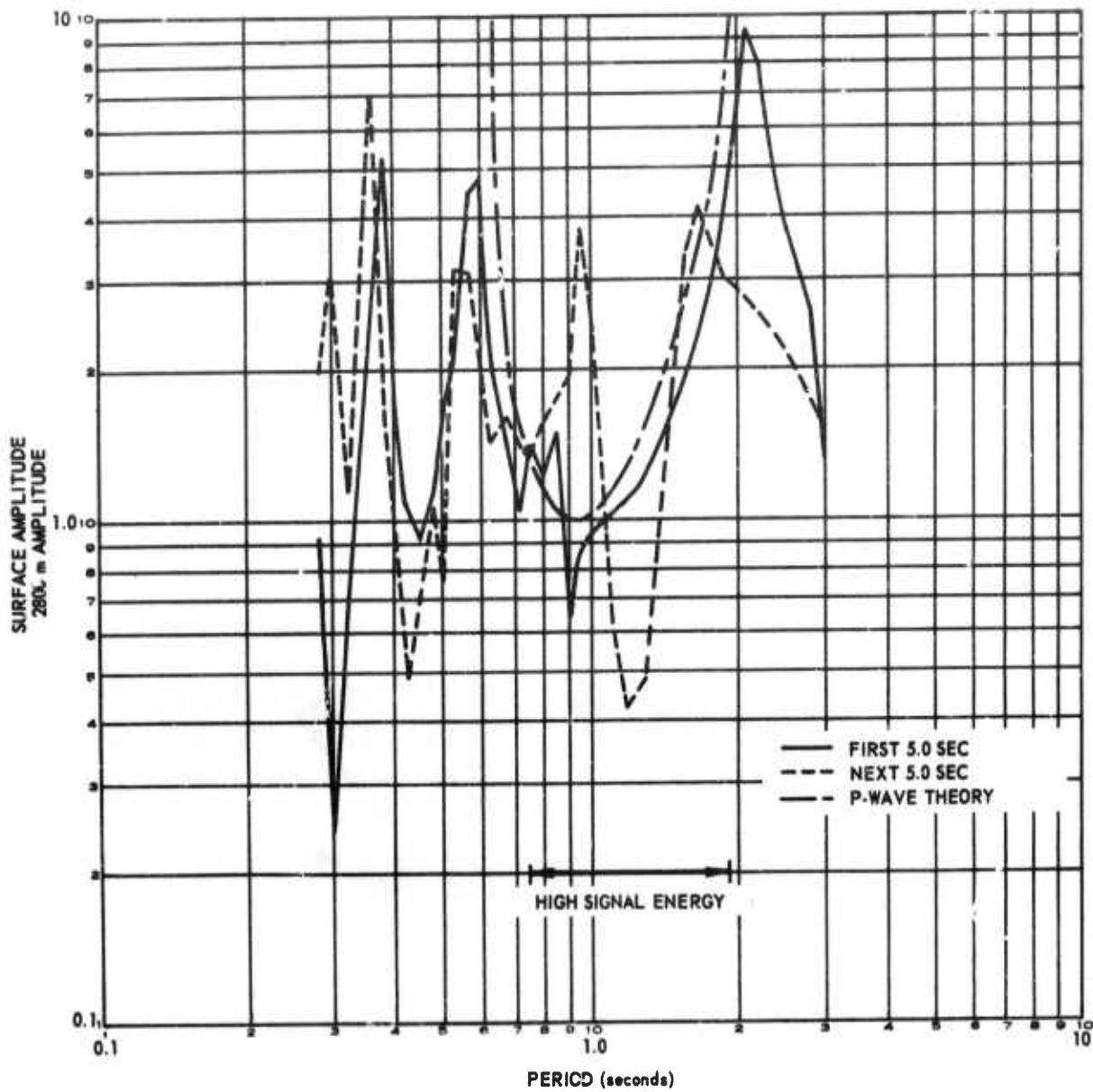
Figure 32. Ratio of surface-divided-by deep-hole amplitude for the first
5.0 sec and the next 5.0 sec of a teleseism from Argentina

G 878

-60-
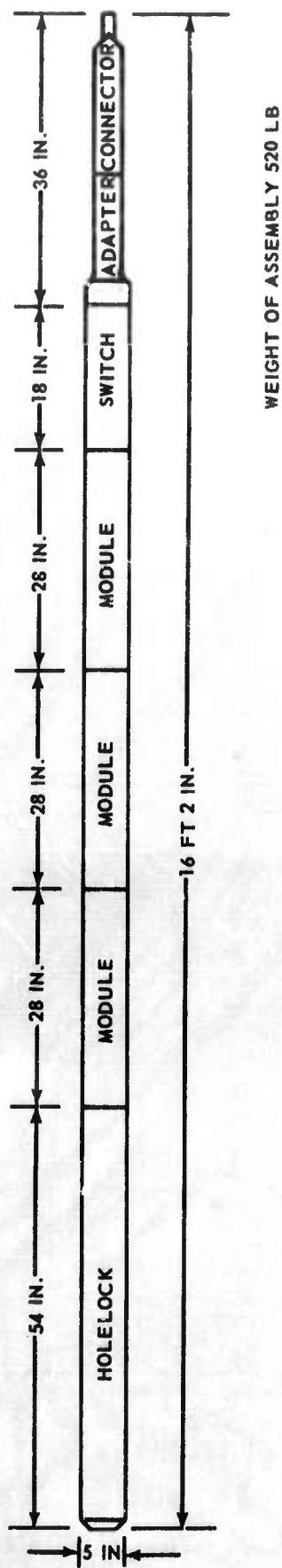
Figure 33. Triaxial seismometer outline drawing

WEIGHT OF ASSEMBLY 520 LB

TR 67-3

G 1347
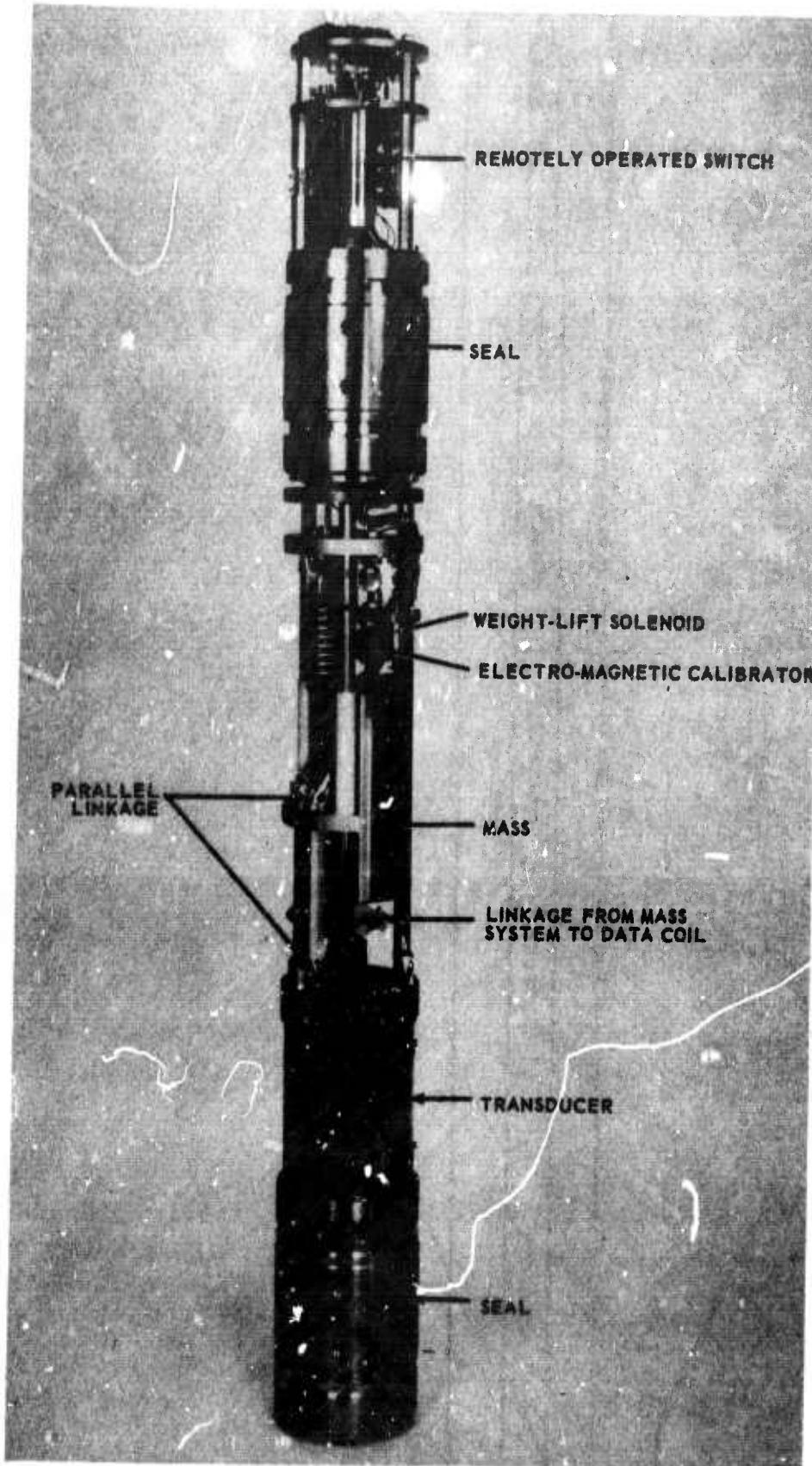
Figure 34.   Triaxial seismometer module and switch

G 1348
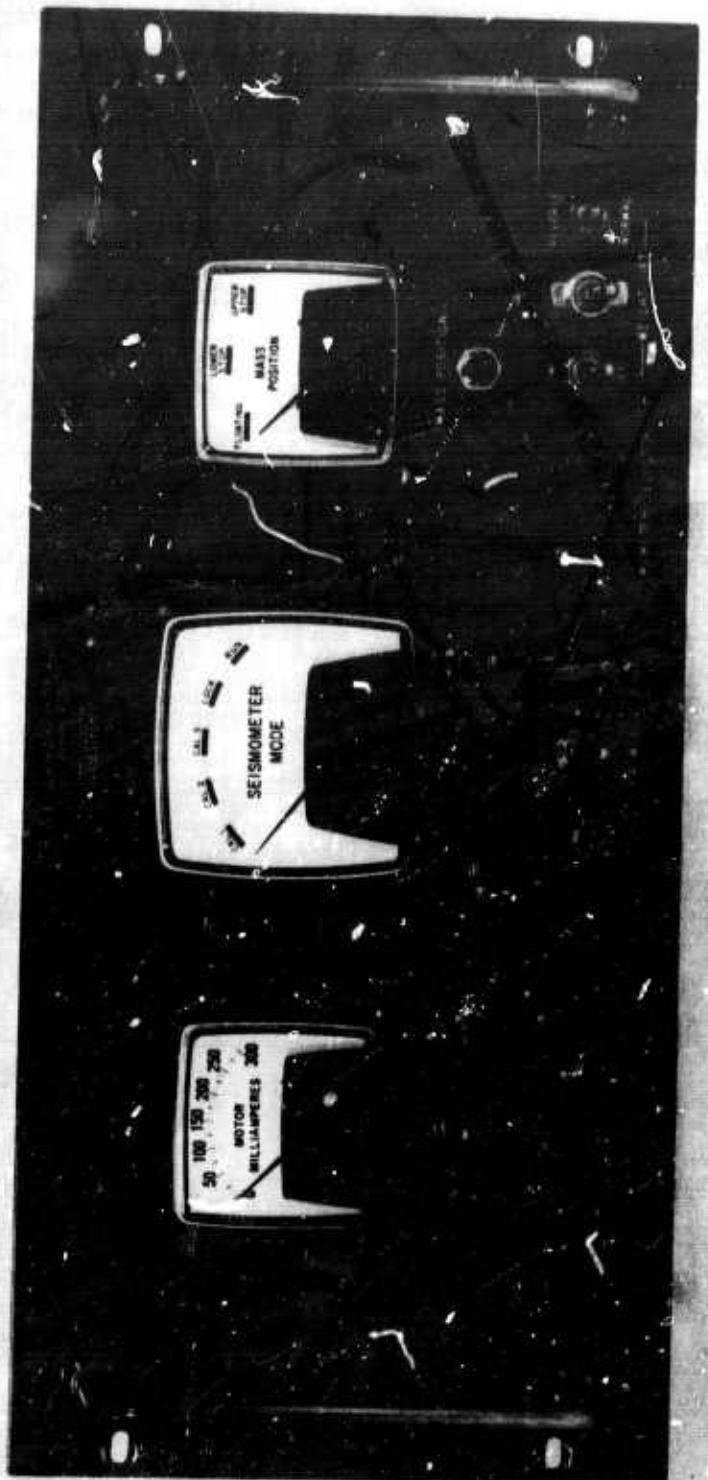
Figure 35. Triaxial array controller G 2231

-63-
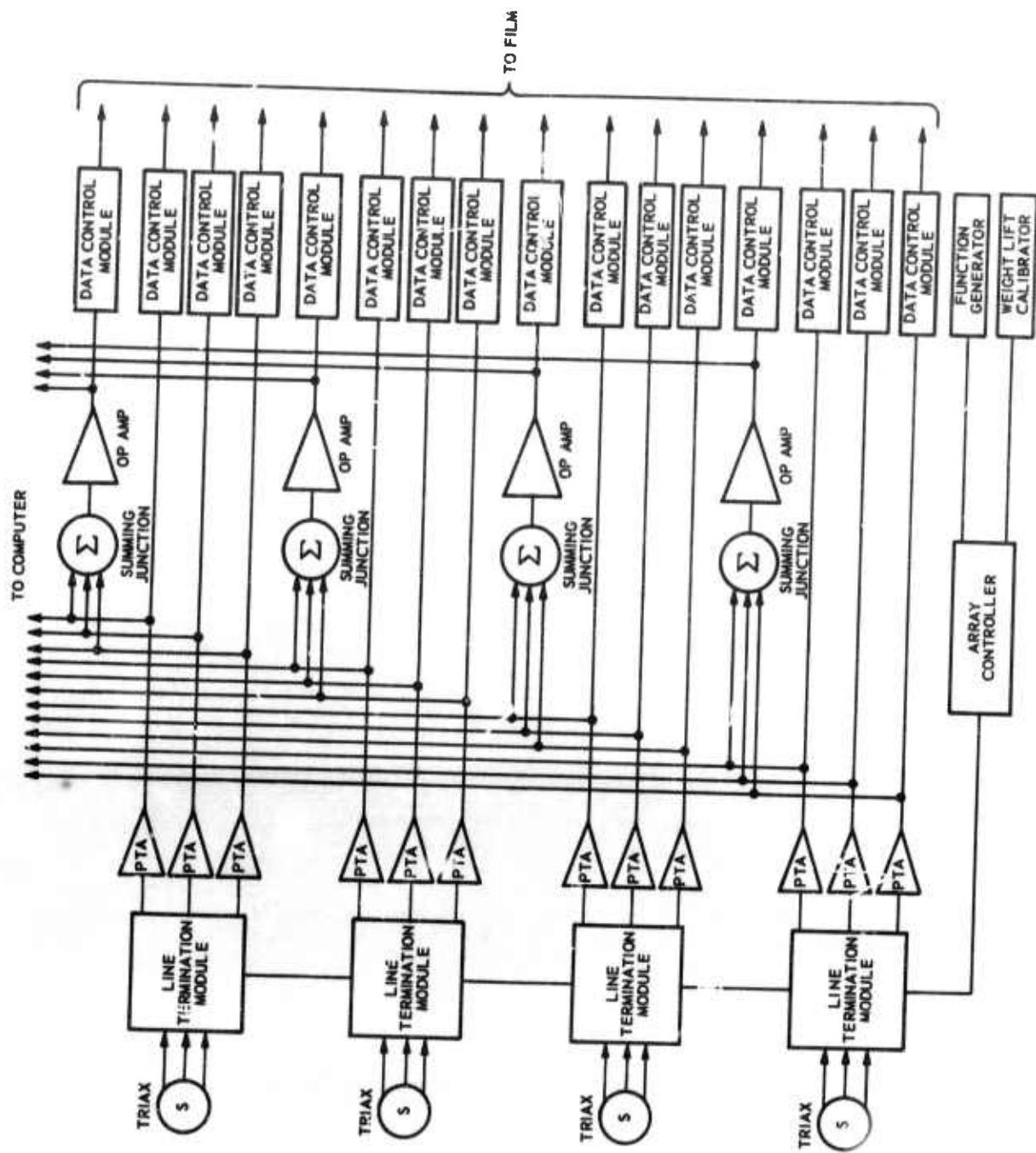
Figure 36. Simplified block diagram of triaxial array system

G 2232

TR 67-3

Figure 37 shows a comparison of background noise recorded at the Grapevine Test Site. Comparisons of the coordinate-transformed output of the triaxial system with the output of the 18300 systems show excellent correlation. In addition to the coordinate-transformed Z output, a direct summation Z is also shown. The correlation, again, is excellent.

7. CONTINUE TO DEVELOP TECHNIQUES, TASK 1f (1)

7.1 INVERSE DIGITAL FILTERS

In processing an array of deep-hole seismographs, two general approaches can be employed: (a) the processes such as optimum Wiener filtering with assumptions about the signals, in which case the signals do not need to be changed, or (b) processes such as maximum likelihood filters or the techniques shown in figures 38 and 39 in which case the signals must be inverse filtered. The simplest approach is to filter the deep-hole signals in such a way as to make them look like the surface signal; however, it is also possible to change all the signals to duplicate any of the deep-hole signals. We will call the filters that change a signal recorded at one depth to the signal at some other depth inverse filters.

The filters that are needed can be expressed as rational functions of Z, where the Z-transform (Jury, 1964) method is employed.

The most general digital inverse filter is given by:

$$F(z) = \frac{A(z)}{B(z)} = \frac{a_0 + a_1 z^{-1} + a_2 z^{-2} + \ldots + a_n z^{-n}}{b_0 + b_1 z^{-1} + b_2 z^{-2} + \ldots + b_m z^{-m}}$$

By rewriting the formula as $B(z) \cdot F(z) = A(z)$, it is apparent that $F(z)$ is the filter that changes the time series $B(z)$ into the time series $A(z)$. In terms of inverse filtering as applied to deep-hole signals, the filter should change the signal recorded at one depth to that recorded at another depth. The time series $A(z)$ and $B(z)$ are the responses that would be recorded at the different depths if the incoming signal were a unit impulse, that is, the impulse response of the layered half space that is taken as model of the section penetrated by the hole.

$F(z)$ can be expanded by long division (Jury, 1964) into a simple polynomial:

$$\frac{A(z)}{B(z)} = f_0 + f_1 z^{-1} + f_2 z^{-2} + \ldots + f_k z^{-k} + \ldots$$

-65-
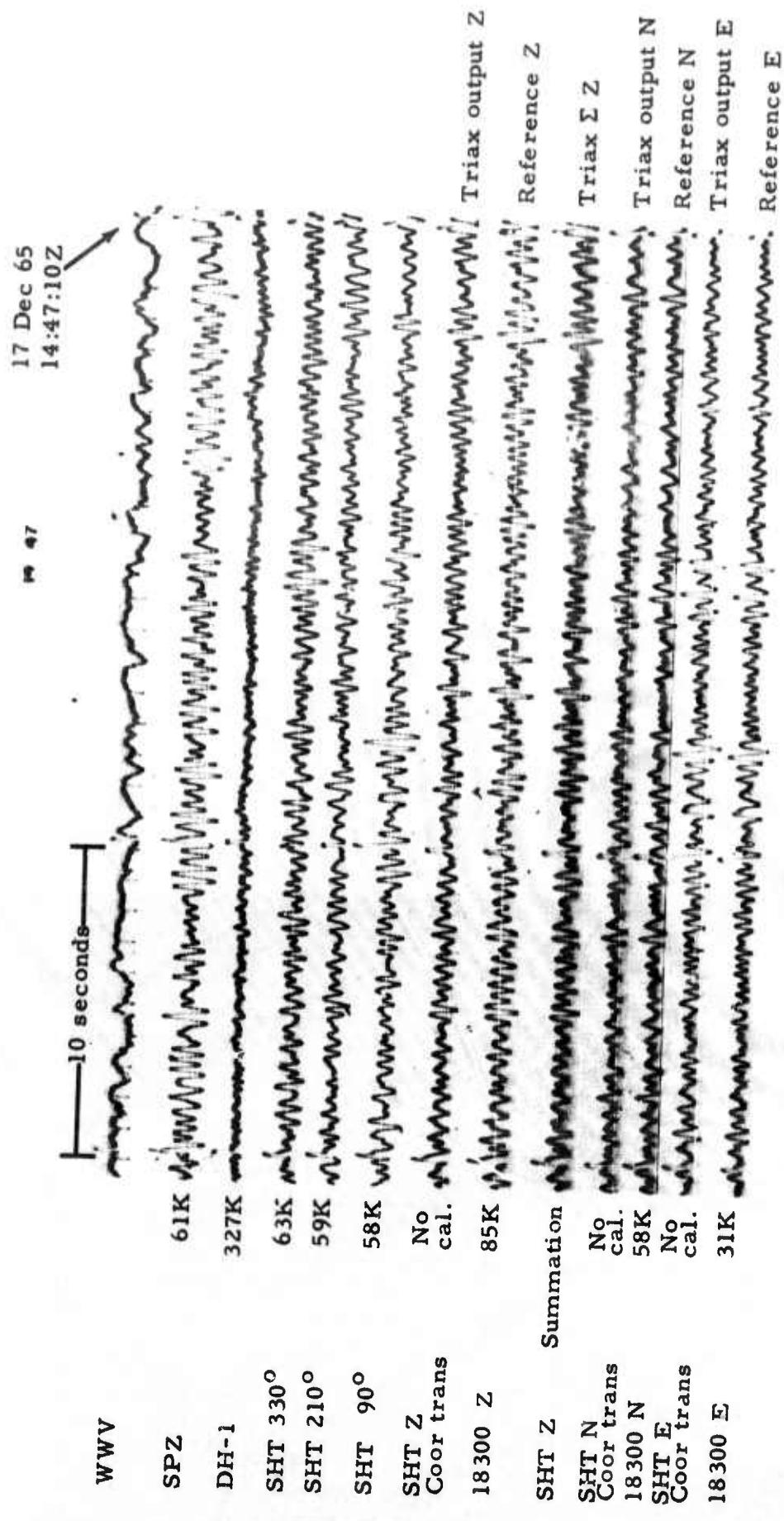
Figure 37. Recording of noise by surface vertical seismograph (SPZ); deep-hole vertical seismograph (DH-1), shallow hole triaxial seismograph (SHT), coordinate transformed triaxial seismograph, and the Model 18300 reference seismograph at Grapevine, Texas. Magnifications at 1 cps (X10 enlargement of 16 mm film). DH-1 at 2901 m.

TR 67-3

-66-

252
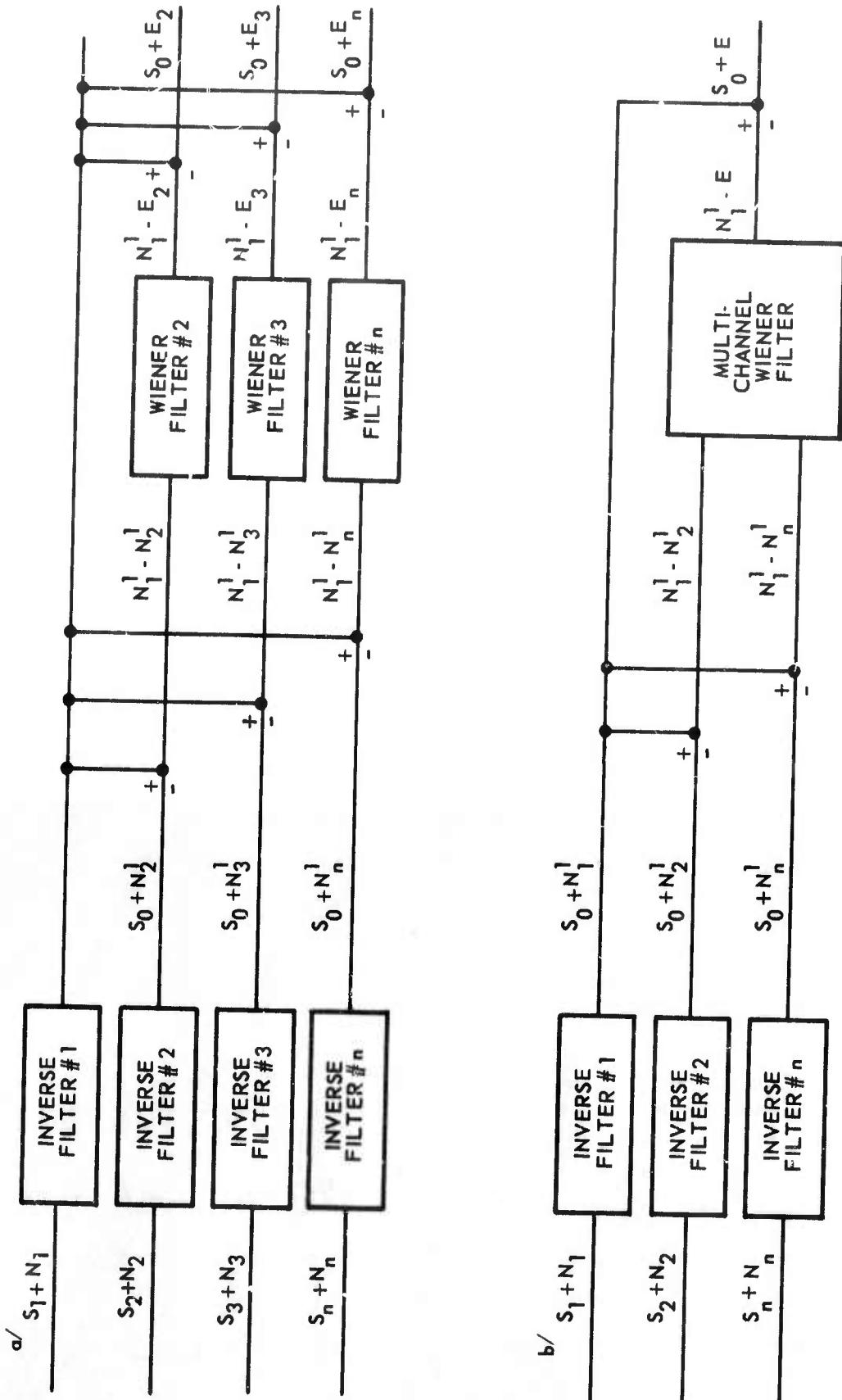
Figure 38. Deep-hole data processing techniques

TR 67-3

G 543A
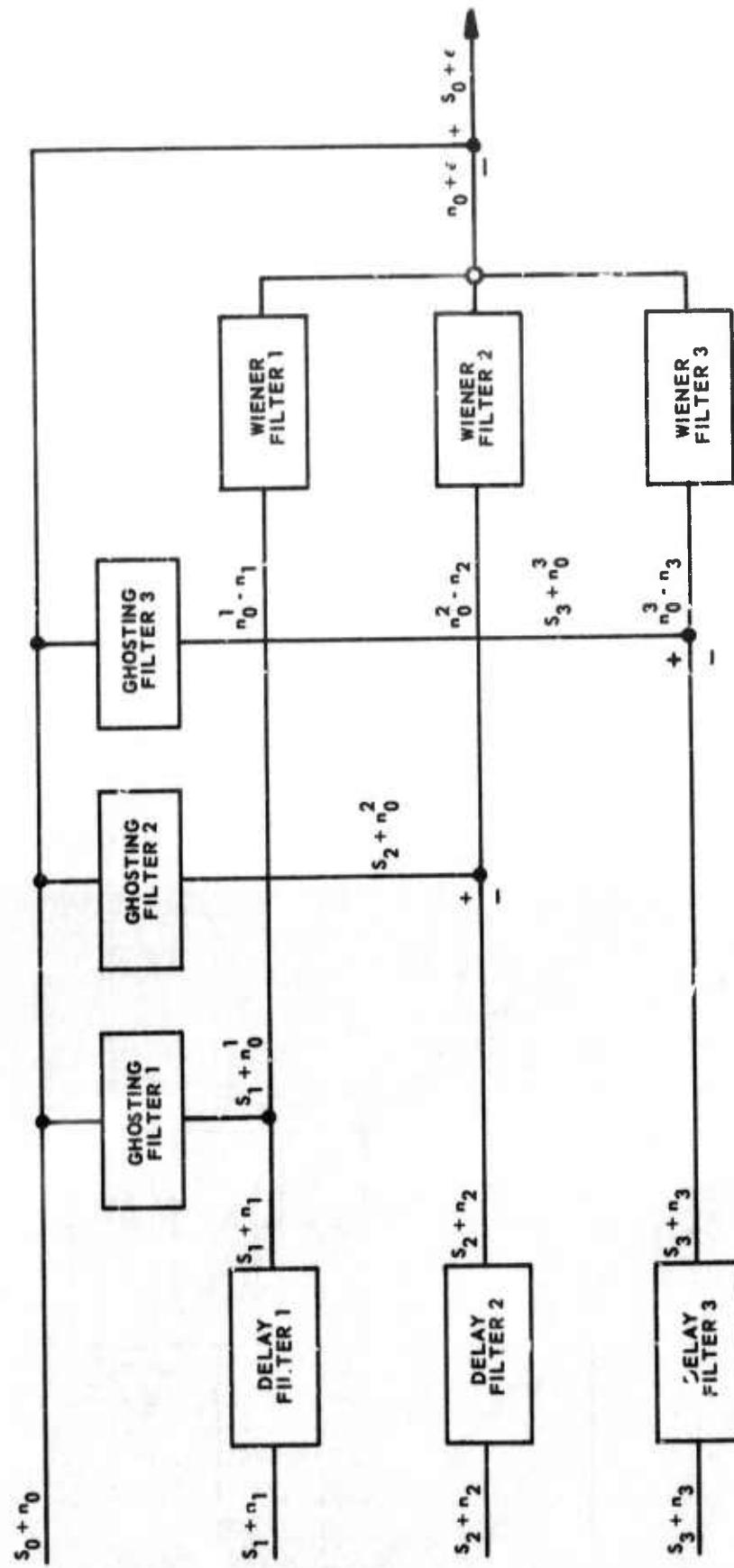
Figure 39. Alternate optimum Wiener process using ghosting filters

G 1245

In general, the expansion of $F(z)$ will result in an infinite series. In the filters used in this work, the deep-hole inverse filters are stable and the coefficients converge to zero; however, they converge only slowly. The series was truncated to a length of 125 points and a cosine taper was applied to smooth the results.

Instead of obtaining an inverse filter by long division and truncation, it is possible to design a one-channel optimum filter of the same length; this approach was also tried. The difference in the results was negligible; therefore, the long division process was employed.

In order to obtain shorter filters that would function more effectively in on-line processing, it was decided to use recursive filters. Consider the following filter, where $X(z)$ is the input and $Y(z)$ is the output:

$$Y(z) = \frac{a_o + a_1 z^{-1} + a_2 z^{-2} + \ldots + a_n z^{-n}}{1 + b_1 z^{-1} + b_2 z^{-2} + \ldots + b_m z^{-m}} \, X(z)$$

where b_o can always be made equal to 1 (unless it is zero) by dividing numerator and denominator by b_o.

By some mathematical rewriting, the formula can be changed into:

$$Y(z) = (a_o + a_1 z^{-1} + \ldots a_n z^{-n}) X(z) - z^{-1} Y(z) (b_1 + b_2 z^{-1} + \ldots + b_m z^{-m + 1})$$

The output $Y(z)$ is thus equal to input convolved by $A(z)$ minus the output delayed one sample interval and convolved with $B(z)$. In case of deep hole processing where the deep-hole signals are usually filtered to approximate the surface signals, it is possible to go one step further and design a filter that uses only the present input and past outputs. This approach is possible in the present case because $A(z)$, the impulse response of the surface seismographs, consist of one large impulse and some very minor reverberations. The desired filter is:

$$F(z) = \frac{A(z)}{B(z)} \approx \frac{1}{C(z)}$$

$C(z)$ can be obtained by synthetic division of $B(z)$ by $A(z)$. Because of the nature of $A(z)$, the result is very nearly $B(z)$ and the length of the filter has

not increased because the values at lags greater than m (the length of B(z))
are extremely small and can be neglected. Thus, the feedback filter presently
being used is:

$$Y(z) = X(z) - z^{-1} \; Y(z) \; (b_1 + b_2 z^{-1} + \; . \; . \; . \; . \; +b_m z^{-m + 1})$$

Figure 40 shows the same signal inverse filtered by the two techniques
discussed. The results are essentially identical for the signal. The noise
appears slightly different; the reason for this behavior is that the feedback
filter is exact while the normal inverse filter is a smoothed approximation.

7.2 Optimum Filtering Techniques

A large variety of optimum filtering techniques can be employed to operate
on the data provided by a vertical array of seismometers. Not all the
processes that will be tried are finished at this time.

The derivation of the Wiener optimum-filter equation has been reported in
numerious publications (for example, Burg, 1964) and will not be discussed
here. Discussions of optimum filtering in this report will be confined to the
Wiener least mean-square technique discussed by Burg (1964).

The most obvious approach is to employ conventional optimum filtering
where the signal model is chosen to conform with the behavior at depth of
teleseismic signals. The noise correlation matrix would be obtained from
actual recordings while the signal would assume to be white over the period
range of interest. The cross-correlation between signal and signal + noise
would assume the signal to be uncorrelated with the noise, and the desired
signal would be taken as the surface; the cross-correlation used would then
be the correlation between the signal at the surface and the signal at the
depths at which the different seismographs are operated. This approach
should be tried in order to compare the results with those obtained from
other techniques. The techniques that have been used to date are shown in
figures 38 and 39. These processing schemes are based on the concept that
elimination of the assumptions made about the signal in conventional optimum
filtering would result in a more effective processor. Whether this concept is
valid cannot be determined until the conventional optimum-filtering techniques
have been tried. Figure 38 shows the filtering technique used in the first
attempts to improve the detection capability of the site. As shown by the
schematic, the signals are first equalized by the inverse filters discussed
in section 6. After inverse filtering, each deep-hole channel is subtracted
from the reference channel to produce a trace that consists only of noise.
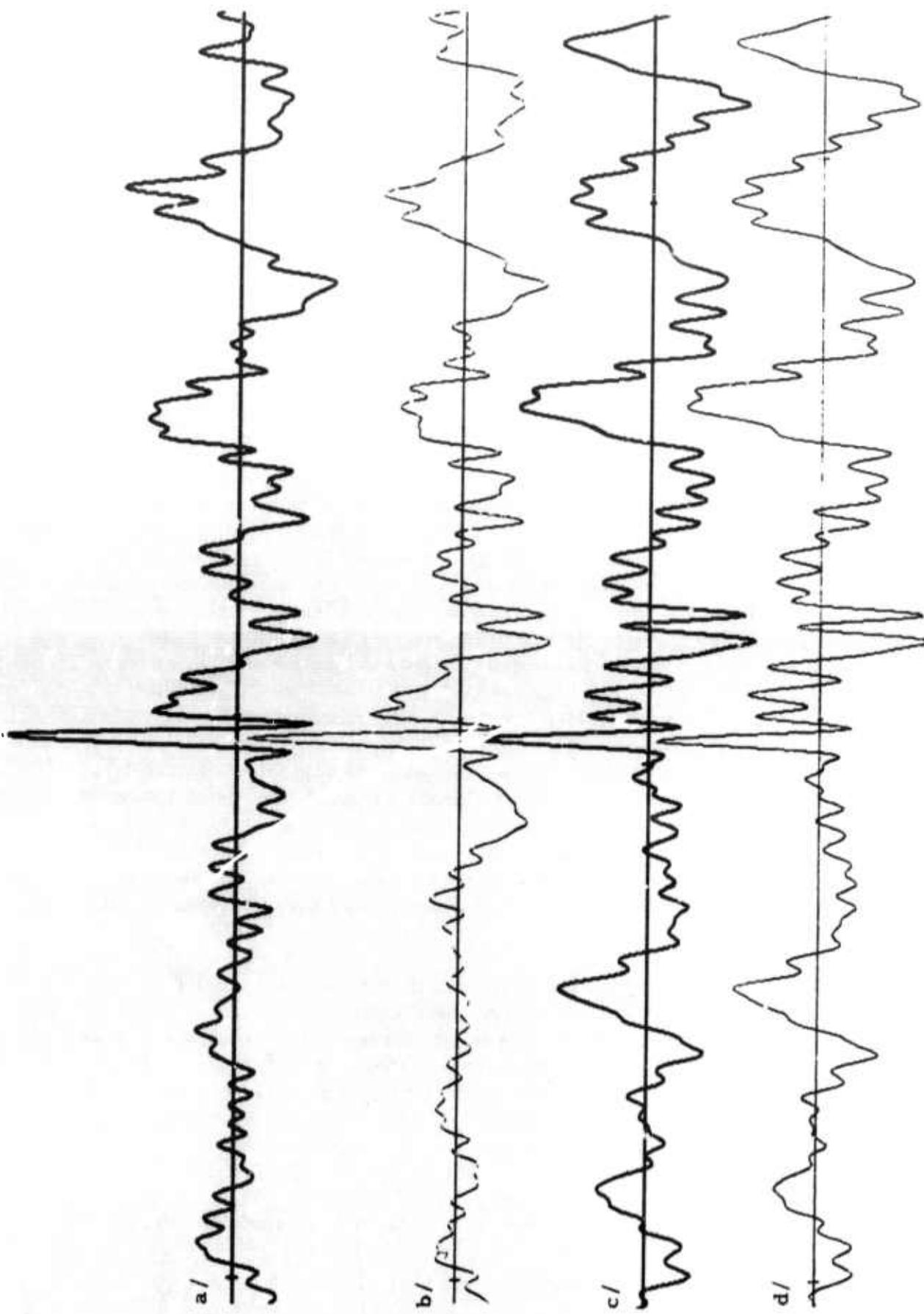
Figure 40. Teleseismic signal as recorded on a/ the surface, b/ through single-channel optimum filter using deep-hole 1, c/ inverse filtered deep-hole 1, d / recursive inverse filtered deep-hole 1

G 2233

-71-

Although the surface channel has been used as a reference channel throughout the present analysis, any channel can be used as a reference. In fact, at sites where there is an appreciable increase of signal-to-noise ratio with depth (which is not the case at AP-OK), the surface must not be used as a reference because it would introduce excessive amounts of noise into the process.

An optimum filter was then constructed where the desired signal is the noise at the surface and the actual noise recorded in the deep hole is to be suppressed. It must be noted that the usual assumption of that desired signal (surface noise) and noise are uncorrelated is not correct; the optimum filters are designed from actual data (including correlation of signal and noise) and no assumptions about the signal are made. The output of optimum filters is then subtracted from the surface to obtain the actual signals. As shown in figure a and b the process can use either multi- or single-channel optimum filters.

Figures 41, 42, 43, and 44 show the spectrum of the noise at the surface and the spectra of the three single-channel outputs of the process. The plastic overlay of surface noise in the envelope at back cover may be used for comparison. The single-channel filters are all one-sided filters using only past data. Figure 45 shows the direct sum of the three single-channel outputs. In this case the output was divided by three to normalize it to equal signal amplitude. The filter lengths employed was 71 points, corresponding to 3.5 sec of real time. In comparing the three single-channel outputs, it is apparent that the noise level was only reduced by a small amount except at 2 cps. The reason for this behavior is probably the fairly low coherence between seismographs at these frequencies together with the fact that the amplitude-depth relationships of signal and noise are almost identical in this period range (for details see section 5.1). The peak at 3.0 sec period was not reduced appreciably by any of the filters mainly because the filter length was not sufficient, however, as these waves are not at the periods where teleseisms are usually detected, no attempt was made to improve the performance.

The 2 cps peak shown on all spectra is one main obstacle to visual detection at this site. Comparison of the results of the single-channel cases indicate that deep-hole 1 (2880 m) was by far the most effective and reduced the power in the 2 cps peak by 12 dB. The single-channel process operating on deep-hole 3 (1060 m) did not reduce the power while deep-hole 2 (1980 m) achieved a reduction of 5 dB. Therefore, a single-channel optimum filter operating on the bottom seismograph is the best processor. Examination of figure 45 which shows the direct sum of the three single-channel cases shows this sum is inferior to the single-channel deep-hole 1 process. The reason for this behavior is that the high noise from deep-hole 3 is introduced by summation.

TR 67-3
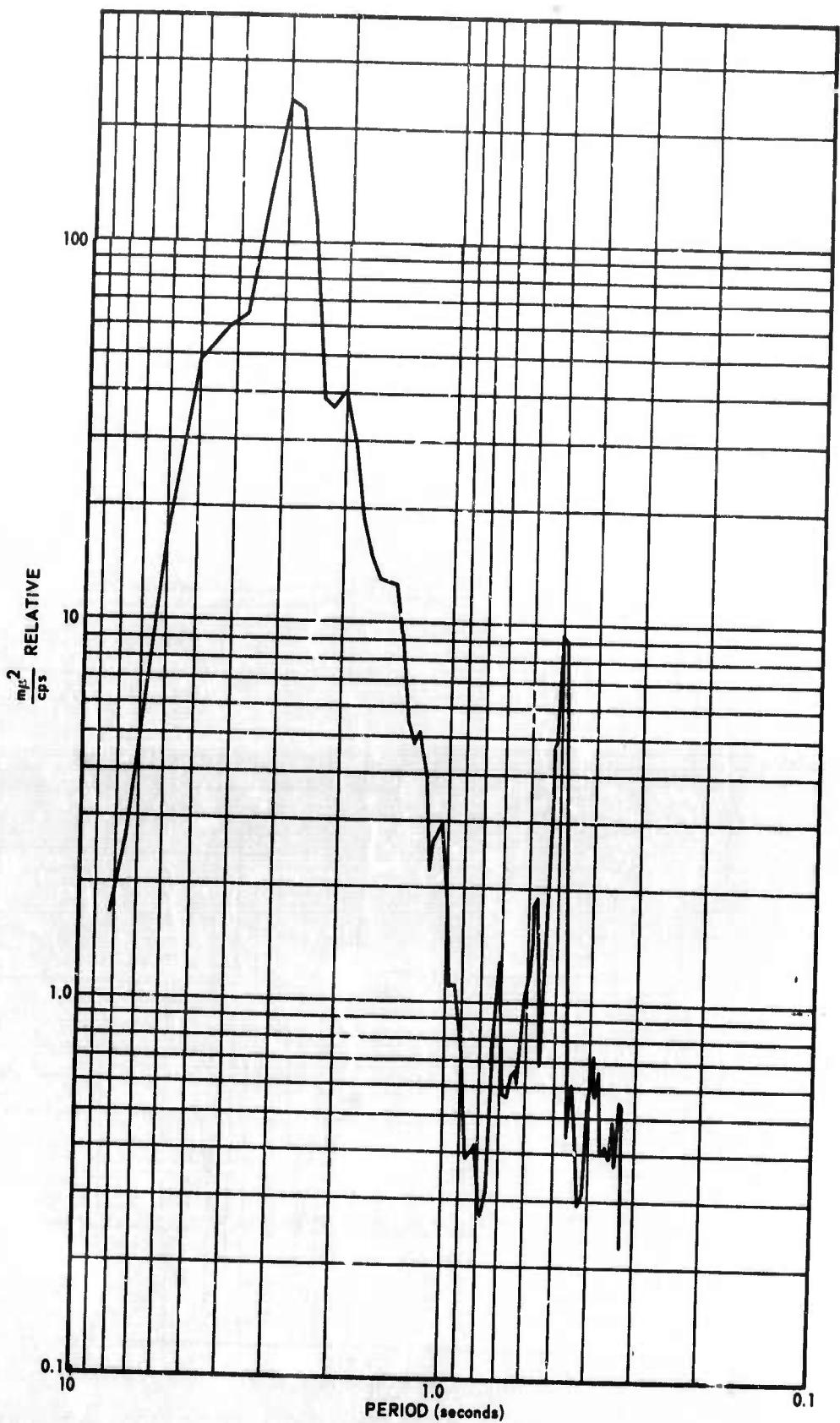
Figure 41. Spectrum of the noise at the surface

TR 67-3
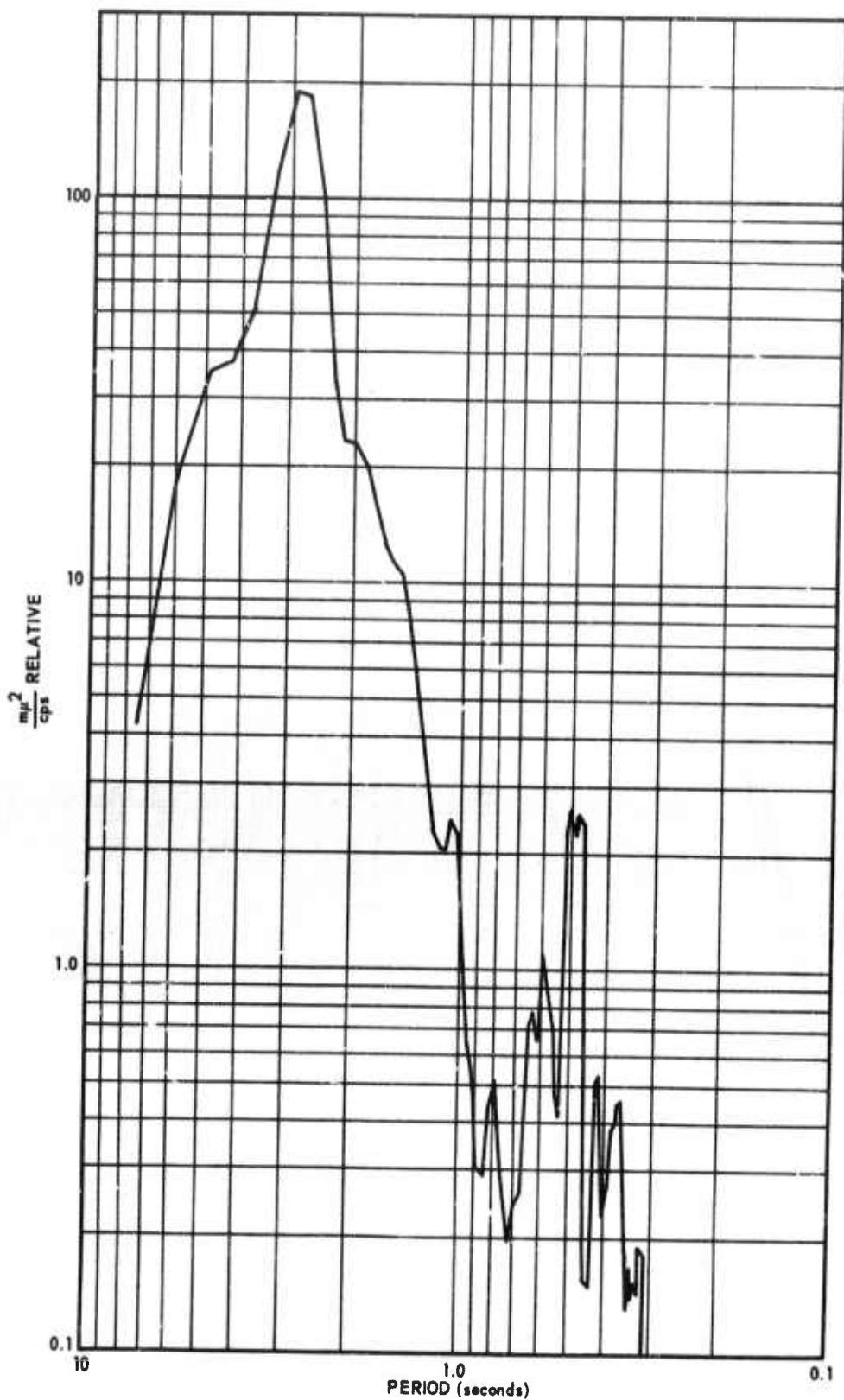
Figure 42. Spectrum of the noise after processing using surface and deep-hole 1 (2880 m) noise

G 2235

-74-
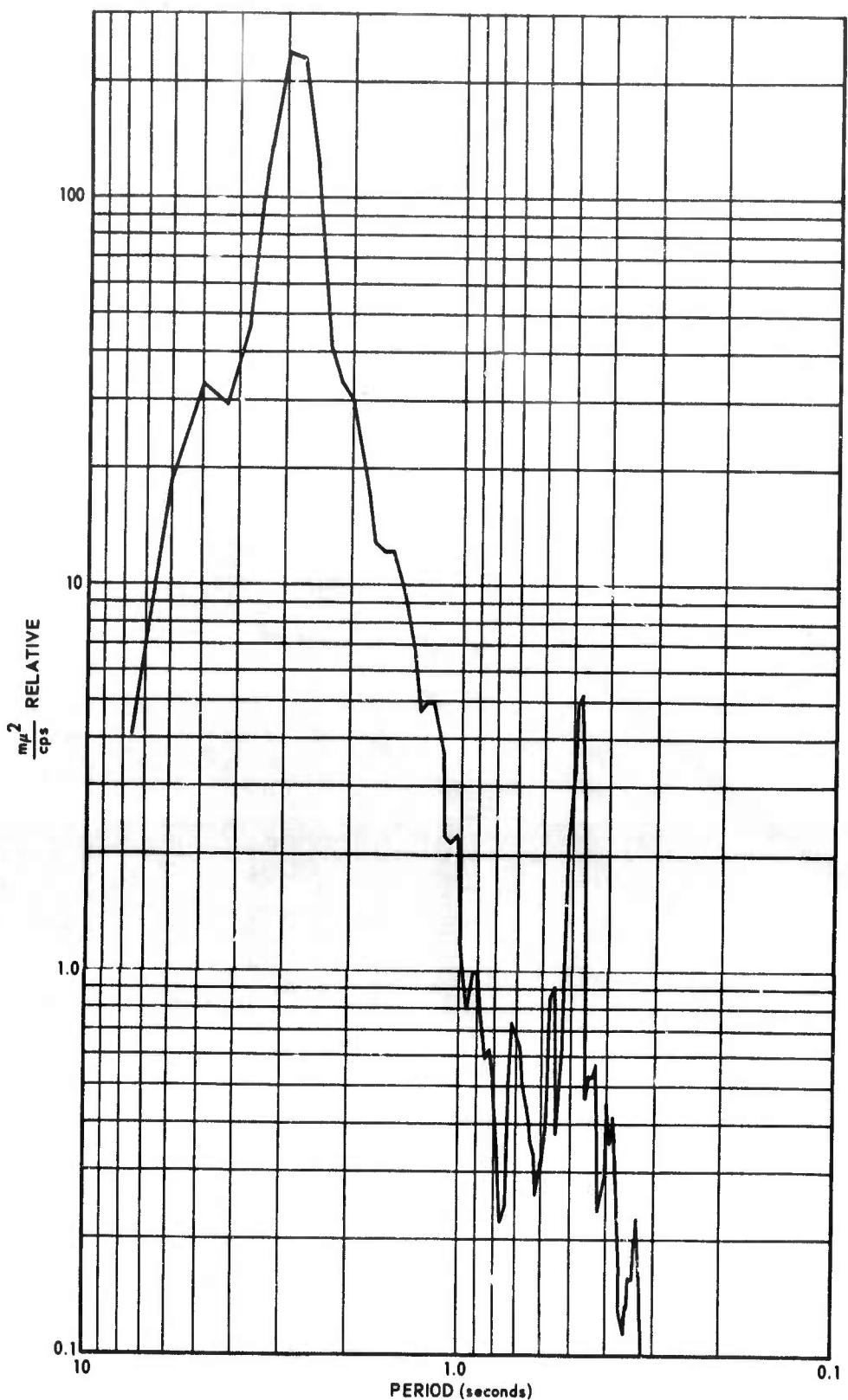
Figure 43.   Spectrum of the noise after processing using
surface and deep-hole 2 (1980 m) noise

G 2236

-75-
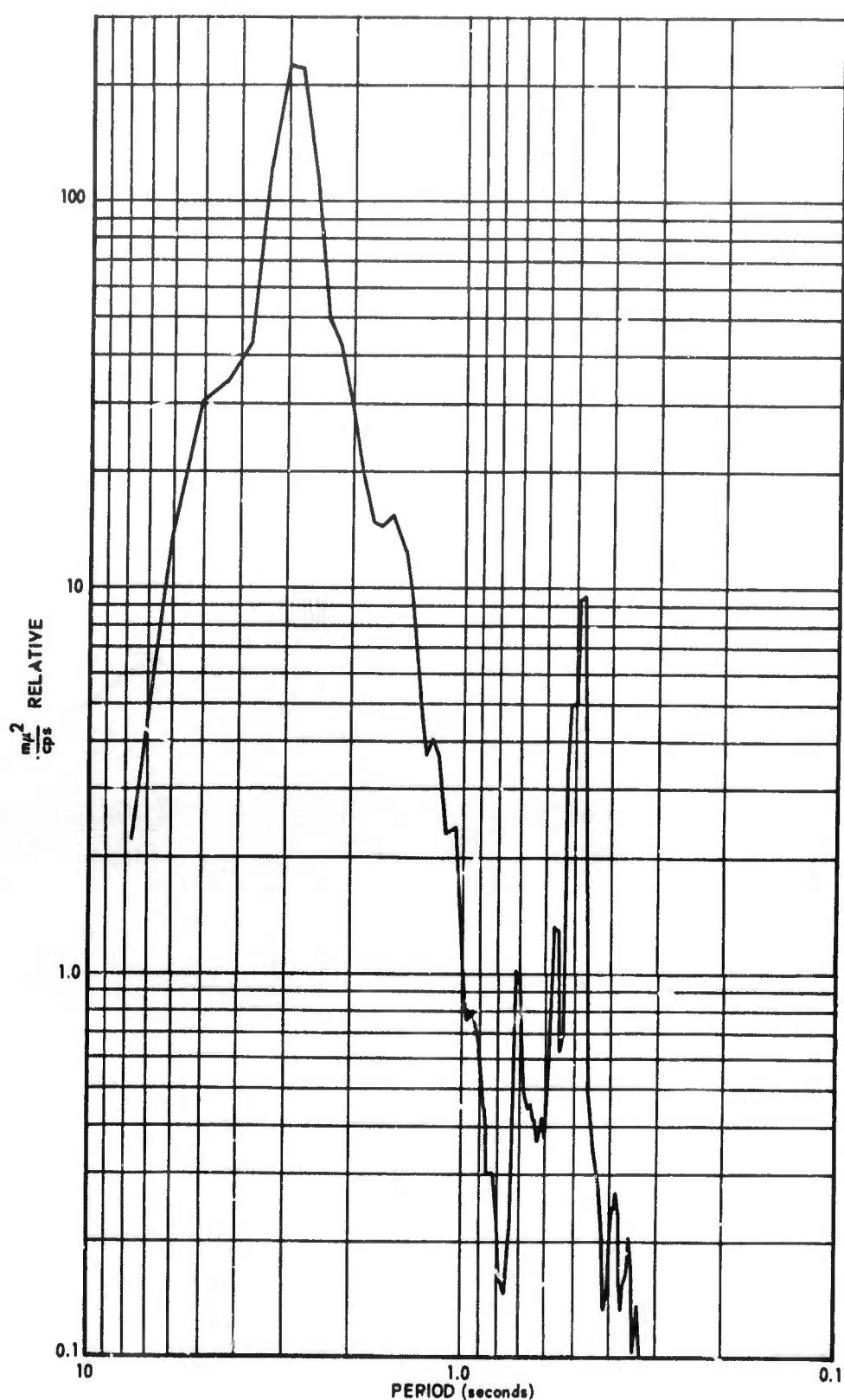
Figure 44. Spectrum of the noise after processing using
surface and deep-hole 3 (1060 m) noise

G 2237

-76-
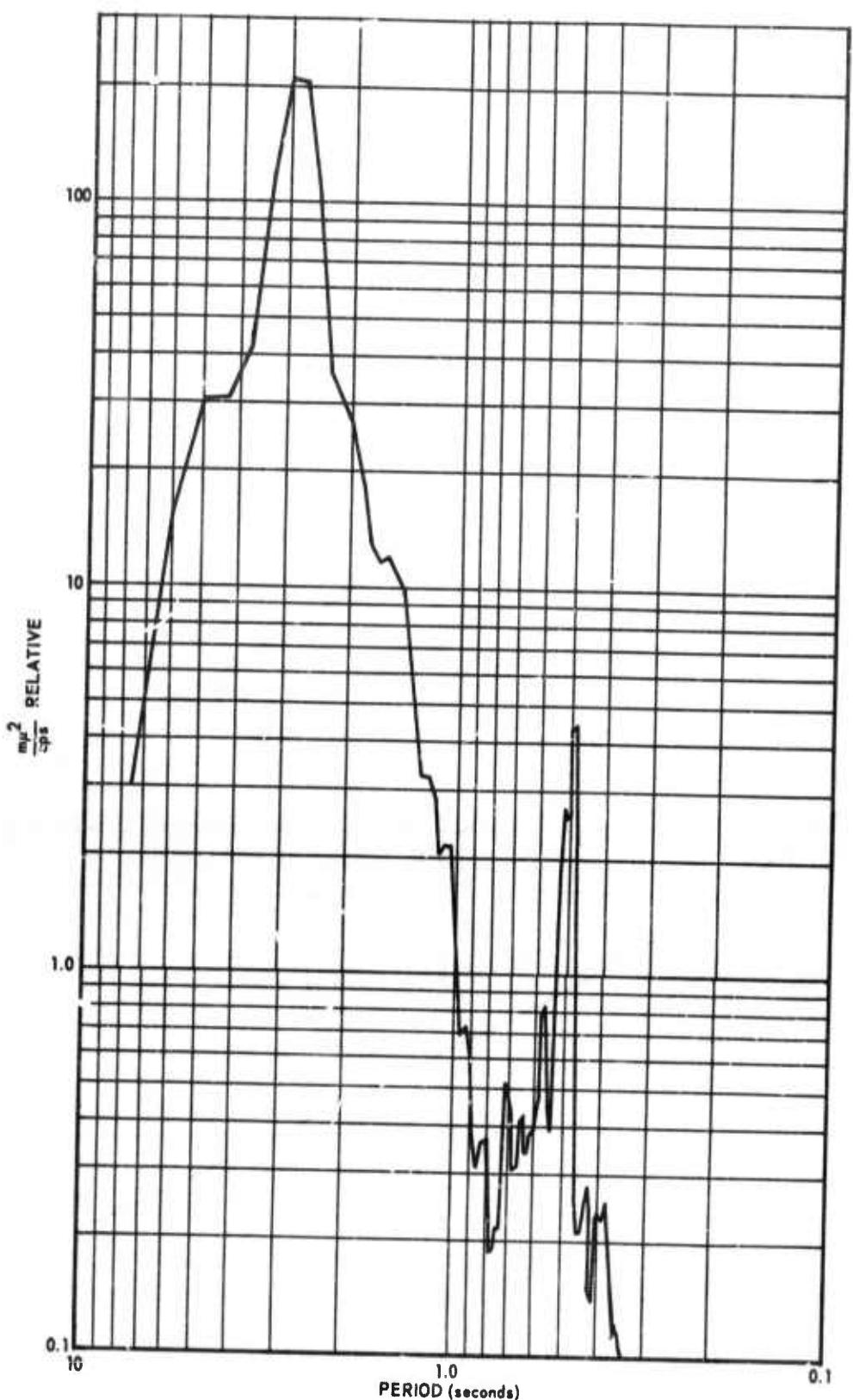
Figure 45. Normalized sum of the sum of the three
single-channel processors

G 2238

-77-

The type of processing discussed above depends heavily on using the correct inverse filters. Any errors in the inverse filters will not subtract correctly and will be operated on by the optimum filters, thus introducing errors.

Figure 40 shows a teleseismic signal as recorded by the surface and deep-hole 1, together with the inverse-filtered deep-hole signal and the signal passed through the single-channel process (using deep-hole 1) discussed above. It will be noted that the inverse-filtered signal is slightly different from the surface signal; however, this difference is caused by noise as is shown by the elimination of the differences when passed through the optimum filter.

It must be noted that the signal used is sharper (higher frequencies) than the usual teleseism and thus constitutes a severe test for the inverse filters.

The inverse filters are expected to show some errors, relative to the noise level, for large signals; however, for large signals, processing of the data is not necessary. Although the noise attenuation shown by the spectra was obtained by processing the same noise sample from which the filters were calculated, the signal occurred several days later. The results indicate that the filters were still effective at this later time.

Figures 46 and 47 show the spectra of the results of using a multichannel optimum filter with deghosting inverse filters (figure 39). Both one-sided (past information) and two-sided (past and future information) filters were used. In both cases the 3.0 sec peak was attenuated in power by approximately 7 dB. The reason that the multichannel filters attenuated the 3.0 sec peak more than single-channel filters is probably that the multichannel filters are able to make better use of slight phase differences between channels after inverse filtering. At the 2 cps peak, the one-sided filter results in an attenuation of noise power practically identical to the single-channel technique operating in deep-hole 1. This result appears to indicate that the multichannel filters essentially only make use of the noise in the deep-hole 1 trace to attenuate this frequency. For reasons that are not understood at present, the two-sided multichannel filters were less effective in suppressing the 2 cps peak than the one-sided ones. Figure 48 shows a signal when passed through the different processors discussed above; in no case was the signal degraded to any appreciable extent.

For comparison with the outputs of the different processors, figure 49 shows the result of the direct summation of the inverse-filtered channels with no optimum filtering. At 2 cps the direct sum is definitely inferior to both the single-channel filter using deep-hole or the multichannel filters. It also failed to attenuate the peak at 0.7 sec period as well as the single-channel filter.

-78-
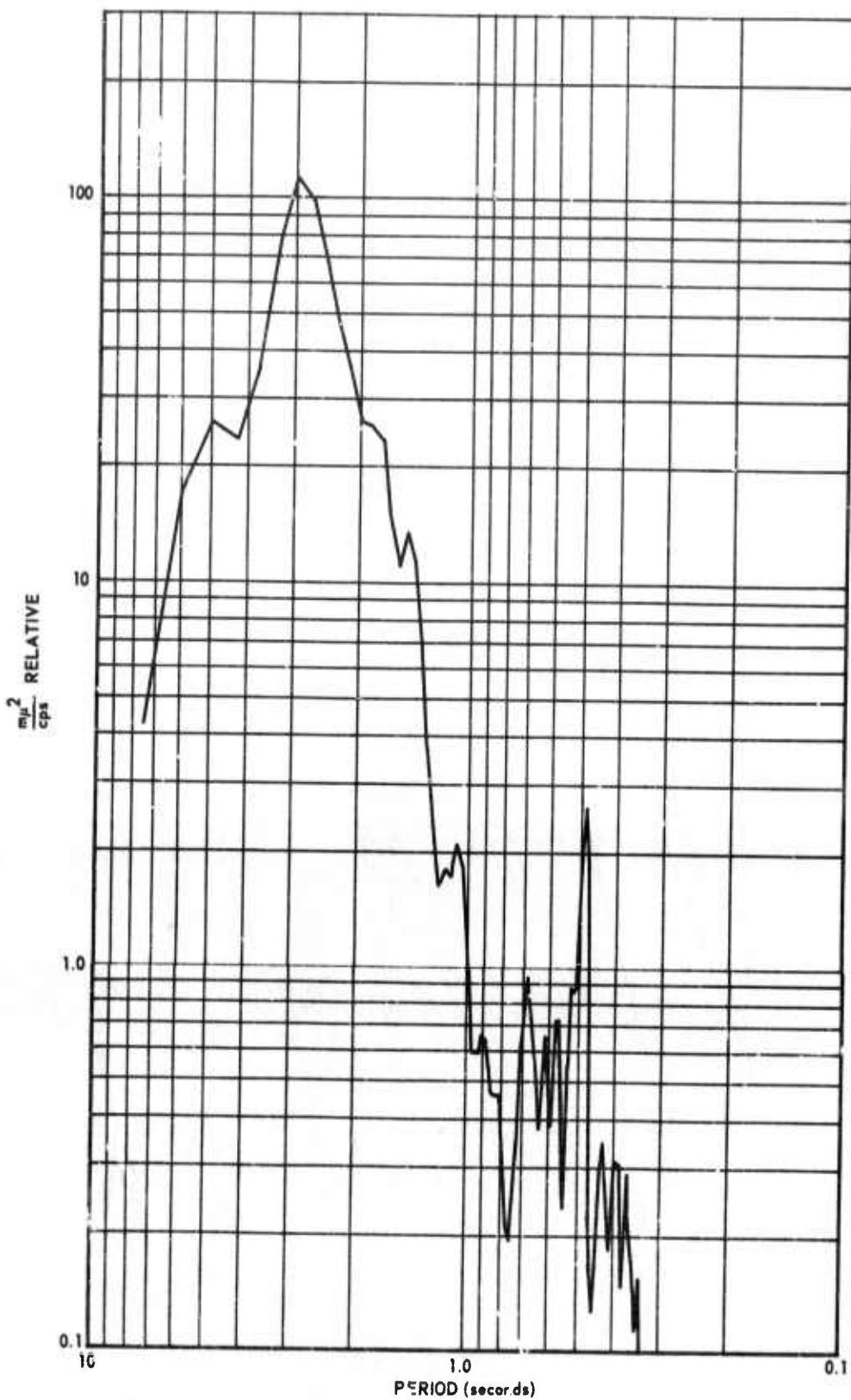
Figure 46.   Spectrum of the noise after one-sided
multichannel filtering

G 2239

-79-
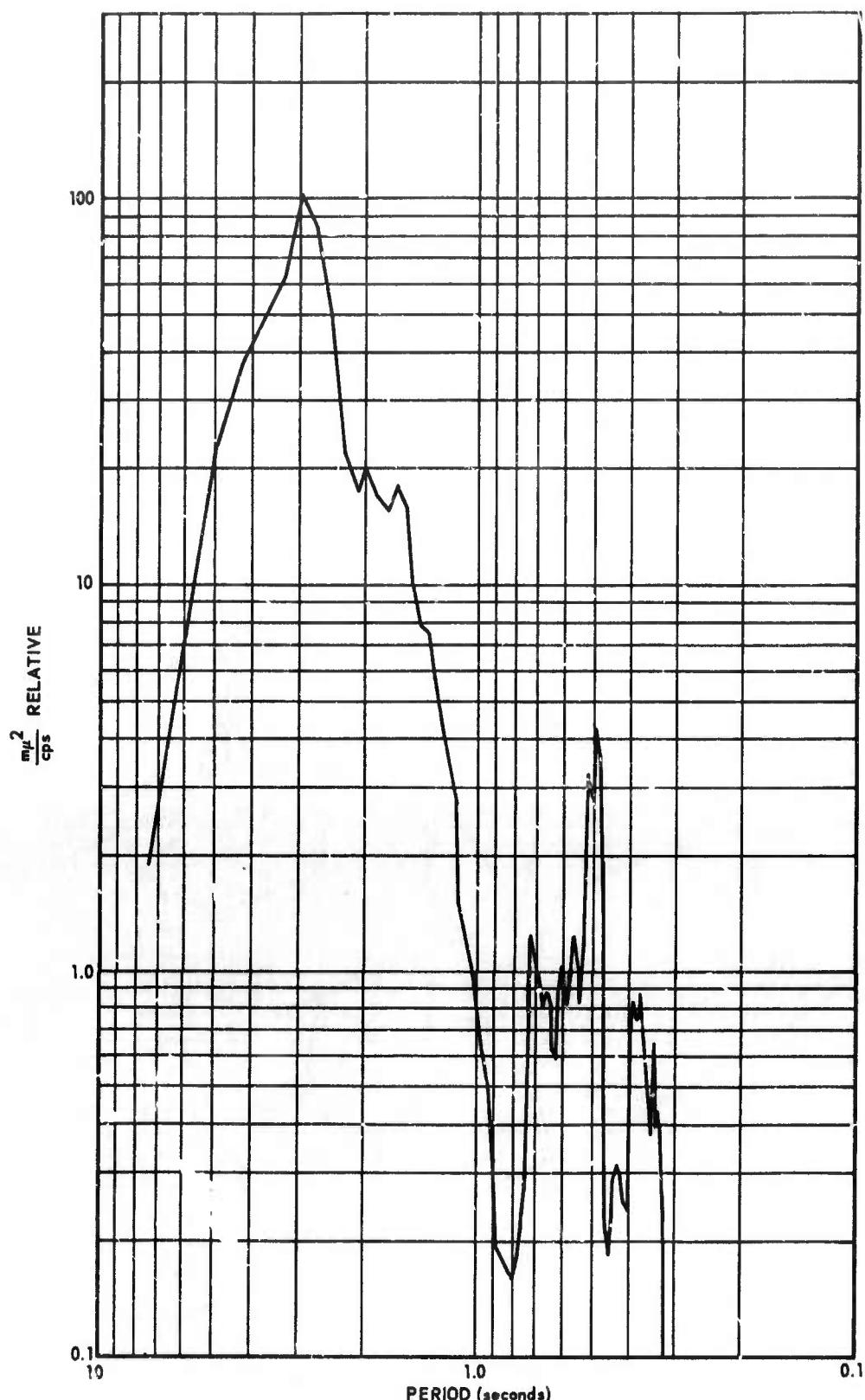
Figure 47. Spectrum of the noise after two-sided
multichannel filtering

G 2240

-80-
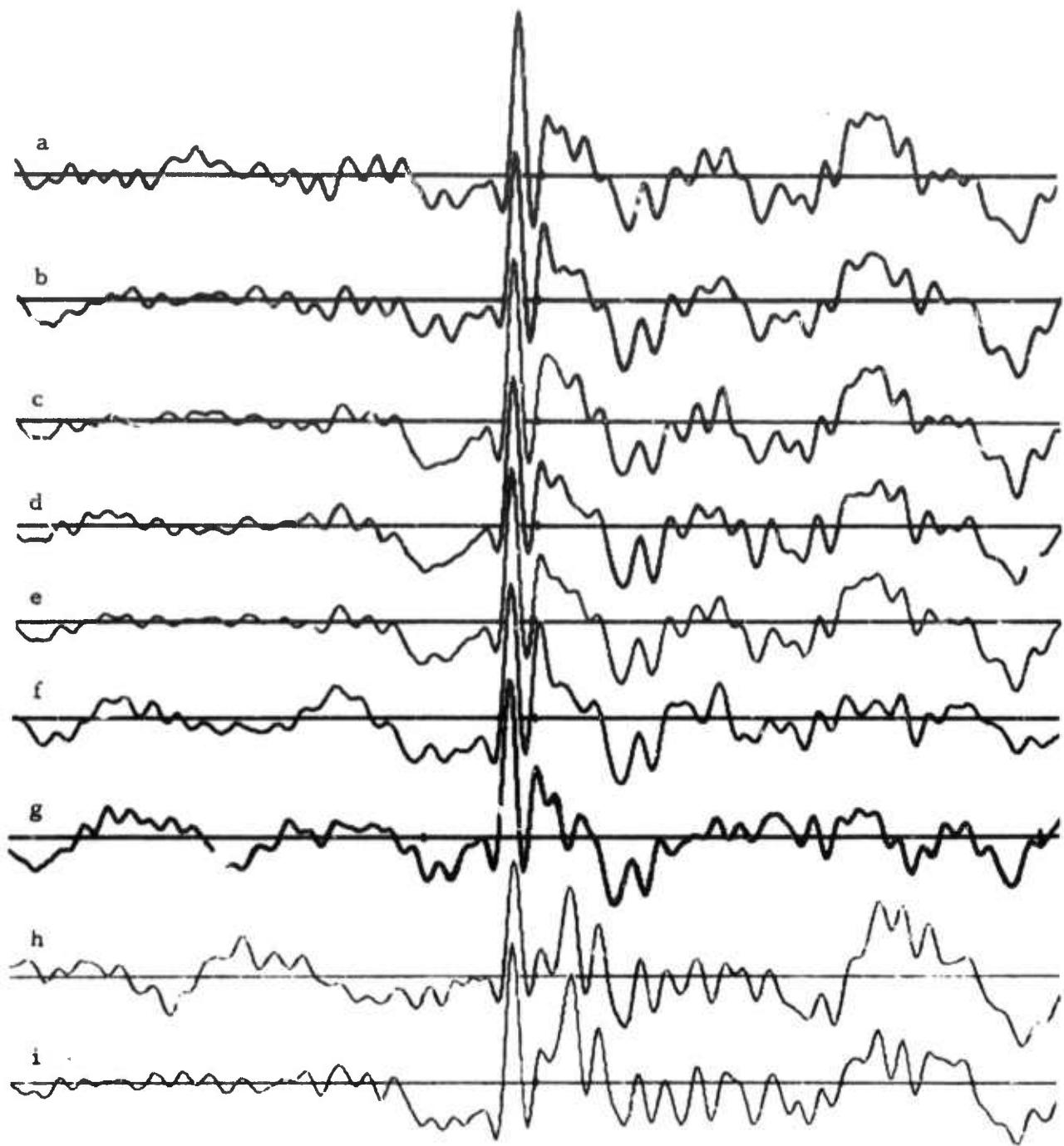
Figure 48. Teleseismic signal operated on by techniques used to increase the signal-to-noise ratio a, surface; b, c, d, single-channel deghosting processes operating on DH3 (1060 m), DH2 (1980 m), and DH1 (2880 m); e, normalized sum of b, c, d; f, g, multichannel deghosting processes with one-and two-sided optimum filters; h, DH1 unfiltered, i/ single-channel ghosting process

G 2241

TR 67-3
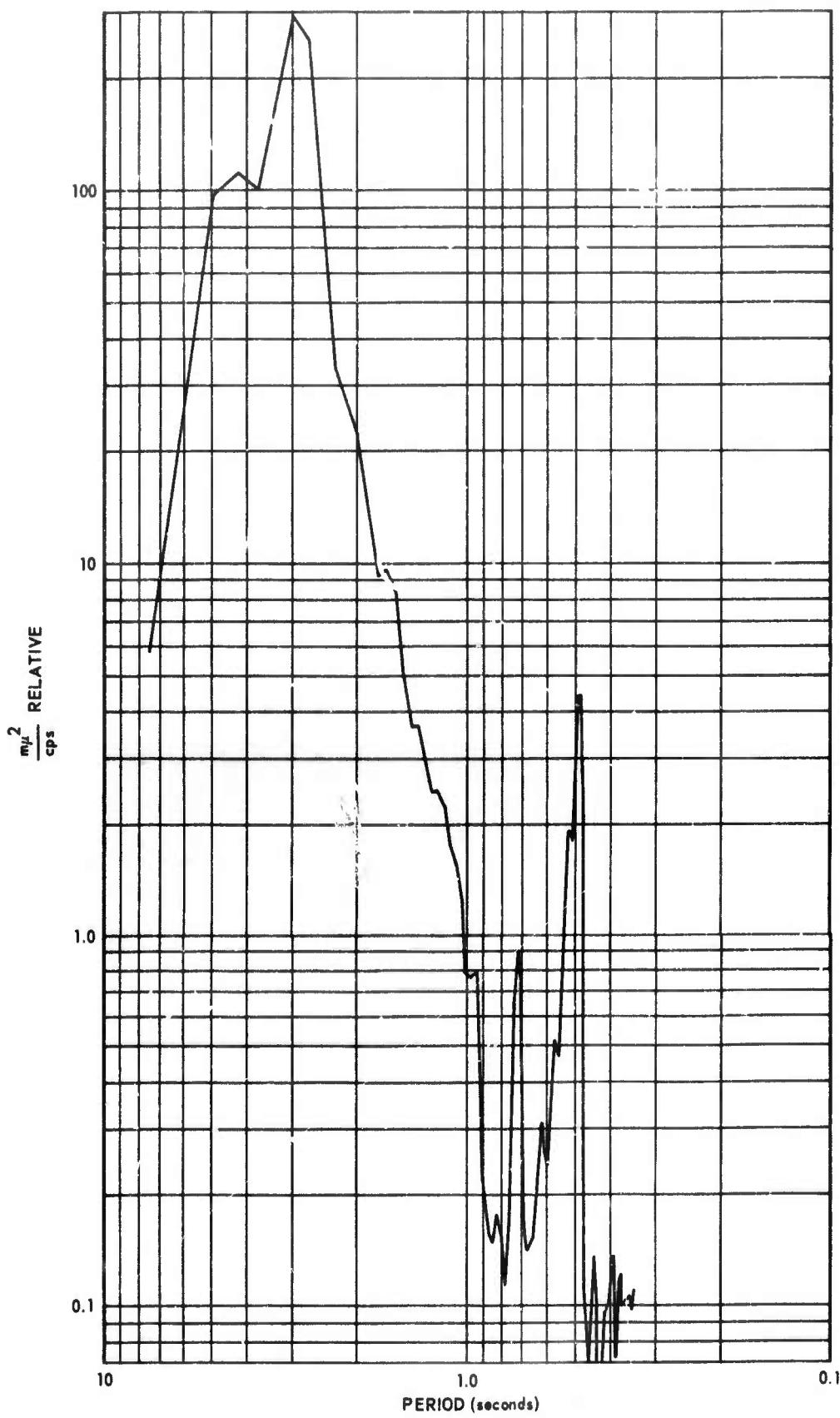
Figure 49. Spectrum of the direct summation of the reverse filtered noise

G 2242

-82-

Figure 50 shows the results of using a single-channel ghosting technique of the type shown in figure 39. For reasons that are not understood at present, the results are inferior to the single-channel deghosting filter technique if the attenuation of the spectral peak at 2 cps is used as the criteria. At 0.5 cps the ghosting technique resulted in a greater attenuation of the noise. The process is working correctly as indicated in figure 48 in which deep-hole 1 (unfiltered) and the final output of the process are shown.

The results obtained to date indicate that the one-sided single-channel optimum filter using the deep-hole 1 and the surface (as reference) is the most effective processor tried to date. The probable reason for this behavior is the similarity between signal and noise, which only at the bottom of the hole shows sufficient differences to allow the filters to effectively operate on them.

Figure 51 shows an example of a small teleseism (epicenter, Crete, magnitude 4.0) as seen by the surface seismograph, and after processing using a deghosting filter and a single-channel optimum filter operating on deep-hole 1. While the signal is obvious on both traces, the first break was noticeably improved on the optimum filter trace.

The principal problem encountered in the processes discussed above is a result of the similarity between the signal and noise. In the computer program, the Levinson reiterative process is used; in general, one of the submatrices in the calculation became singular within the limits of accuracy before 71 points of the filter were calculated. Usually, the problem could be resolved by adding sufficient white noise (5 to 10 percent) to the correlation matrix. However, even using this approach, many of the optimum filters used were not at long as 71 points. The filter's computation is stopped when the mean-square error shows an increase, which often indicates a singularity in a submatrix. However, great care must be employed when this happens because the singularity often occurs before it appears in the mean-square error. Therefore, the last set of filter points is not valid, and a previous set (before the error) must be used. The correct set can only be determined by careful inspection of the filter points. It is expected that the program will be changed in the future so that it prints out warnings when singularities occur.

It must be emphasized that this problem is caused by the particular signal and noise correlation used, and is not a problem in the more usual filter computations.
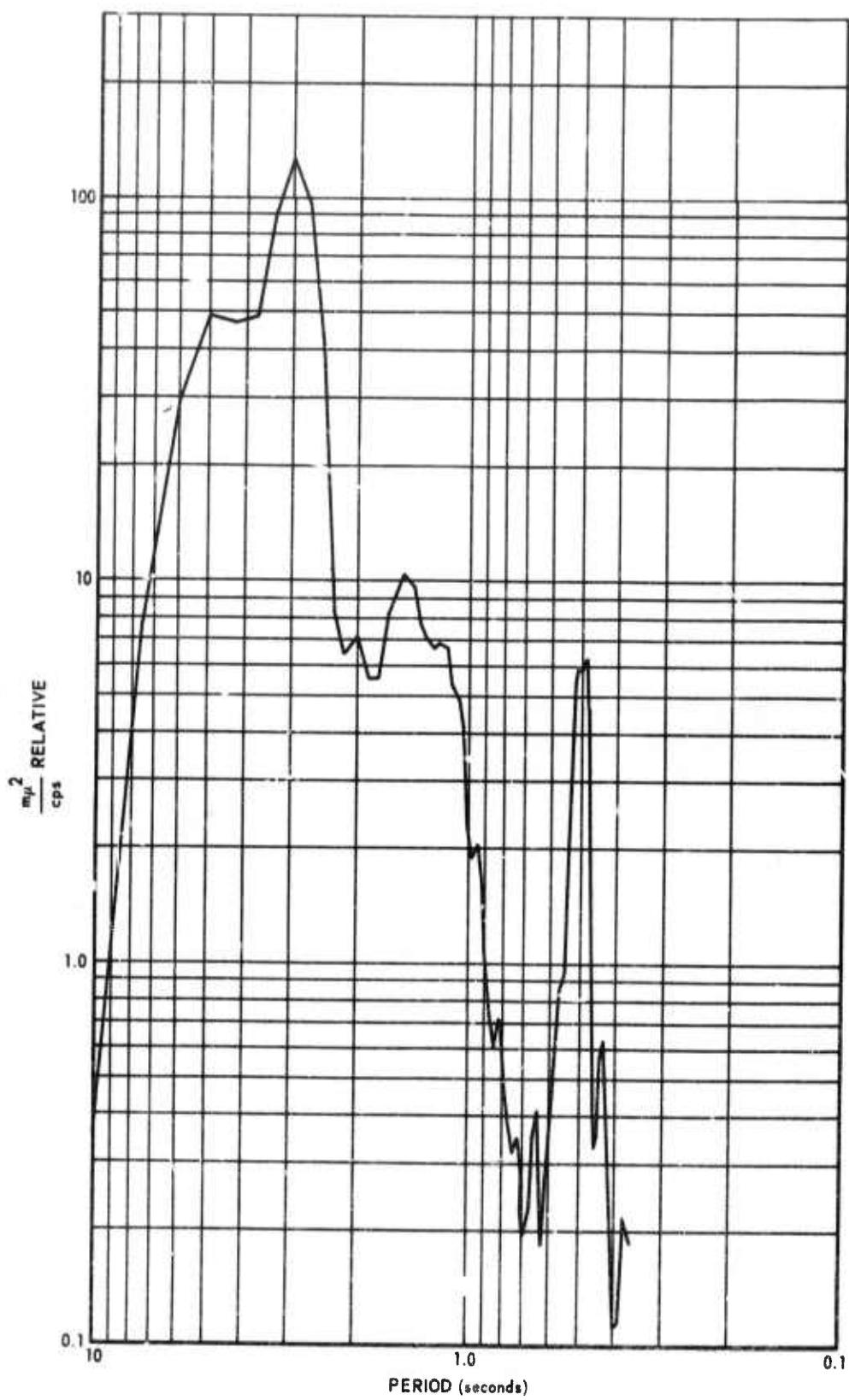
Figure 50. Spectrum of the noise after single-channel optimum
filtering using the ghosting method

-84-

Surface

DH1 after processing

first break
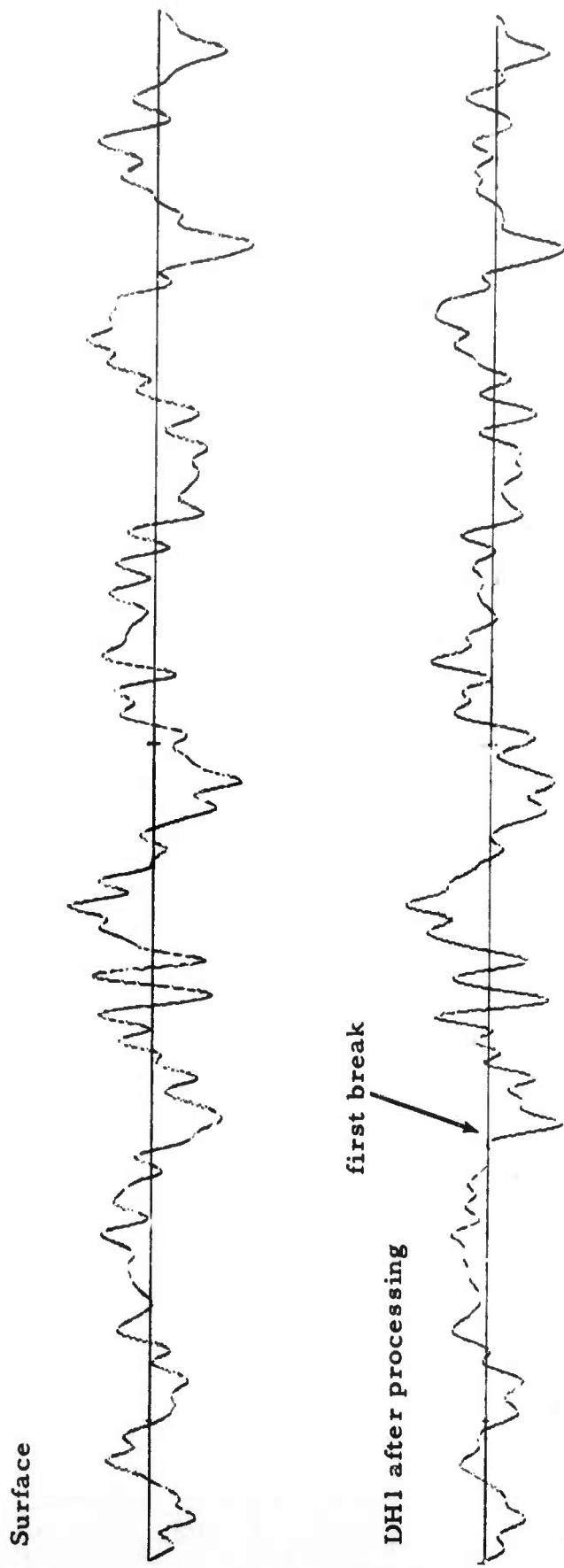
Figure 51. A small teleseism recorded at AP-OK as seen on the surface and after single-channel processing using deep-hole 1 (2880 m). Epicenter Crete. Magnitude 4.0 (PDE cards)

G 224

TR 67-3

8. PROVIDE AND MAINTAIN AN ON-LINE SIGNAL PROCESSOR, TASK 1f (2)

8.1 COMPUTER

A number of digital systems were considered for use in this task. The general specifications for the system were as follows:

Number of channels	32, minimum
Samples per second	20, maximum
Resolution, bits	14 (13 + sign)
Input impedance	>50 K Ω
Tape format	Gapped, IBM compatible

The final choice of an on-line processor was the Adage Inc., Computer, the Ambilog 200. The specifications for this computer met our requirements, and the equipment was procured and installed in an LRSM recording van that was transferred to this project. Figure 52 shows the arrangement of racks in the van and figure 53 shows the operator's console.

8.2 PROGRAMMING

Because of the need to do real-time processing of data, all programs for the computer were written in machine language. Included among the programs were a digitizing program (GTCH6), an on-line inverse filter program (GTCHY) and a data listing program (DALST). GTCH6 and GTCHY provide for operator input so that station identification, day of year, year, starting time, and sampling rate is included in each record on the tape. The time in the record is updated programatically. Figure 54 shows the format used to digitally record data. DALST is a useful program for listing data from the tape on the typewriter.

8.3 DIGITAL SYSTEM PERFORMANCE

The digital system was installed in a recording van in April 1966. When the software was received, it was learned that the requested digitizing program had not been written. Consequently, some time was lost while this was done. In August, the memory was increased to 16K and ambilogical subsystems were installed to permit on-line processing of data. During the intervening time, difficulty was experienced in using the Adage-furnished systems programs. The difficulty was finally traced to a tolerance buildup between machines. Adage subsequently rewrote their programs to remedy the problem. Another problem that caused considerable difficulty was the presence of spurious noise pulses as illustrated in figure 55. These pulses
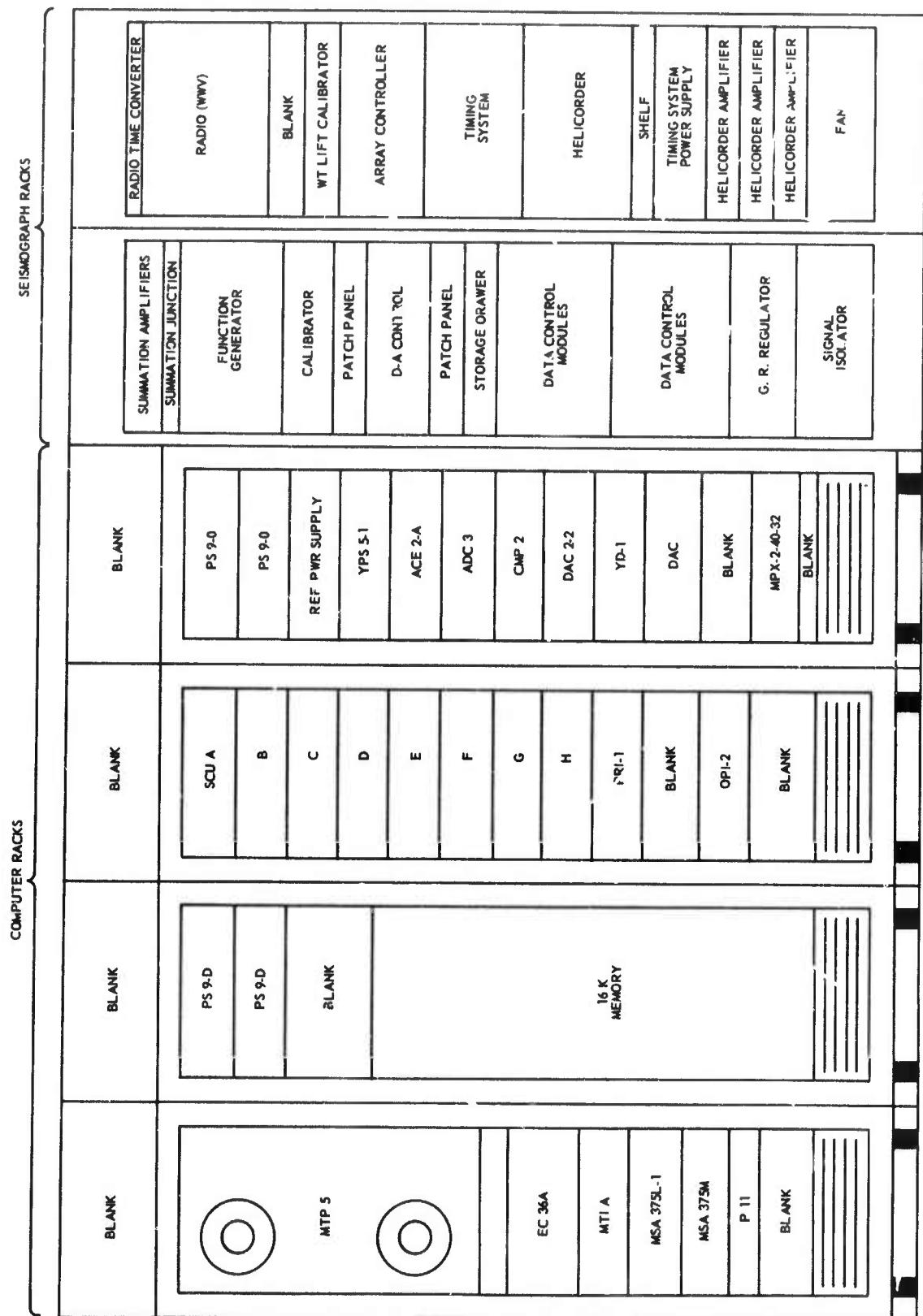
Figure 52. Configuration of racks in recording van   G 2245

-87-

TR 67-3
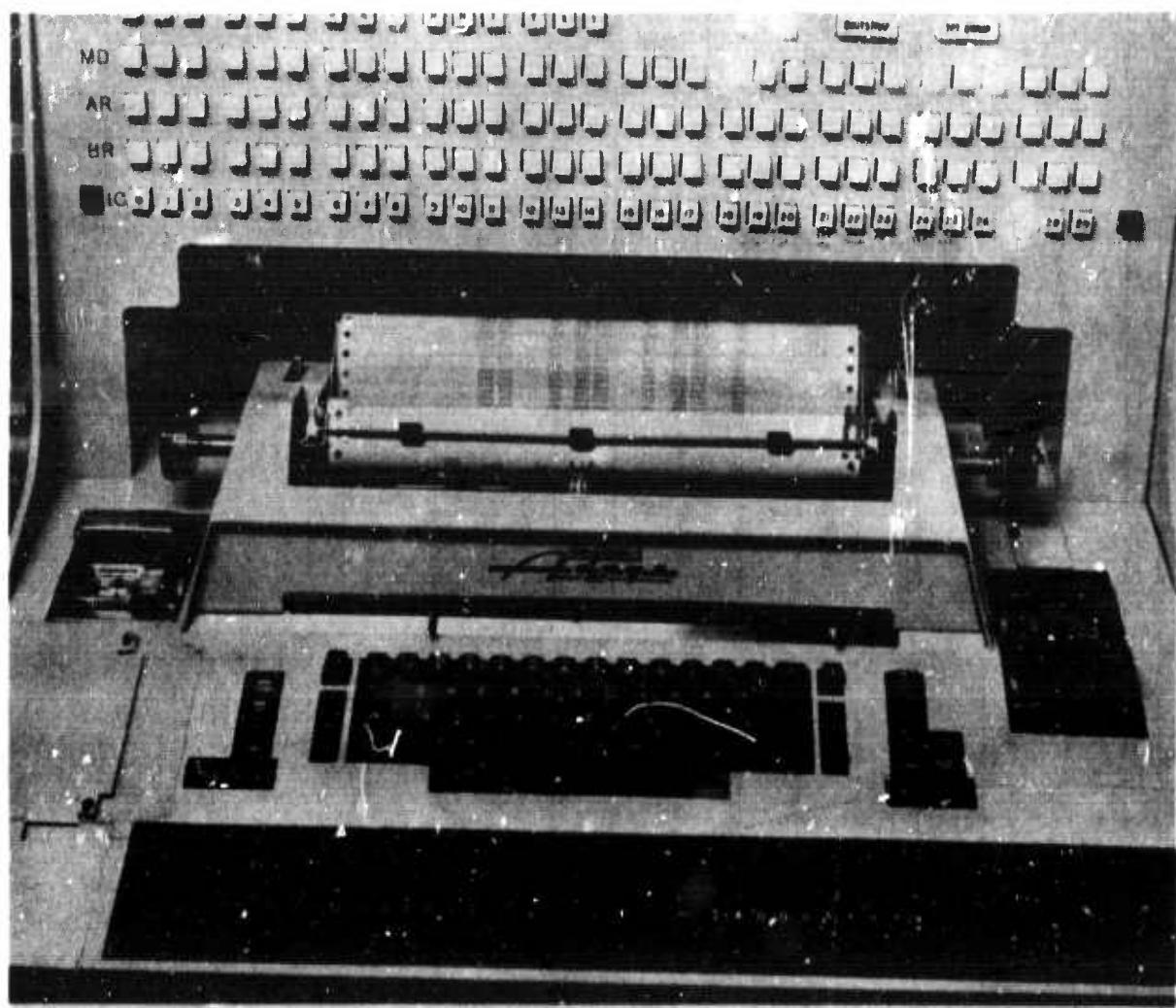
Figure 53. Operator's console, ambilog 200 computer

G 2246

TR 67-3

WORD

CHARACTER

ONE PHYSICAL TAPE RECORD

| 1 | 2 | 3 | 4 | 5 | 6 | | 7 | 8 | 9 | 10 – 25 | 26 | 27 | 28 | 29 | 30 – 509 |

RECORD NO.

FILE NO.

FILE NAME

NUMBER OF WORDS

TYPE RECORD
FIRST CORE ADDRESS

STATION IDENTIFICATION

RECORD NO.

FILE NO.

CLOCK RATE

NO. OF CHANNELS

SCANS PER CHANNEL PER RECORD

NO. 6 BIT TAPE CH. PER 2 SAMPLES

CHSQ

CHANNEL ASSIGNMENTS

UNUSED

YEAR

DAY

HOUR
MINUTE

SECOND
MILLISECOND

DATA

ADAGE HEADER
5 CHARACTERS PER WORD

GEOTECH HEADER
4 CHARACTERS PER WORD

DATA

DATA

PARITY

NOTE:
1. ADAGE HEADER IS WRITTEN IN WORDS 1–4, 5 CHARACTERS PER WORD
GEOTECH HEADER IS WRITTEN IN WORDS 5–29, 4 CHARACTERS PER WORD
DATA WRITTEN IN WORDS 30–509, 4 CHARACTERS PER WORD

= 20 CHARACTERS
= 100 CHARACTERS
= 1920 CHARACTERS
2040 CHARACTERS

2. UNPACKING ROUTINES USED OFF-LINE TREAT WORDS 1–4 AS HAVING
FOUR CHARACTERS. THUS, THERE ARE 510 WORDS, EACH OF FOUR
CHARACTERS FOR A TOTAL OF 2040 TAPE CHARACTERS PER RECORD.

Figure 54. Format of tape records   G_247

-89-
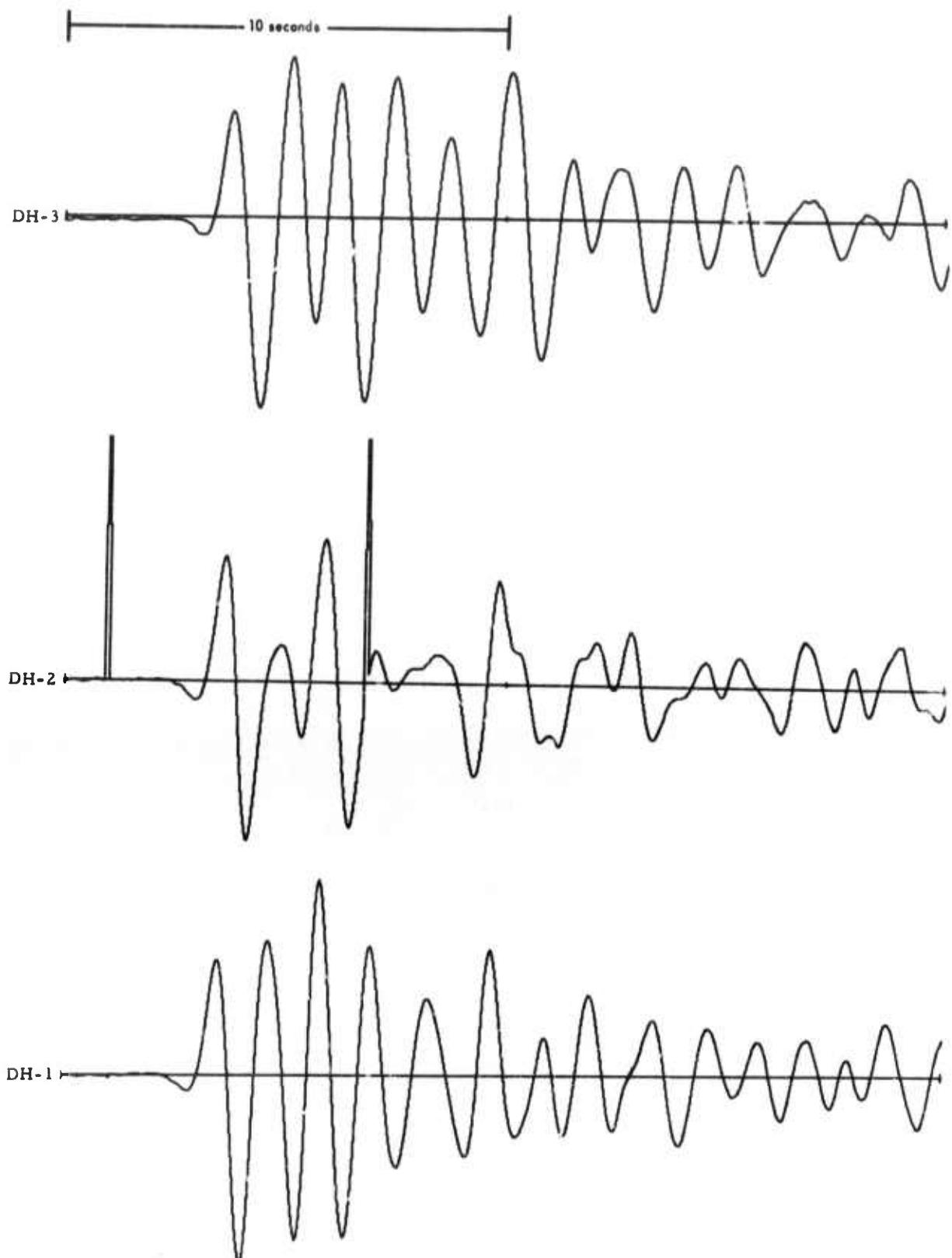
Figure 55. Plot of three triaxial seismometer summations.
DH-1 at 2897 m, DH-2 at 198? m, DH-3 at 1067 m.
AP-OK 19 May 1966

G 2248

-90-

occurred at 3-sec intervals, coincident with the tape-writing operation. Adage worked with us in finding the cause. In August, they made hardware modification to the computer and assisted us in revising our digitizing program in an attempt to eliminate the problem.

In September, we experienced an intermittent memory failure, and personnel from Adage and Fabritec (the manufacturer of the memory) attempted to find the cause. The failure was of such a nature that it was not conclusively found.

In June and again in October, we experienced a catastrophic failure of the computer. Each time, approximately 25 transistors were destroyed in the system control unit (SCU). Adage has taken the position that the cause was either a line transient or a lightning strike. A difference of opinion exists between their company and ours that may never be resolved.

During September and October, we were troubled by frequent failure of the computer and/or programs that caused the computer to fail to execute our data-gathering programs. The exact cause is still not clearly understood by us or Adage. During this period, Adage made hardware modification and again revised our software.

During November, we continued to have difficulty loading the Adage programs and difficulty operating our own programs. Further, the noise pulses were again observed, as shown in figure 56. A service man from Adage came to the site to find the difficulty. Another Adage employee came to repair a minor difficulty with the typewriter. The cause of the difficulties with the computer was not found.

During October, November and December, we found that an alarming number of parity errors were detected while working off-line with the data. It was established that the errors were the result of failure of the system to write the parity bit, rather than errors in the data. Toward the end of December it became impossible to read program tapes at all. Through use of an alignment tape it was determined that the tape transport was not reading tracks 1 and 4 of the tapes. Two defective transistors were found and replaced. This seems to have cured the problem and was possibly the cause of the parity bit problem. During testing to find the cause of this failure, a failure occurred in the memory. A defective transistor was replaced and the system was again operational and remained so to the end of the technical program.

8.4 PERFORMANCE COMMENTS

Although many problems were encountered with the digital system, it was still used for its intended purpose as described in an earlier portion of this report. Further, we found the manufacturer of the equipment to be

-91-
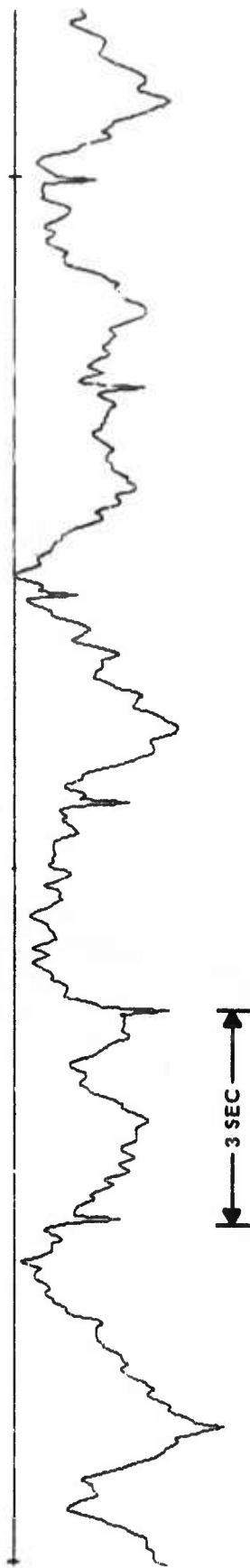
Figure 56. Computer noise   G 1878

3 SEC

cooperative and as anxious as we to find and cure the sources of difficulty. Any criticism of the computer should be tempered by the fact that it was remotely situated with respect to Adage service centers and that the identification of the cause of intermittent failures can be extremely difficult in a large scale computer.

9. REFERENCES

Amos, D. E., and Koopmans, L. H., 1963, Tables of the distribution of the coefficient of coherence for stationary bivariate Guassian processes: Sandia Corporation Monograph SCR 483

Backus M., and others, 1964, Wide-band extraction of mantle P waves from ambient noise: Geophysics, vol. 29, p. 672-692

Benioff, H., 1932, A new vertical seismograph: Bull Seism. Soc. Am., vol. 22, p. 155-169

Blackman, R. B., and Tukey J. W., 1958, The measurement of power spectra: Dover Publications, Inc., New York

Burg, J. P., 1964, Three-dimensional filtering with an array of seismometers: Geophysics, vol. 29, p. 693-713

Douze, E. J., 1964, Rayleigh waves in short-period seismic noise: Bull. Seism. Soc. Am., vol. 54, p. 1197-1212

Ewing, W. M., and others, 1957, Elastic waves in layered media: McGraw-Hill Book Company, Inc., New York

Geotechnical Corporation, 1964, Deep-hole site report, Meridian unit No. 1 well, White Pine County, Nevada: TR 64-68, Project VT/1139, Contract AF 33(600)-43369

Gupta, I., 1965, Standing-wave phenomena in short-period seismic noise: Geophysics, vol. 30, p. 1179-1186

Gutenberg, B., 1958, Advances in geophysics: Academic Press, New York

Jury, E. I., 1964, Theory and application of the Z-transform method: John Wiley and Sons Inc., New York

Oliver, J., and Ewing, M., 1958, Normal modes of continental surface waves: Bull. Seism. Soc. Am., vol. 48, p. 33-49

Roden, R. B., 1965, Horizontal and vertical arrays for teleseismic signal enhancement: Geophysics, vol. 30, p. 597-608

Sax, R. L., and Hartenberger, R. A., 1964, Theoretical prediction of seismic noise in a deep borehole: Geophysics, vol. 29, p. 714-720

Seriff, A. J., Velzeboer, C. J., and Haase, R. J., Possible P-wave observations in short-period seismic noise: Geophysics, vol. 30, p. 1187-1190

10. CONCLUSIONS AND RECOMMENDATIONS

10.1 CONCLUSIONS

10.1.1 The deep-hole vertical arrays were effectively used to gather data for use in work designed to increase understanding of the composition of noise and the behavior of signals.

10.1.2 The vertical array of triaxial seismometers was operated routinely.

10.1.3 Although intermittant problems were experienced with the on-line processor, it was, nevertheless, useful in digitally recording data for off-line use.

10.1.4 Additional programming effort will be required to implement on-line data processing techniques.

10.1.5 The inverse filters were shown to operate correctly on the teleseismic P-wave signals for which they were designed. Failure of the filters to operate correctly was shown to be caused by the presence of wave types other than the P waves for which the filters were designed, resulting in a degradation of results.

10.1.6 The best processor found was a single-channel optimum filter using a deghosting filter operating on the bottom seismograph (2880 m) and on the surface.

10.2 RECOMMENDATIONS

10.2.1 Before additional short-period triaxial seismometers are constructed, redesign should be undertaken to increase their ruggedness.

TR 67-3

10.2.2 The digital system should be further improved to increase its reliability before it is used in a continuous (24 hr/day) application.

10.2.3 The techniques to improve the S/N ratio discussed in this report need to be tried at other sites where different kinds of noise fields are present.

10.2.4 Several other optimum filtering techniques such as the maximum likelihood type need to be tried and the results compared with the results discussed in this report.

10.2.5 Only a small amount of effort was expended on the horizontal data obtained because the vertical motion processing was considered to be more important. A great deal more effort is needed to gain an understanding of the horizontal-motion noise field and to examine the processing techniques that can be used.

TR 67-3

APPENDIX 1 to TECHNICAL REPORT NO. 67-3

STATEMENT OF WORK TO BE DONE
AFTAC PROJECT AUTHORIZATION NO. VELA T/5051
AND AMENDMENTS

STATEMENT OF WORK TO BE DONE
AFTAC PROJECT AUTHORIZATION No. VELA T/5051

1. **Tasks.**

   a. Conduct systems engineering on deep-well instrumentation to obtain a capability of operating up to 6 seismometers in a borehole simultaneously. Evaluate the applicability of multiconductor data cable with quick disconnect features between instruments in a vertical array. No major redesign of the deep-well seismometer is anticipated although mass size may be reduced to meet size and weight limitations. Following design approval by the government, assemble and conduct operational tests on the recommended deep-well seismographic system.

   b. Maintain and operate the deep-well test facility near Grapevine, Texas, for the purpose of testing equipment modifications, developing new handling and emplacement techniques, and qualifying calibration and operational procedures for the deep-well seismograph. In this regard, field evaluation of new or improved deep-well devices, such as the borehole triaxial SP seismometer under Project VELA T/072, will be conducted at Grapevine prior to use in field measurements tasks.

   c. Continue to measure signals and noise in deep and shallow boreholes where additional data are required. These field measurements do not anticipate any preparation of new deep-well sites but provide for occupancy of several boreholes previously conditional and available. Data should be obtained for the purpose of supporting analysis of the behavior of seismic signals and noise with depth. A limited number of shallow boreholes may be required in support of this task.

   d. Provide for complete and detailed analysis of data resulting from field measurements and develop means of processing multiple signals from borehole arrays of 3 to 6 sensors. Major effort should be devoted to prediction of deep- and shallow-buried arrays under varying conditions of surface noise, environmental influences, geological structures, and geographic location. Large scale computer support of the CDC 1604 class is not authorized but will be provided by separate arrangement with the AFTAC project officer.

2. **Reports.**

   a. A monthly letter-type management and progress report in 14 copies, summarizing work through the 25th of the month, will be dispatched to AFTAC by the end of each month. Specific topics will include technical and financial status, major accomplishments, problems encountered, future plans, and any action required by AFTAC. The financial status in each report should

include estimated expenditures and commitments to date, estimated funds available to complete the work, and estimated excess or deficiency of funds. Illustrations and photographs should be included as applicable. In addition, the monthly report submitted for the reporting period occurring 6 months prior to the scheduled contract completion date shall contain specific statements concerning recommendations or requirements and justifications for extensions, modifications, or expiration of work and any changes in cost estimates which are anticipated by the contractor. The heading of each report should contain the following information:

AFTAC Project No. VELA T/5051
Project Title
ARPA Order No.
ARPA Project Code No.
Name of Contractor
Date of Contract
Amount of Contract
Contract Number
Contract Expiration Date
Project Scientist's or Engineer's Name and Phone Number

b. A list of suggested milestones will be dispatched to AFTAC in 14 copies not later than 20 September 1964. Milestones are defined as accomplishments which present significant progress when completed. Each milestone should be briefly described and completion dates should be estimated. Upon arrival of milestone information, copies of SD Form 350 will be furnished for reporting progress against the milestone schedule. The SD Form 350 will be attached to the monthly report.

c. Special reports of major events will be forwarded by telephone, telegraph, or separate letter as they occur and should be included in the following monthly reports. Specific items are to include (but are not restricted to) program delays, program breakthroughs, and changes in funding requirements.

d. Special reports, as requested by the AFTAC project officer, may be required upon completion of various portions of the work.

e. An initial technical summary report in 50 copies, covering work performed through 30 January 1965, will be submitted to AFTAC within 15 days after the close of the reporting period. A semiannual technical summary report in 50 copies, covering work performed through each 6-month period following the close of the initial reporting period, will be submitted to AFTAC within 15 days following the close of the reporting

2

period. These reports will present a precise and factual discussion of the technical findings and accomplishments during the reporting period. The heading of the report will contain the heading information indicated in paragraph 2a.

3. Technical Documents. The contractor will be required to furnish the following technical documents:

a. All seismograms and operating logs, to include pertinent information concerning time, date, type of instruments, magnifications, etc., as requested by the AFTAC project officer.

b. Technical manuals on the installation and operation of all technical equipment installed during the duration of the contract for this project.

c. Two sets of reproducible engineering drawings and specifications for any changes or modifications in standard operational equipment and instruments, and for any new equipment designed, together with 2 sets of prints of these same drawings.

5. Miscellaneous. DD Form 1423, Contract Data Requirement List is attached. All technical reports and documents are to be forwarded to:

Hq USAF (AFTAC/VELA Seismological
Center/Maj Meek)
Wash DC 20333

3

AMENDED STATEMENT OF WORK TO BE DONE
AFTAC Project Authorization No. VELA T/5051

1. Tasks.

    a. Under Task 1a, add: Assemble and operate 2 deep-well vertical
array systems at locations designated by the AFTAC project officer.
Each system will consist of up to 6 sensors suitable for borehole use
and appropriate surface recording instrumentation. Ground handling
equipment, derricks, rigging, and instrument winching shall be easily
transportable between sites and capable of maximum flexibility in
field measurements operations.

    b. Under Task 1d, add: Develop, provide, and maintain an array
signal processing apparatus capable of processing multiple data inputs
from borehole arrays. This processing apparatus must ultimately be
suitable for on-line operation and may be composed of digital as well as
analog components.

2. Reports. In lieu of the report requirements in paragraphs 2a,
b, c, d, and 3, provide monthly, quarterly, final, and special reports
in accordance with sentence 1, paragraph 1 of Data Item S-17-12.0,
AFSCM 310-1; however, if that data item conflicts with Attachment 2,
Amendment 1, Project VT/5051, the latter will take precedence.

AFTAC Project Authorization No. VELA T/5051

1. **Monthly Progress Reports.** Monthly progress reports will be submitted in 15 copies, commencing the 5th day of the second month after the effective date of the contract. The report will include identification information as outlined in paragraph 3b. These reports will include but not be limited to the following subject areas:

    a. Technical Status.

        (1) Major accomplishments.

        (2) Problems encountered.

        (3) Future plans.

        (4) Action required by the government.

        (5) Illustrations and photographs, as applicable.

    b. Financial Status.

        (1) Expenditures to date.

        (2) Man-months expended to date.

        (3) Statement concerning overrun possibilities.

2. **Quarterly Progress Reports.** Quarterly progress reports will be submitted in 50 copies and in accordance with the format established for semiannual reports under Contract AF 33(657)-13668. The requirement for monthly status reports is to be deleted when quarterly reports are submitted. Quarterly reports will be submitted by the 15 day following the end of each quarter. Reports will include notices and identification information as outlined in paragraphs 3a and 3b, respectively. DD Form 1473, Document Control Data - R&D, will be attached to each report (reference AFR 80-29).

3. **Final Report.** The final report will be submitted in 50 copies not later than 2 months after the contract period. Format for this report will be in accordance with the final report format established under Contract AF 33(600)-43369. DD Form 1473, Document Control Data - R&D, will be attached to each report (reference AFR 80-29). Report will include the following:

    a. Notices on the cover, first page, or title page as follows:

        (1) Sponsored by: Advanced Research Projects Agency, Nuclear Test Detection Office, ARPA Order No. 624.

<div style="text-align: right">Atch 1</div>

<div style="text-align: right">S/A # 1 - AF 33(657)-13668</div>

<div style="text-align: right">REPRODUCTION</div>

(2) _Availability_: Qualified users may request copies of this document from:

> Defense Documentation Center
> Cameron Station
> Alexandria, Virginia 22341

(3) _Acknowledgment_: This research was supported by the Advanced Research Projects Agency, Nuclear Test Detection Office, and was monitored by the Air Force Technical Applications Center under Contract AF 33(657)-13668.

b. Identification Information:

AFTAC Project No. VELA T/5051

Project Title

ARPA Order No. 624

ARPA Program Code No. 8100

Name of Contractor

Contract Number   *

Effective Date of Contract

Amount of Contract

Contract Expiration Data

Project Manager's, Scientist's, or Engineer's Name and Telephone Number

c. All seismograms and operating logs to include pertinent information concerning time, date, type of instruments, magnification, etc., will be provided when requested by the project officer.

4. _Special Reports_.

a. Special reports of major events will be forwarded by telephone, telegraph, or separate letter as they occur and should be included in the following monthly report. Specific items are to include, but are not restricted to, program delays, program breakthroughs, and changes in funding requirements.

b. Special technical reports will be required for instrument evaluations, project recommendation, and special studies when it is more desirable to have these items reported separately from the quarterly or final reports. Specific format, content, number of copies, and due dates will be furnished by this headquarters.

2

JUN 10 1965

CONTRACT CHANGE NOTIFICATION

46230

1. MASTER SERIAL NO.	5N-2827
2. CCN NO.	1
3. PAGE 1 OF 1 PAGES	

4. TO:	5. FROM:
The Geotechnical Corporation 3401 Shiloh Road Garland, Texas	ASD (ASWKS) Special Projects Division Directorate of Specialized Subsystems & Equipment, Wright-Patterson AFB, Ohio

6. PURCHASE REQUEST NO.	7. CONTRACT NO. AND/OR PURCHASE ORDER NO.	8. PROPERTY CLASS
WK-5-RD-2103	AF 33(657)-13668	N/A

9. Pursuant to the clauses of the contract relating to changes, the above named Contractor is hereby authorized and directed to accomplish the changes listed below in respect to the articles called for under said contract as the same has heretofore and may hereafter be amended; subject, however, to the terms and provisions set forth on the reverse side hereof. Whenever both a purchase order number and a contract number are shown above, both numbers will be used in any shipping paper, packing sheet, invoice, correspondence, or related document, the purchase order number preceding the contract number.

I. The Statement of Work To Be Done, referred to in PART I is amended to include work under Project Authorization No. VELA T/5051/ASD/31 Amendment # 2 dated 26 May 1965, as follows:

" Task 1c of Project Authorization No. VELA T/5051 is amplified to include operational testing of the deep-well seismometer on the ocean bottom in approximately 15,000 feet of water at location designated by the AFTAC Project Officer.

" Four identical systems of deep-well seismometers, cables, transmitters, buoys and anchors will be provided, of which three (3) systems will serve as spares.

" This work shall be included in reports required by basic contract.

" Work shall begin 1 June 1965 and be completed by 1 August 1965"
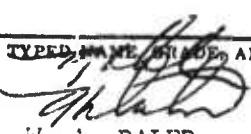
II. It is anticipated that incorporation of the changes cited above will increase the contract price by an estimated amount of One Hundred and Twenty Thousand Dollars ($120,000.00). Funds in the amount of One Hundred and Twenty Thousand Dollars ($120,000.00) are hereby obligated to cover the estimated increase in price resulting from this CCN. This obligation is for administrative purposes only and will not affect the right of either party to negotiate an equitable adjustment according to the provisions of the clause pursuant to which this CCN is made.

MAILING DATE JUN 7 1965

FUND ALLOTMENT: 97X0400.1302 6124 P5810 920F VT/5051 S595600/591600

Effective Date: 26 May 1965

10. DATE	11. TYPED NAME, GRADE, AND SIGNATURE OF CONTRACTING OFFICER
26 May 1965	W. A. DALER

12. DISTRIBUTION
Dallas C&D, 500 Ervay Street, Dallas, Texas   75201

AFPI FORM 35
APR 59

PREVIOUS EDITIONS OF THIS FORM MAY BE USED.

1. Tasks 1a, 1b, and that portion of Task 1c pertaining to oceanbottom testing, which have been completed, are deleted.

2. Task 1d and the rest of Task 1c, which are still applicable, are retained and enhanced by the following specific tasks:

    a. Task 1e: Assemble and operate an easily transportable vertical-array system employing 3 to 6 triaxial short-period deep-well seismometers. Record deep-hole three-component data at deep-well sites to be designated by the AFTAC Project Officer. Analyze the data obtained to determine the behavior with depth of the horizontal and vertical components of signals and noise.

    b. Task 1f: Continue developing techniques for improving signal/noise ratios and detecting low-level signals by processing data from vertical-borehole arrays of vertical and triaxial seismometers. Relate parameters of the processing techniques to varying conditions of seismic noise, seismographic system characteristics, geological structure, and geographic location. Provide and maintain an on-line vertical-array signal processing device and field test it at sites to be designated by the AFTAC Project Officer.

APPENDIX 2 to TECHNICAL REPORT NO. 67-3

OFF-SHORE MEASUREMENTS PROGRAM VT/5051

TO: MEMORANDUM

FROM: Richard M. Shappee

SUBJECT· Off-Shore Measurements Program,
             Ref. P-436, Project VT/5051

ABSTRACT

A deep-ocean seismograph was installed in the ocean approximately 200 nautical miles [1] off Cape Hatteras in water with a depth of approximately 2000 fathoms [2]. The seismograph consisted of: a Model 20171 seismometer modified to withstand high pressure and further modified to permit remote mass locking, unlocking, and centering; a Texas Instruments RA-3 amplifier; a voltage controlled oscillator; a telemetry transmitter; a programmed calibrator; and a seven-conductor, deep-hole cable. Other portions of the seismograph included a telemetry receiver, a discriminator, a Helicorder, and a tape recorder. Four attempts were made to install the seismograph, and the last attempt was partially successful.

INTRODUCTION

The Statement of Work to be Done of Project VT/5051 was amended on 26 May 1965 to include " .... operational testing of the deep-well seismometer on the ocean bottom in approximately 15,000 feet of water at locations to be designated by the AFTAC Project Officer." In accordance with the Project Officer's recommendation, a simple system was designed and made ready for measurements at sea on 19 June. This date was chosen so that measurements might be made of explosions scheduled as part of the East Coast On-Shore Off-Shore Experiment (ECOOE). The appendix shows the planned locations of explosions and the locations at which we planned to install our equipment.

INSTALLATION OF EQUIPMENT

The design of the original system taken to sea is shown in figure 1. Figures 2 and 3 show block diagrams of the electronic equipment used throughout the work.

A vessel (R. V. rospector) was leased and set out from Newport News with equipment and personnel on 17 June. The ship was on station on 18 June but the initial installation was delayed by severe weather until 20 June 1965.

---

[1] 1 nautical mile = 1.853 kilometers
[2] 1 fathom = 1.828804 meters
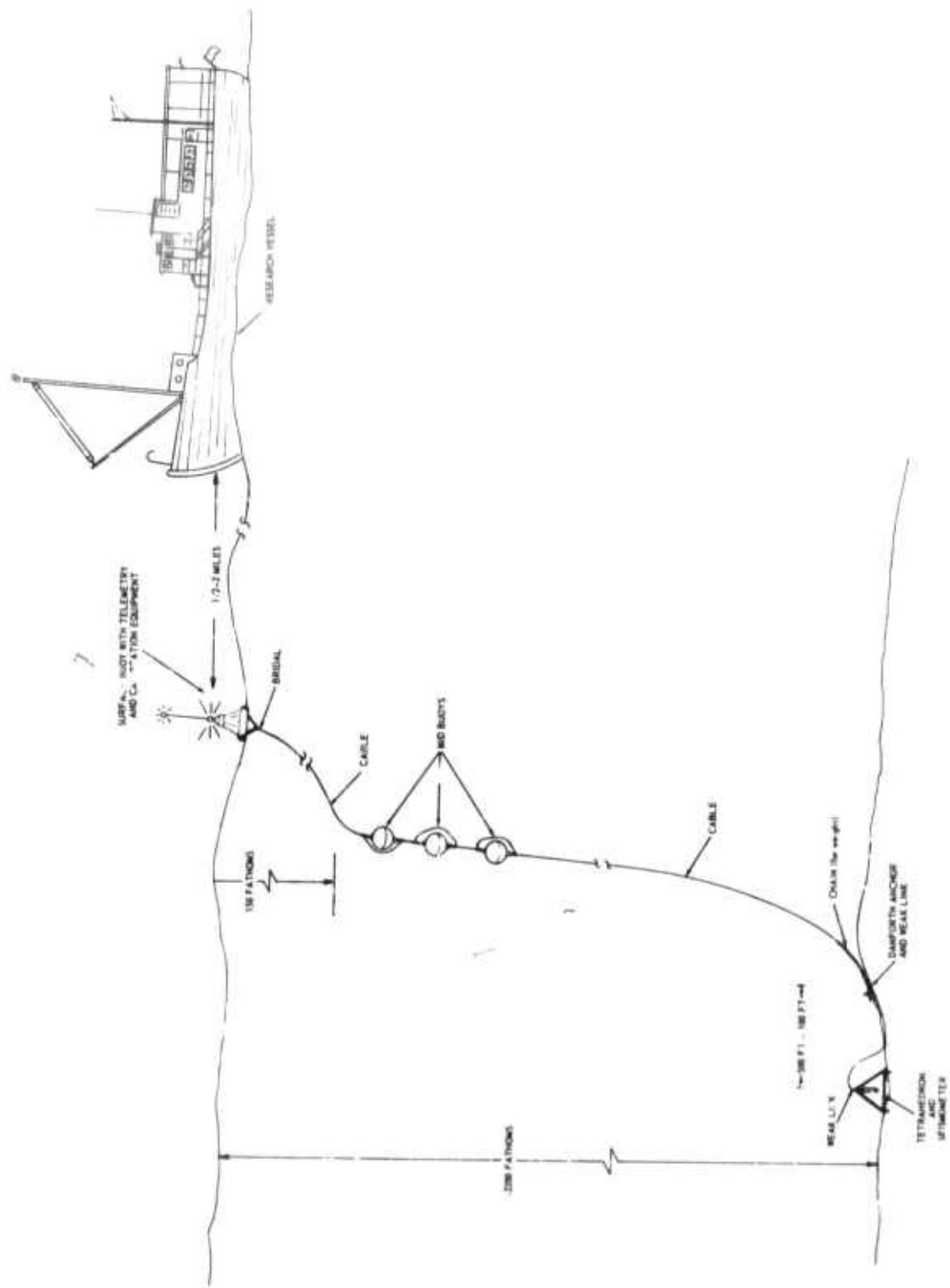
Figure 1. First system, off-shore measurements   G 2249

Figure 2. Data transmission and calibration
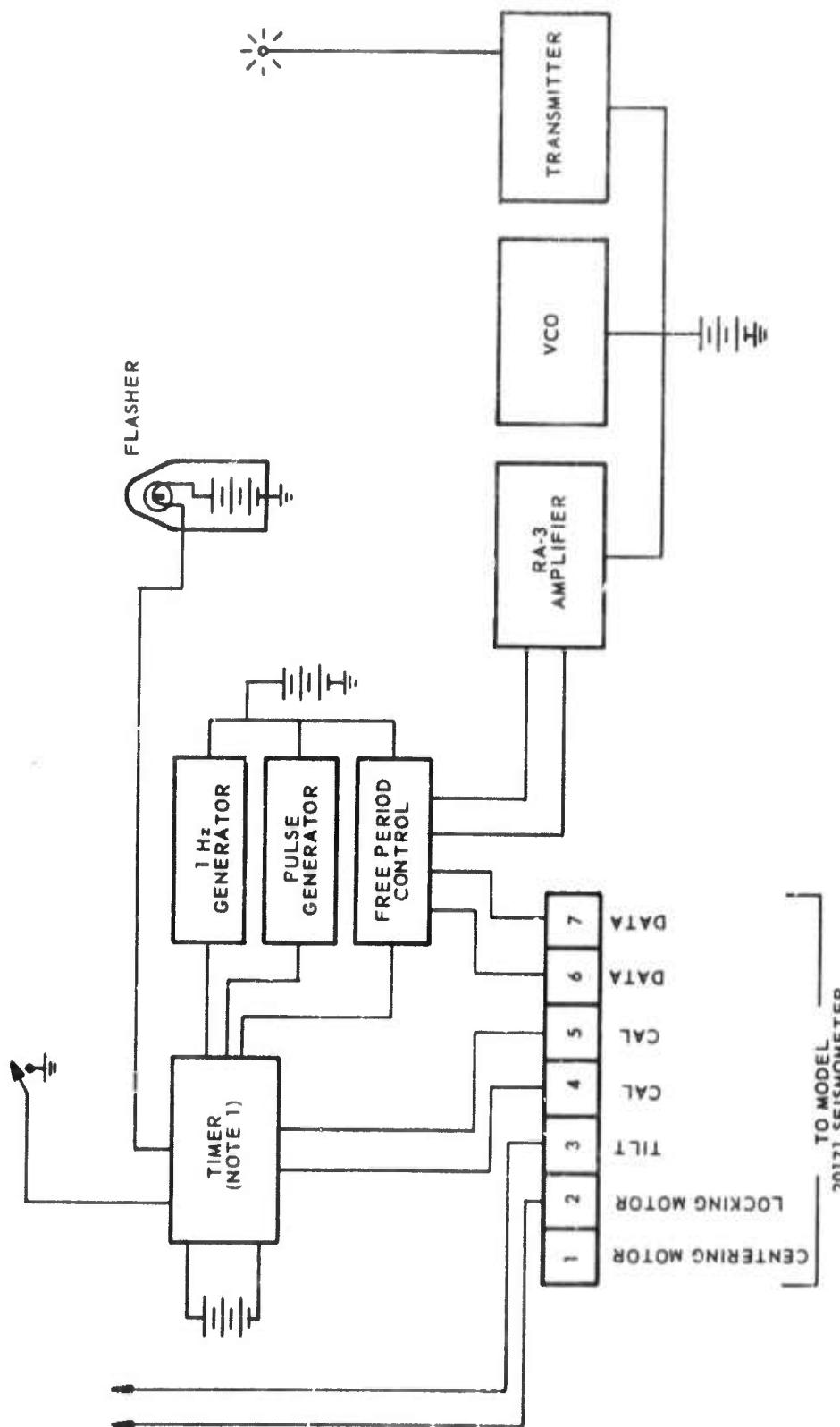
NOTE: TIMER APPLIES CALIBRATION SIGNAL, PUTS SEISMOMETER INTO FREE PERIOD AND APPLIES DC PULSES ONCE EACH DAY OR WHEN MANUALLY OPERATED SWITCH IS ACTUATED.

G 2250
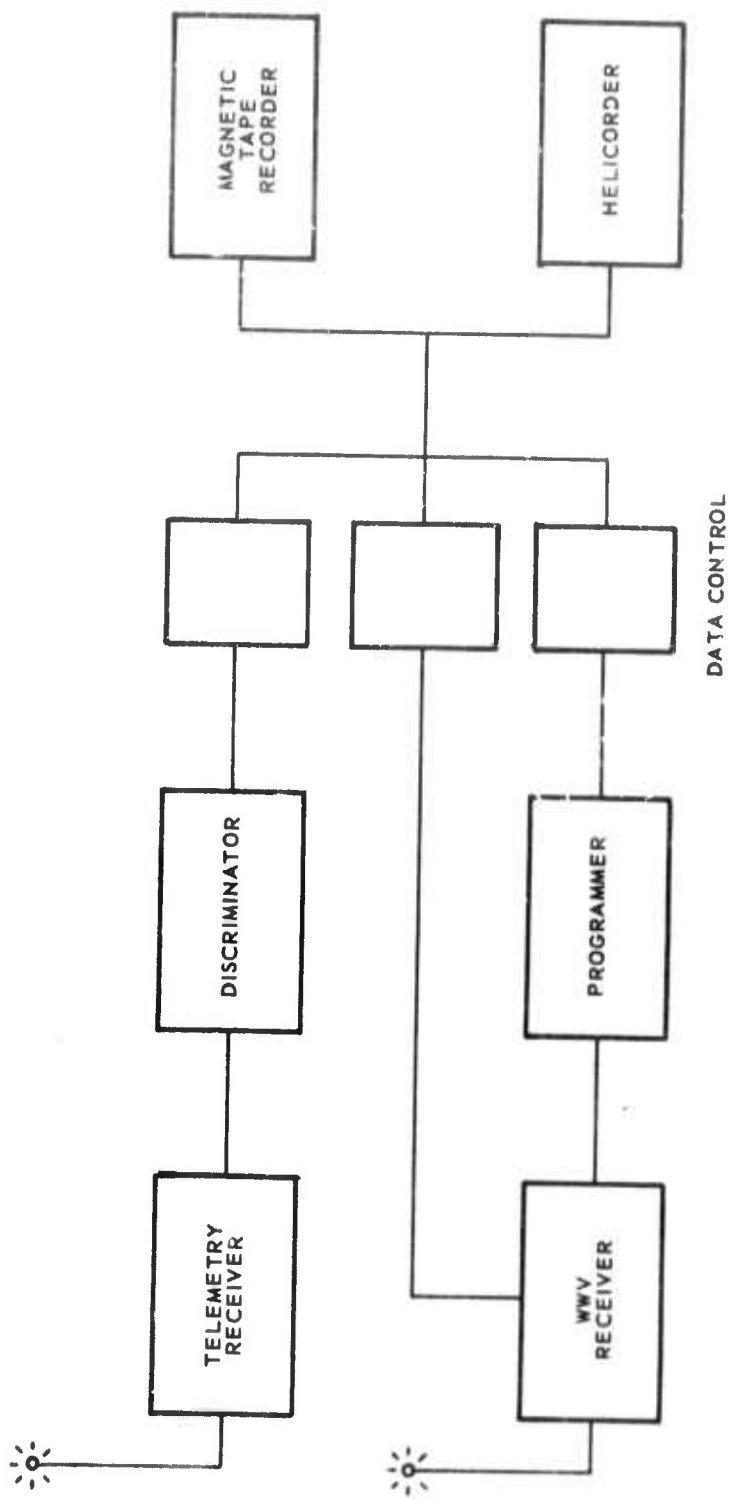
Figure 3. Receiving and recording   G 2251

Difficulty was experienced in putting the system into the ocean. It was found that the subsurface buoys, chain, and anchor caused severe kinking of the cable with resultant electrical shorts in the cable. The kinking was thought to be caused by rotation of the subsurface buoys and tetrahedron and by nontorque balance in the cable. Figure 4 illustrates the type of kinking. A second attempt was made to put the system into the sea, replacing the chain weight with zinc coring weights. The cable kinked again and the ship and equipment returned to port, arriving at Newport News on 24 June 1965.

Modifications to the design were made. These included changing the cable from 9.5 mm to 11 mm in diameter, construction of an ocean bottom "sled" (figure 5) that was designed to stream into the ocean current, revision in the surface buoy so that subsurface buoys were not required, and revisions to the anchor weights to increase their symmetry. The revisions were all intended to minimize cable rotation. This system is shown in figure 6.

After the modifications were completed, the ship set out for sea on 3 July 1965. The oceanbottom system was installed with a minimum of difficulty but it was found impossible to unlock the seismometer mass because of a motor failure. Later examination of the motor revealed that the failure was caused by mechanical binding in the gear box. The system was raised to the surface without having installed the surface buoy and all equipment was recovered except the sled and anchor. In order that the system might be at sea for the resumption of the ECOOE shot program on 6 July, a duplicate sled had not been constructed. It seemed reasonable to assume that if the system was not adequate, redesign would be required and a duplicate sled would be of little value. The ship returned to port and a new sled was constructed. The loss of time that resulted from the return to Newport News to construct a new sled did not greatly affect the recording schedule, as shots were not detonated during most of this time.

The new design was similar to the original design but included runners on the bottom of the sled in the belief that the sled might more readily be installed and retrieved. Additionally, a smaller anchor (39 kg) was used rather than the 230 kg anchor used previously. As before, weak links were provided between the cable and the seismometer, the seismometer and the sled, the sled and the cable, and between the anchor and the cable. Figure 7 illustrates some of the weak links.

Adverse weather prevented installation of the system until 12 July. When weather permitted, the system was lowered to bottom, the mass unlocked, and preparations started to connect the cable to the buoy. With approximately 8-1/2 turns of cable remaining on the winch drum and 3290 fathoms of cable

-5-

Figure 4. Kinked cable, 9.5 mm diameter

G 2252

TR 67-3, App 2
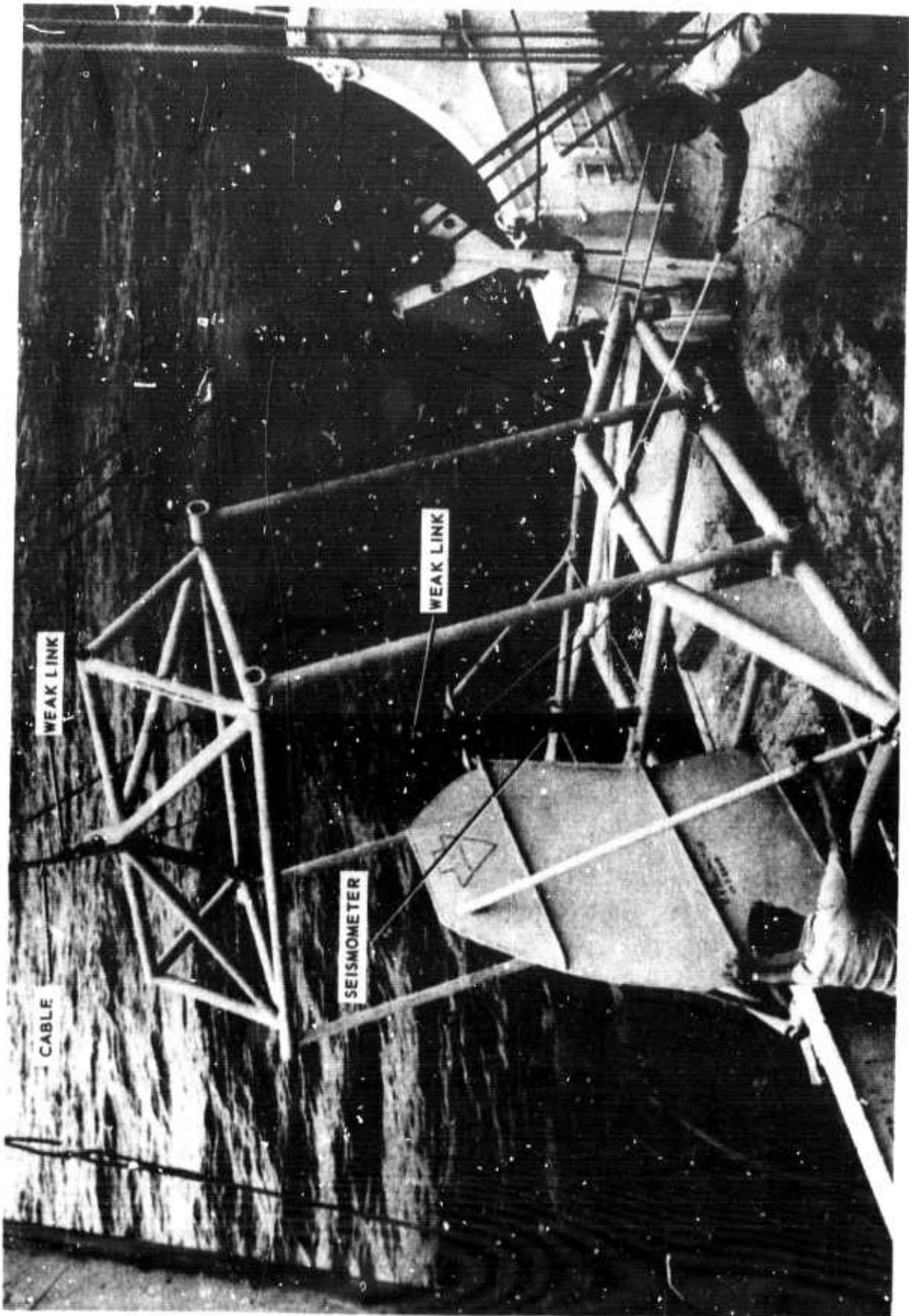
Figure 5. Sled being put over the side   G 2253

- 7 -

TR 67-3, App 2
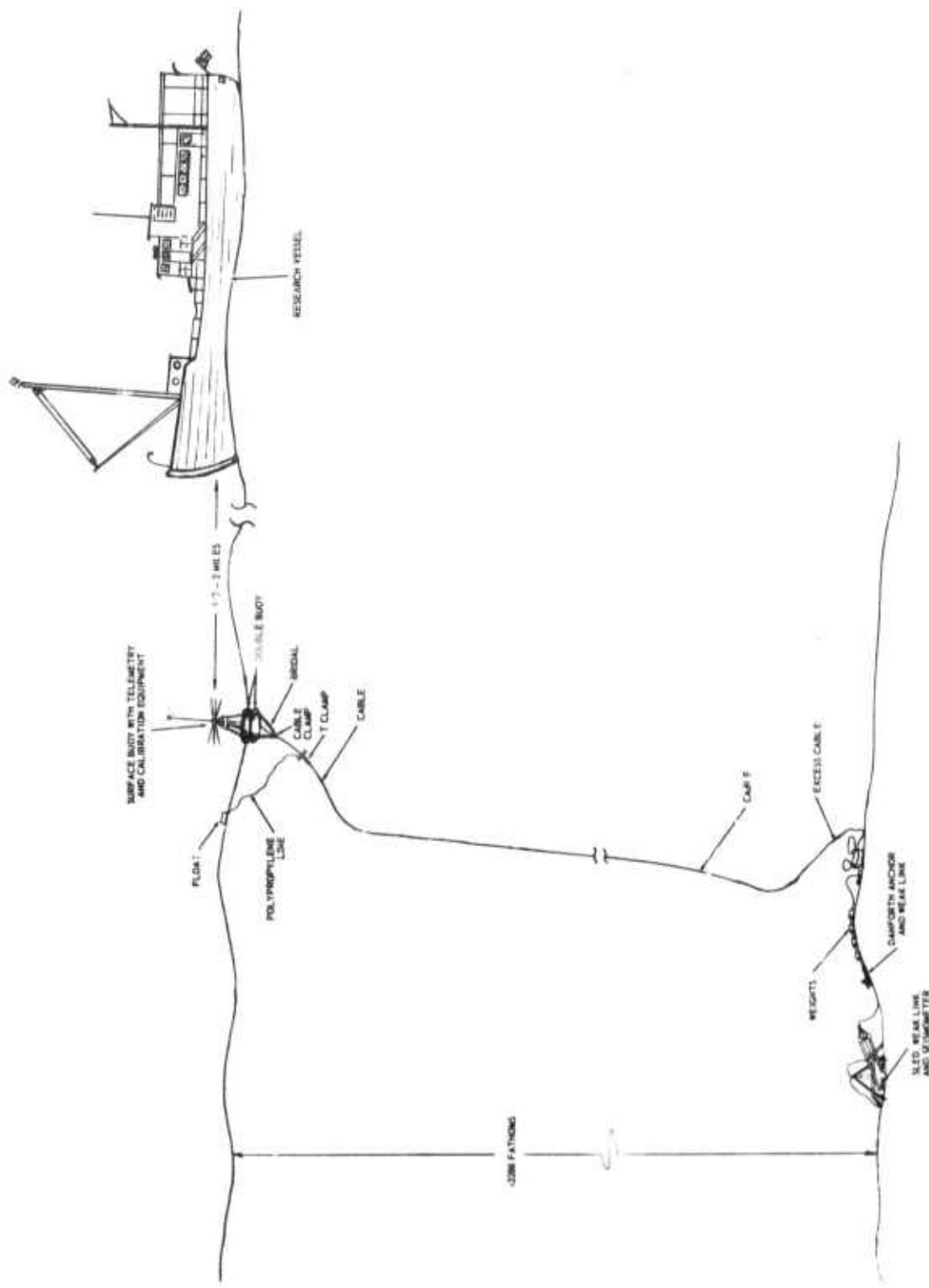
Figure 6. Second system off-shore measurements

G 2254
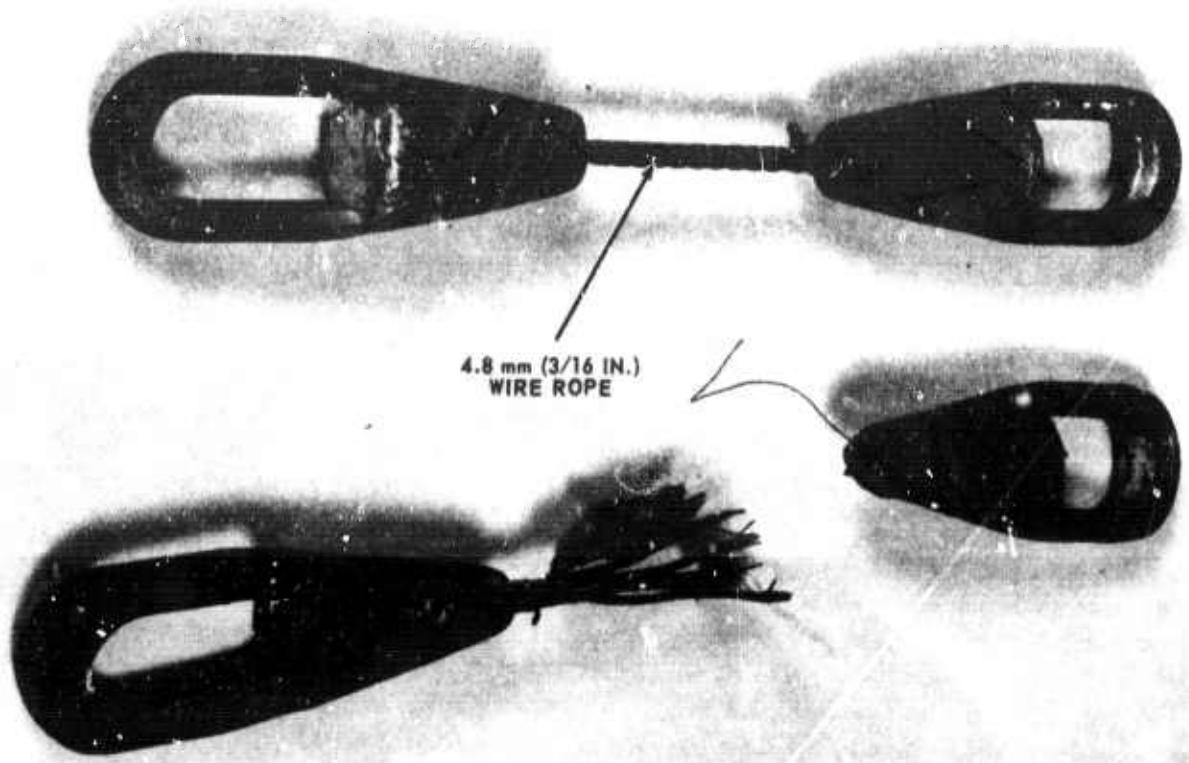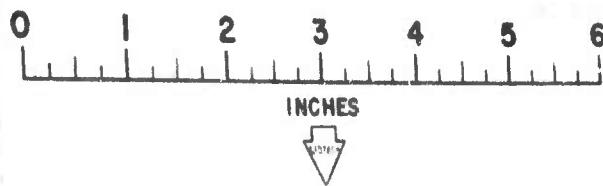
Figure 7. Weak link (1590 kg breaking strength)

TR 67-3, App 2

in the water, the T clamp was attached to the cable and secured with a doubled length of 16 mm polypropylene line. When the load of the cable was partially transferred to the 16 mm line, it appeared unsafe to continue to transfer the load. Then a 25.4 mm nylon line with a breaking strength of 11,800 kg was attached. With approximately 1/2 the load transferred to the nylon line, it was observed that the line was stretching excessively. Therefore, the load of the cable at the T clamp was taken by a 13 mm steel rope attached to the winch boom while a 16 mm steel line and swivel from the winch was prepared to take the load. The 16 mm line appeared safe and the signal line was disconnected at deck level by breaking apart the connectors in the line. A manila "tag line" was used to hold the clamp and signal line to the side of the ship while the work proceeded. A tendency for the signal line to kink was noted when it was slacked. The connector was made up to the buoy and the system operated with the buoy on the ship's deck. A calibration was performed and all appeared satisfactory. Next the manila tag line was released, prior to lowering with the 16 mm line. Upon doing so, the signal line revolved approximately 15 times at a high velocity. In doing so, the signal line was severely wrapped about the T clamp (figure 8), damaging the line. Since it then appeared impossible to respool the cable, it was decided to provide a strain relief between the T clamp and the buoy so the signal line would not be stressed and further damaged. The system was still electrically operational at this time. Four strands of 16 mm polypropylene line were used and the T clamp was lowered into the water while the buoy was lowered into the water using a cargo boom. When the weight of the cable was supported from the buoy, the 16 mm wire rope was cut. A line supporting the buoy from the cargo boom was cut and the system was then free of the vessel. Simultaneously, the data line failed electrically, undoubtedly from damage at the T clamp.

The installation of the system began at 1300 EDST and was finished the following morning at 0300 EDST. Work was concluded at that time, with the telemetry transmitter and the flasher on the buoy operational. The buoy was kept in sight throughout the night.

At daylight, the ship was brought near the buoy and it was observed that the ocean current was about 4 kt[3] rather than 0.8 kt expected and shown on charts. This greater current probably increased the cable load from about 450 kg to about 1820 kg. Figure 9 shows the buoy in the water. Note that both floats are below water.

---

[3] 1 kt = 1 nautical mile per hour
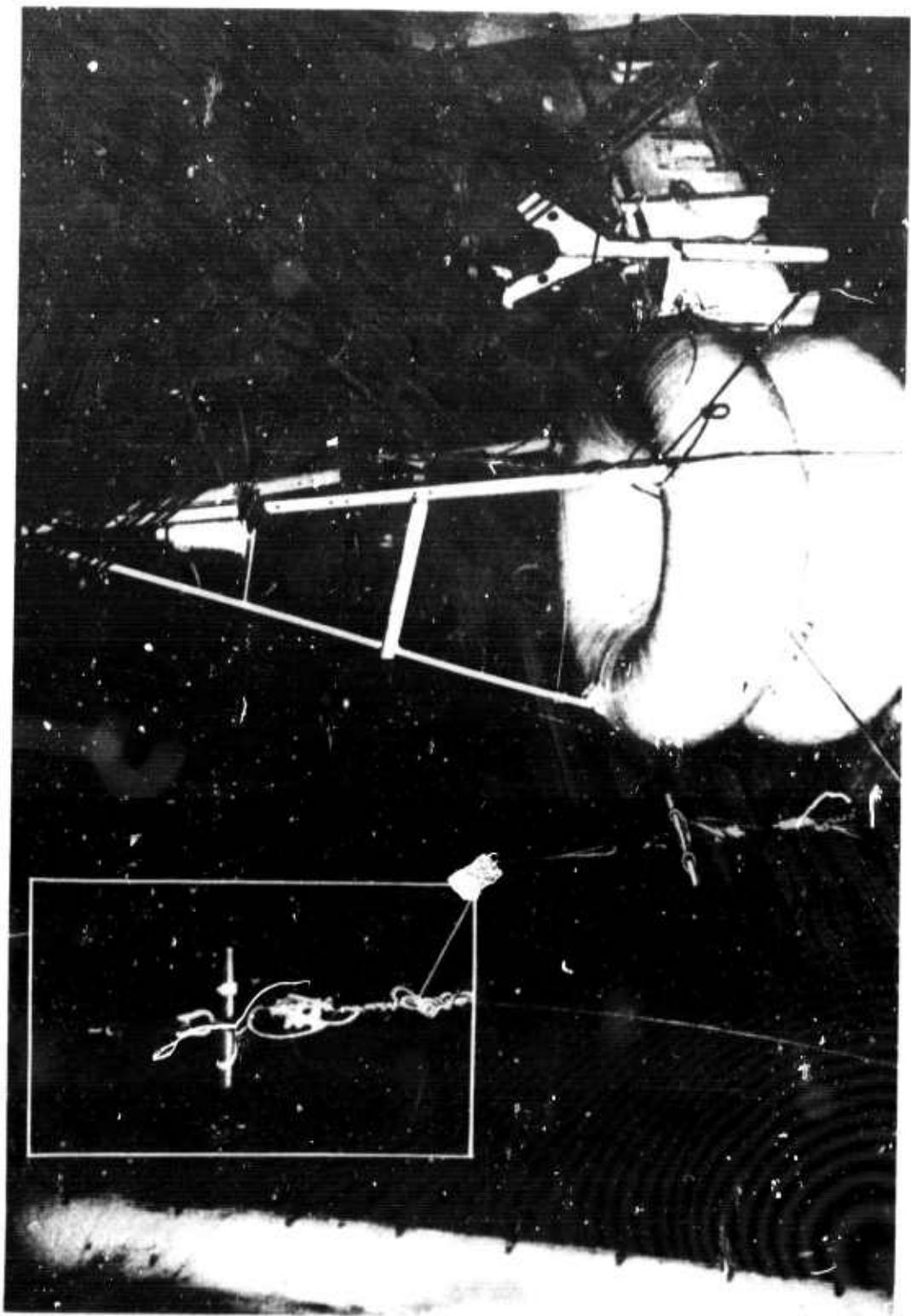
Figure 8. Cable twisted at T clamp G 2256

-11-
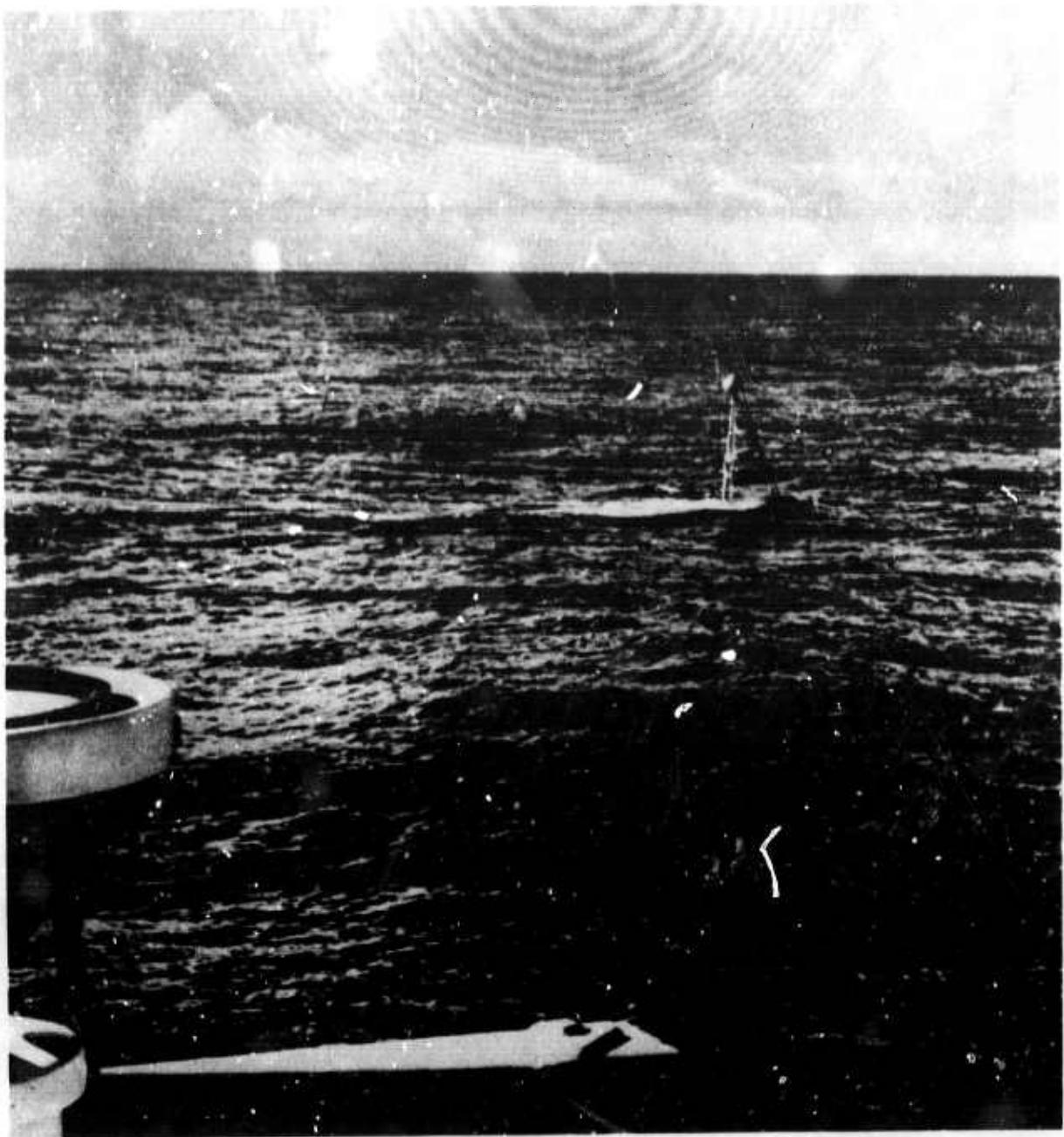
Figure 9. Buoy in the water G 2257

-12-

Because the signal cable was severely kinked and believed likely to break
at any time, no attempt was made to retrieve the buoy, cable, or subsurface
equipment. If the cable had broken during recovery operations, it was possible
that the buoyant force of the buoy would propel it upward with a resultant
injury to personnel nearby. We were advised by the Captain of the Prospector
that no liability would result from leaving the equipment in the ocean.

RESULTS

The system operated from the time the cable was connected to the buoy until
the buoy was put in the water. The programmed calibrator was cycled sev-
eral times during this interval and operated satisfactorily. Although some
noise appears on the recordings that may be the result of movement of the
buoy while on the ship's deck, approximately 30 minutes of data were recorded
with the seismometer on the ocean bottom. Figure 10 shows a portion of
recorded noise which is believed to be representative of the noise at the ocean
bottom.

CONCLUSIONS AND RECOMMENDATIONS

1. The techniques developed during this work were, for the most part,
satisfactory.

2. Improvement must be made in the method by which the weight of the
cable is transferred from the ship and winch to the buoy.

3. Future installations will have a greater likelihood of success if they are
made at a location where the ocean currents have lower velocity.
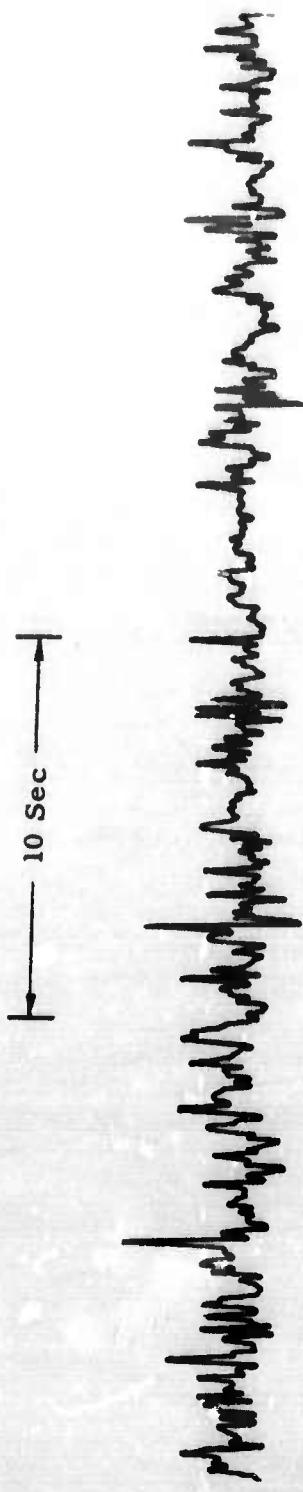
Figure 10. Noise recorded on 13 July 1965 on ocean bottom at 72°03'W. 36°11'N. Depth of water 3600m. Magnification 125K at 1 Hz

G 2258

10 Sec

APPENDIX

The East Coast On-Shore Off-Shore Experiment was planned as a part of the Transcontinental Geophysical Survey. Figures 1 and 2 show scheduled shot points and positions where the ocean bottom installations were attempted.

APPENDIX 3 to TECHNICAL REPORT NO. 67-3

EAST COAST ON-SHORE OFF-SHORE EXPERIMENT
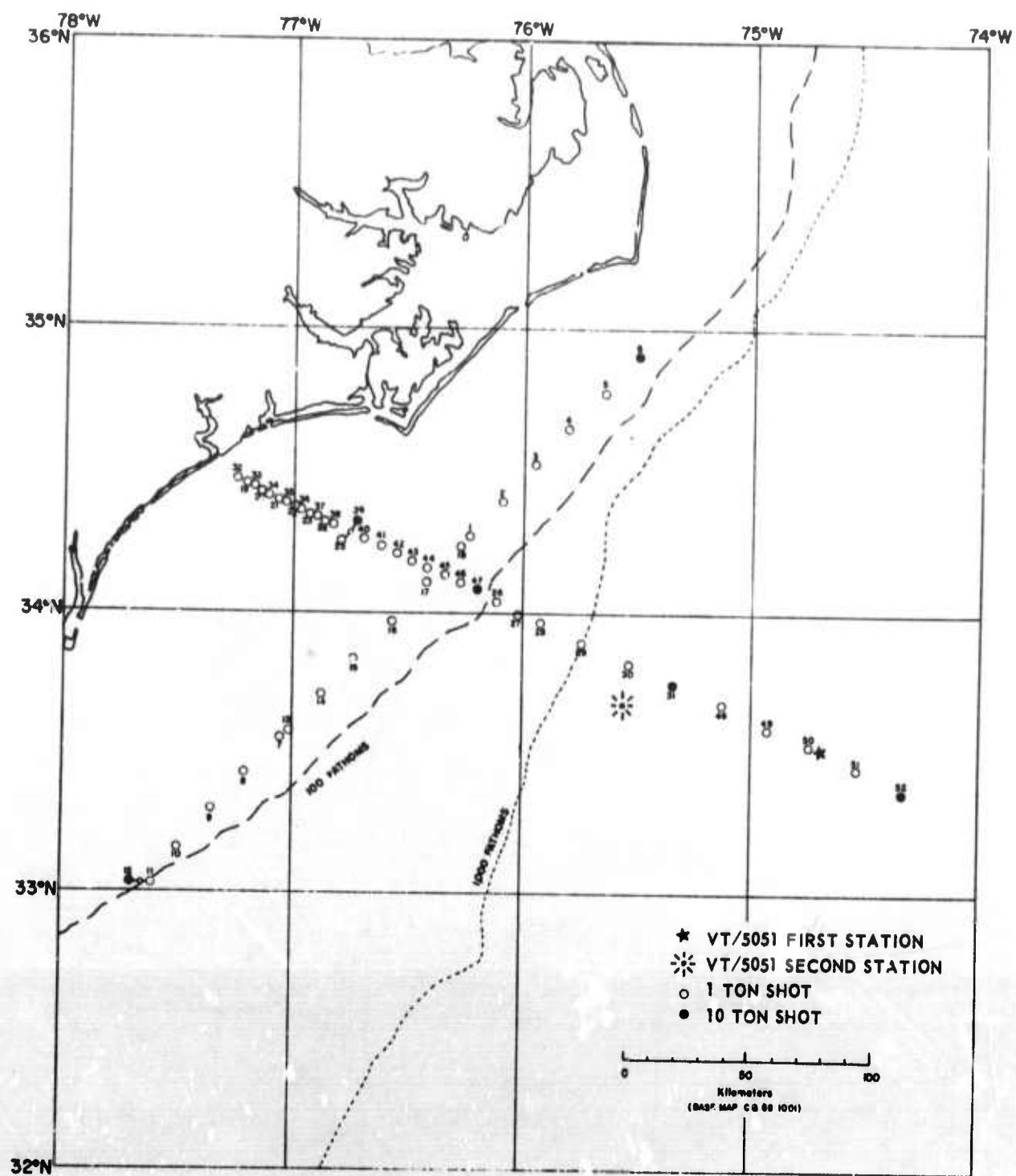
Figure 1. ECOOE shot point locations, southern lines

G 2259

-1-
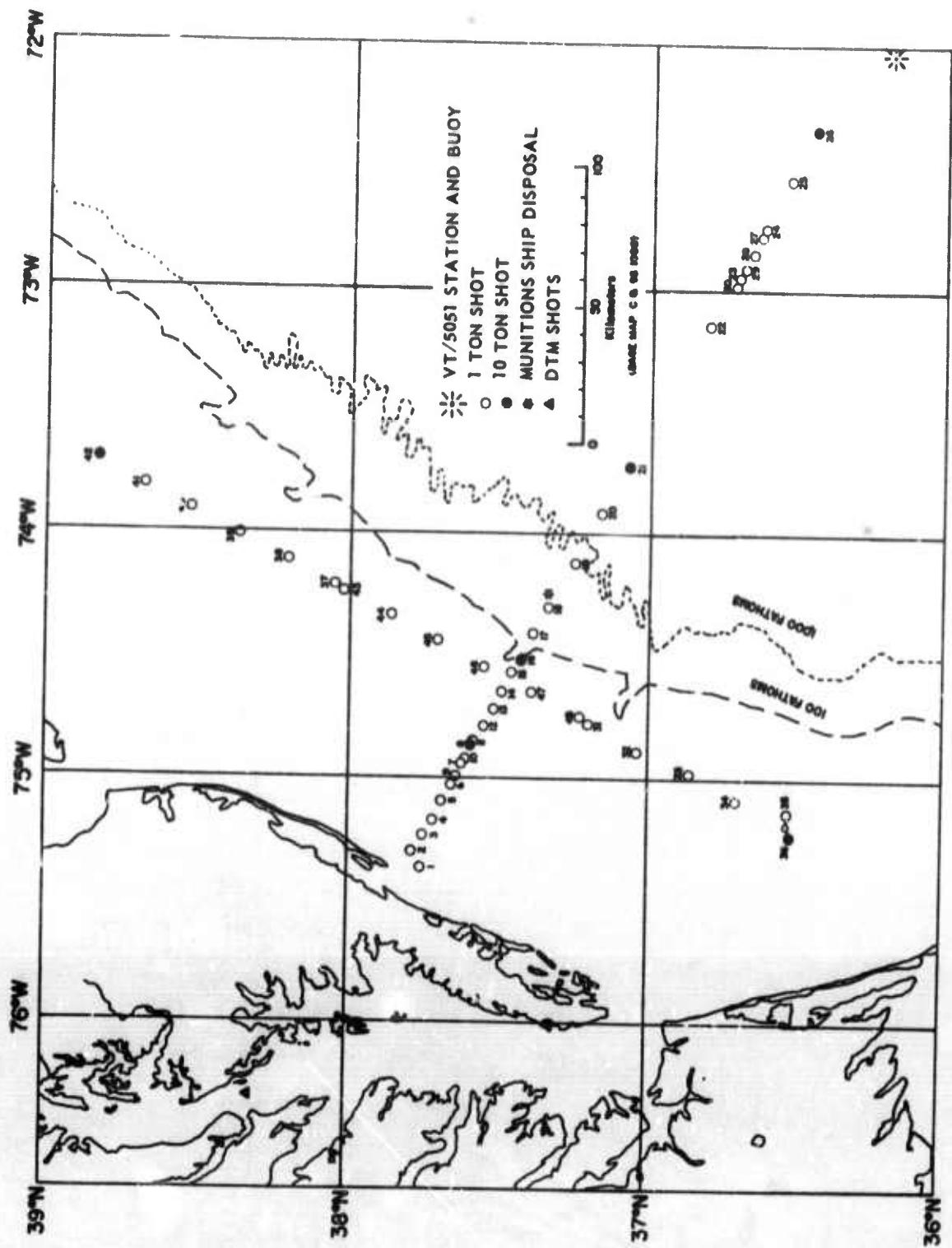
Figure 2. ECOOE shot point locations, northern lines   G 2260

TR 67-3, App 3

APPENDIX 4 to TECHNICAL REPORT NO. 67-3

DESIGN OF A DEEP-HOLE VERTICAL ARRAY

TECHNICAL REPORT NO. 65-3

DESIGN OF A DEEP-HOLE VERTICAL ARRAY

by

Richard M. Shappee

THE GEOTECHNICAL CORPORATION
3401 Shiloh Road
Garland, Texas

15 January 1965

IDENTIFICATION

AFTAC Project No: VT/5051
Project Title: Deep Well Research
ARPA Order No: 104-60
ARPA Project Code No: 8100
Contractor: The Geotechnical Corporation,
                            Garland, Texas
Date of Contract: 16 July 1964
Amount of Contract: $470,150.00
Contract No: AF33(657)-13668
Contract Expiration Date: 30 September 1965
Program Manager   Richard M. Shappee, Garland, Texas
                            BR8-8102, Area Code 214

TR 65-3

CONTENTS

ILLUSTRATIONS

DESIGN OF A DEEP-HOLE VERTICAL ARRAY

ABSTRACT

The design of a Deep-Hole Vertical Array was completed. The array was designed in groups of three seismometers. As a result, the vertical array can be operated with any multiple of three instruments.

The array used standard deep-hole seismograph components and new components designed for use in the vertical array. These new components included remotely operated line termination modules, motor-driven switches added to the seismometers, a control mechanism to select desired functions of the surface and subsurface equipment, special connectors, and handling equipment.

Preliminary tests indicated that the design of the array was satisfactory. Detailed measurements made with the array will be required to demonstrate its usefulness.

TR 65-3

DESIGN OF A DEEP-HOLE VERTICAL ARRAY

1. INTRODUCTION

This report discusses a project of research in deep-hole seismology. The work reported herein covers the design of a deep-hole vertical array suitable for use at depths up to 3040 m.

The purpose of this report is to present the technical findings, accomplishments, and design details of the vertical array. The report is submitted as a special report in compliance with paragraph 2, Reports, of the Statement of Work to be Done, Project VT/5051.

The body of the report is organized to first describe the basic system and design philosophy, then describe the design details of the new components required in the vertical array, and finally, describe operational tests of the system.

The work done was authorized in the Statement of Work to be Done of Project VT/5051 as Task 1a. The project was under the technical direction of the Air Force Technical Applications Center (AFTAC) and under the overall direction of the Advanced Research Projects Agency (ARPA).

Task 1a is as follows:

"a. Conduct systems engineering on deep-well instrumentation to obtain a capability of operating up to six seismometers in a bore-hole simultaneously. Evaluate the applicability of multiconductor data cable with quick-disconnect features between instruments in a vertical array. No major redesign of the deep-well seismometer is anticipated although mass size may be reduced to meet size and weight limitations. Following design approval by the government, assemble and conduct operational tests on the recommended deep-well seismographic system."

Our letter of 17 August 1964 (appendix 1) requested approval of our design, as required in the Statement of Work. Approval was received on 21 September 1964 (appendix 2) and the comments of the Project Officer were carefully

considered. As a result, the design of the system was modified to more nearly fulfill the objectives set forth in paragraph 3 of appendix 2. Consequently, the final design of the system was somewhat different than that described in appendix 1.

2. DESCRIPTION OF THE VERTICAL ARRAY, MODEL 22625

Figure 1 illustrates the components of the vertical array. As shown, three seismometers are operated on each of two cables. Each cable contains seven electrical conductors. Each of the top two seismometers on each cable has provisions for quick connection of two cables. Each of these seismometers also has an assembly added to permit surface control of subsurface switching of cable leads as required to perform calibration or operation of the seismometers.

The holelocks used with each of the top two seismometers on each cable were modified to use "cams" rather than the normal locking arms. This was done so that the seismometers could be locked at any position in the casing rather than just at casing joints. The holelocks were further modified to guide the cables so they would not be damaged by the holelock cam.

The process of installing the seismometers in the hole may be summarized as follows:

a. The seismometers are in the rack at the surface, ready for installation.

b. The cable and connectors are reeled onto the winch, and the end of the cable is threaded over the sheaves, ready to connect to seismometer No. 1.

c. The cable is connected to seismometer No. 1; the instrument is picked up from the rack and is lowered into the hole to a depth equal to the separation desired between instruments. The cable is then clamped at the well head to support the seismometer and cable weight.

d. The cable connectors are parted at the first joint and are connected to seismometer No. 2. Seismometer No. 2 is hoisted into the air, lifting seismometer No. 1 and the cable clamp at the well head.
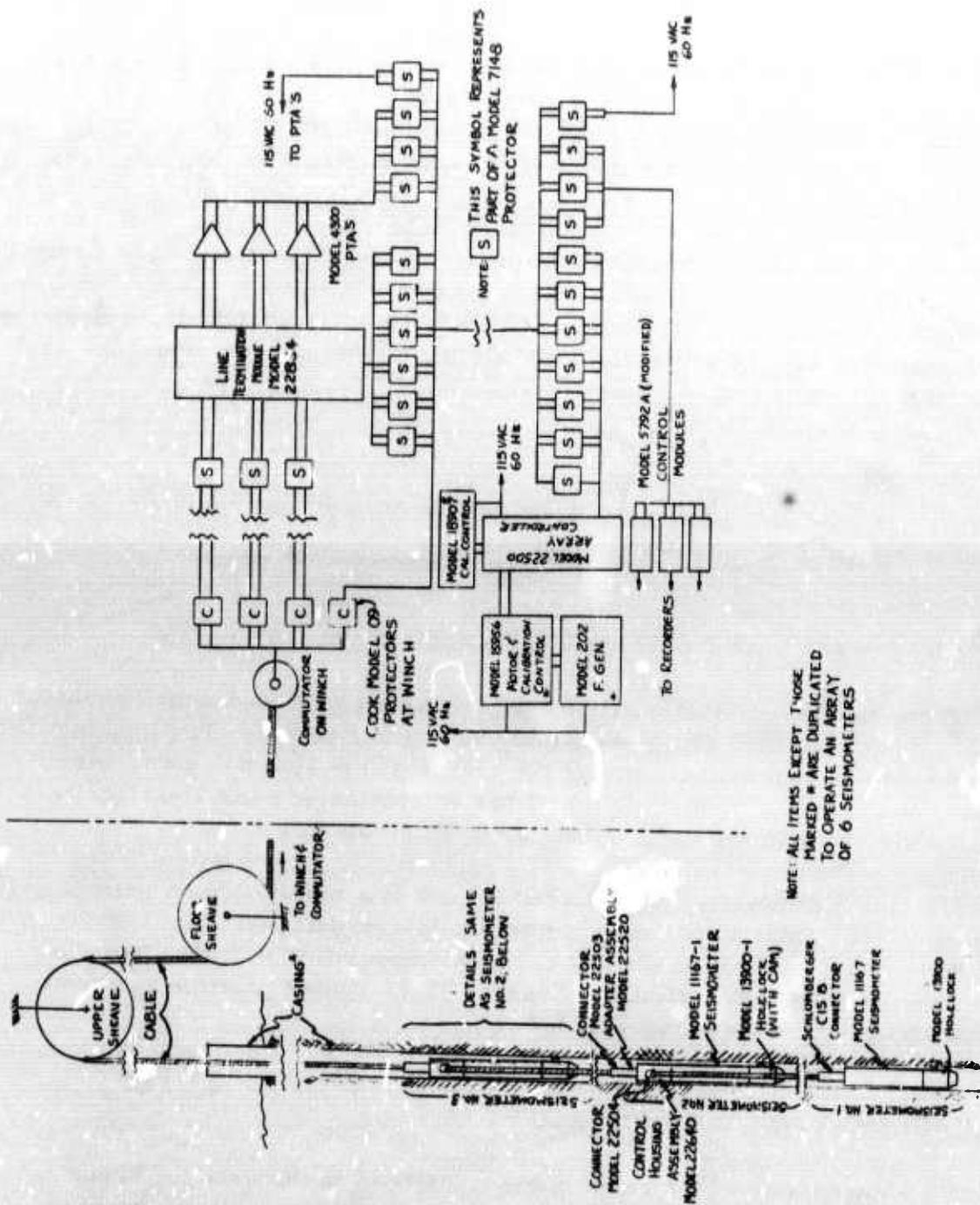
Figure 1. Deep-Hole Vertical Array, Model 22625

e. The cable clamp is removed at the well head, and seismometers Nos. 1 and 2 are lowered until seismometer No. 2 has been lowered to a depth equal to the separation desired between instruments.

f. These steps are repeated to pick up seismometer No. 3 and all instruments are lowered to total operating depth.

g. All seismometers are locked into the casing with the holelocks.

By selecting the conductor leads in the deep-hole cable with the Array Controller, Model 22500, Housing Assembly, Model 22640, and Line Termination Module, Model 22834, each seismometer is calibrated. After the calibration is completed, the conductor leads are again switched to connect the seismometers to the phototube amplifiers, so that all seismographs are in operation.

3. DESCRIPTION OF THE COMPONENTS OF THE VERTICAL ARRAY

3.1 CONTROL HOUSING ASSEMBLY, MODEL 22640

The control housing assembly, figure 2, contains cable connector receptacles and the motor-operated switch assembly shown in figure 3. The housing assembly provides terminations for the cables at the seismometer, permits remote selection of a given function of the seismometer, and electrically connects the appropriate cable leads to the seismometer.

The switching function is accomplished by use of a motor-driven geneva drive to rotate cams, which in turn operate Microswitches. The geneva drive provides a long dwell time at each switch position in order that the switch operation will be reliable. Sensing of the switch position is accomplished as described in paragraph 3.3.

3.2 CABLE CONNECTORS AND ADAPTER

Figure 4 shows some of the cable connectors used in the array. These connectors are substantially smaller than standard deep-hole connectors.
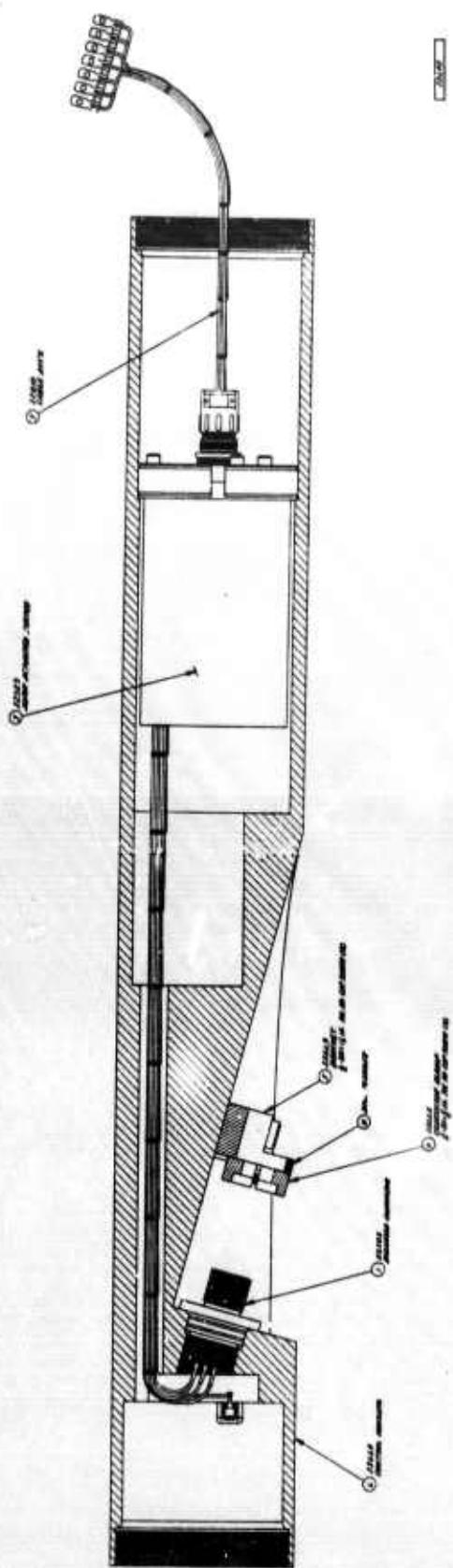
Figure 2. Control Housing Assembly, Model 22640
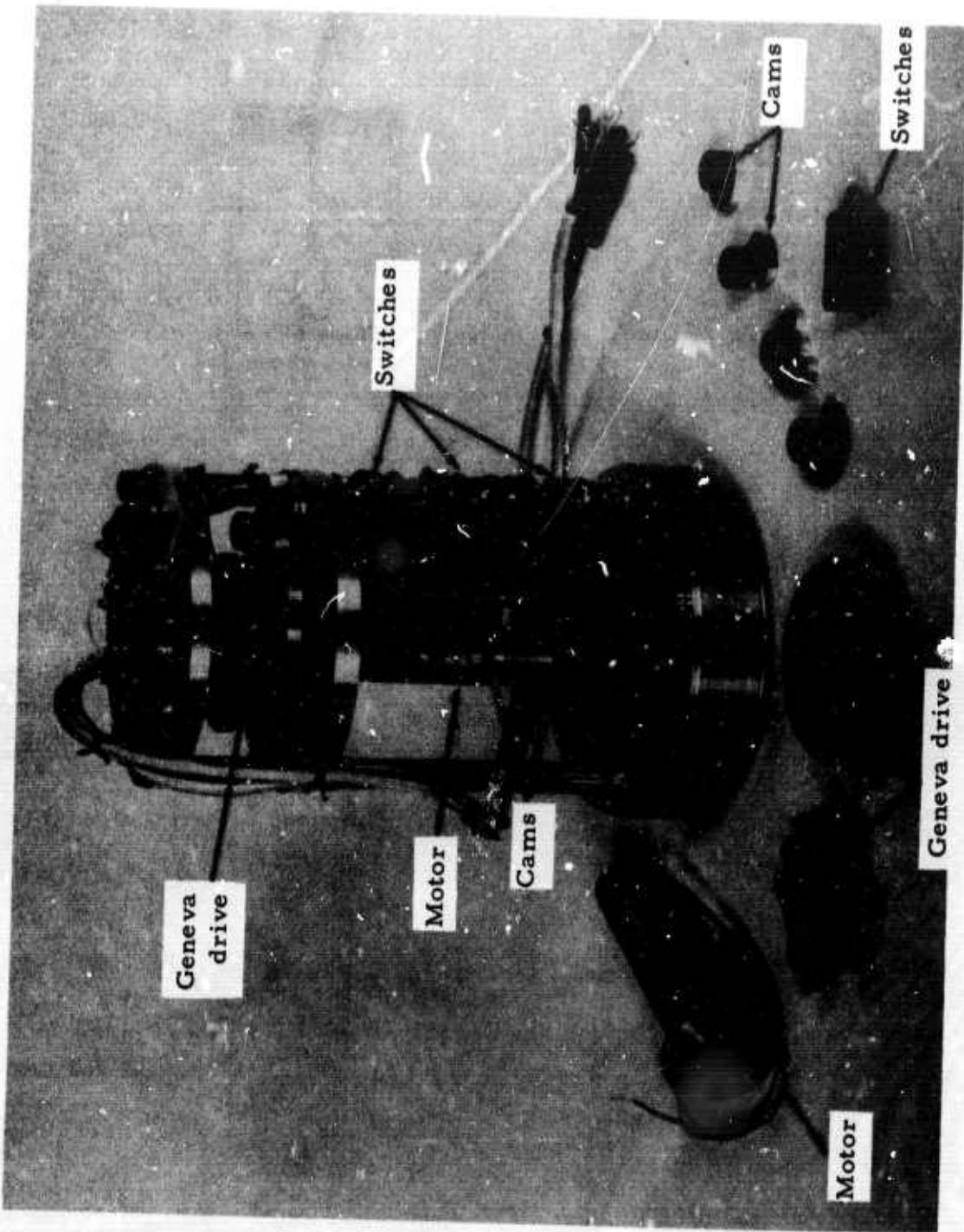
Figure 3. Motor Actuated Switch, Model 22523
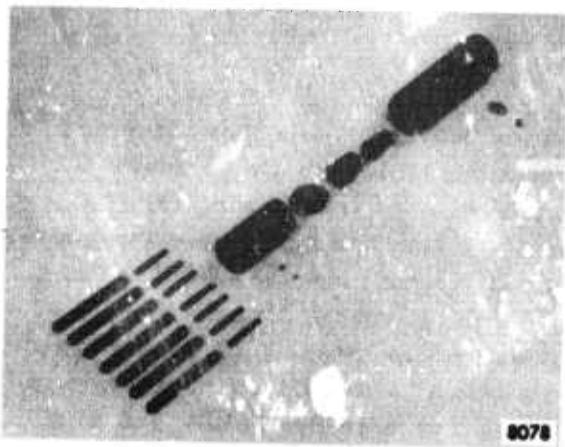
Connector, Model 22504
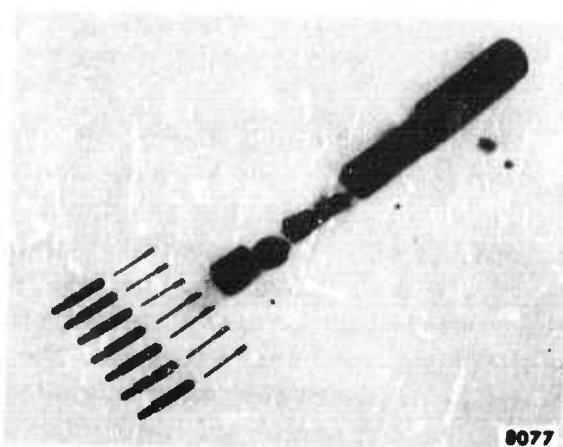
Connector, Model 22503
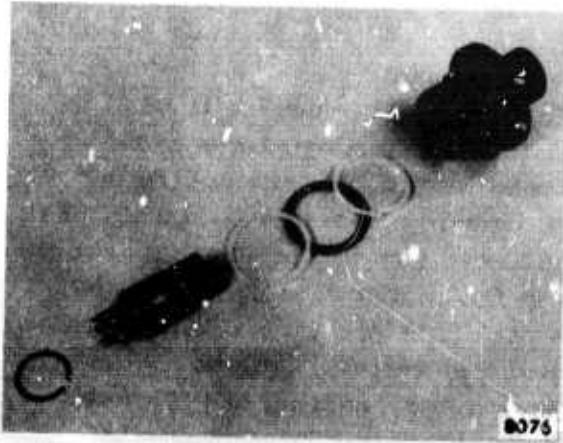
Connector, Model 22502
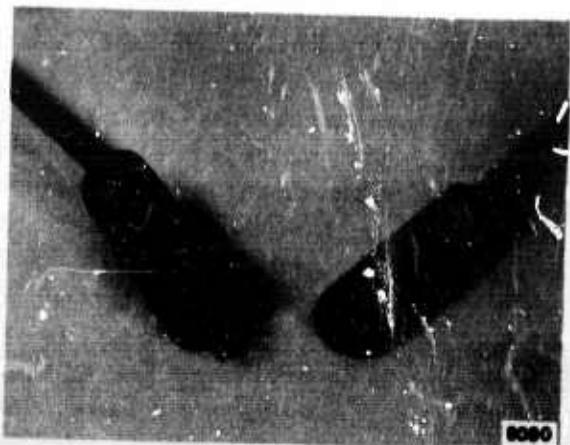
Connectors, Models 22503 and 22504

Adapter, Model 22520
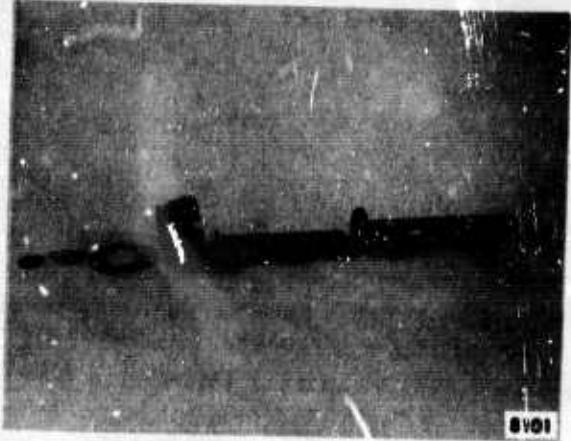
Figure 4. Connectors

Short lengths and small diameters are essential because the connectors are required to pass around sheaves and spool onto the winch drum. Figure 4 also shows an adapter that is used at the tops of four of the seismometers in the array of six. (Schlumberger adapters are used on the bottom seismometer of each group of three instruments.) The adapter functions as a fishing head and weak link for the seismometer, in addition to providing electrical connections. If it is necessary to break the cable away from the seismometer while at depth, screws at the top of the adapter will fail at a predetermined tension and the inner assembly of the connector will pull out with the cable, leaving an exposed, unobstructed fishing head.

3.3 ARRAY CONTROLLER, MODEL 22500

Figure 5 shows the Array Controller, Model 22500. This device is used to control the functions of three seismometers; two array controllers are necessary to control an array of six seismometers. The array controller provides voltage to operate the motors in the Housing Assembly, Model 22640, described in paragraph 3.1. The position of the switch in the housing assembly is sensed by monitoring the current flowing in the motor circuit; resistors are shunted across the motor at the various positions in its rotation, and the current change is used to sense the position of the switch. The resistors are isolated from the motor by a low-voltage zener diode; sensing of the motor position may be accomplished without operating the motor by applying a voltage less than the zener voltage and measuring the current through the resistors. The array controller also contains switches to remotely operate the Line Termination Modules, Model 22834, described in paragraph 3.4.

3.4 LINE TERMINATION MODULE, MODEL 22834

Figure 6 shows the Line Termination Module, Model 22834. This unit provides termination for three signal circuits and is electrically equivalent to three Line Termination Modules, Model 5874A, except that the free-period function is relay controlled, and a relay is provided to permit switching of the signal lines to an external circuit rather than to the phototube amplifier. The Model 22834 fits a Data Line Terminal, Model 7149, in the same space as three Model 5874A modules.

3.5 OTHER COMPONENTS OF THE ARRAY

Appendix 3 lists all components of the array.
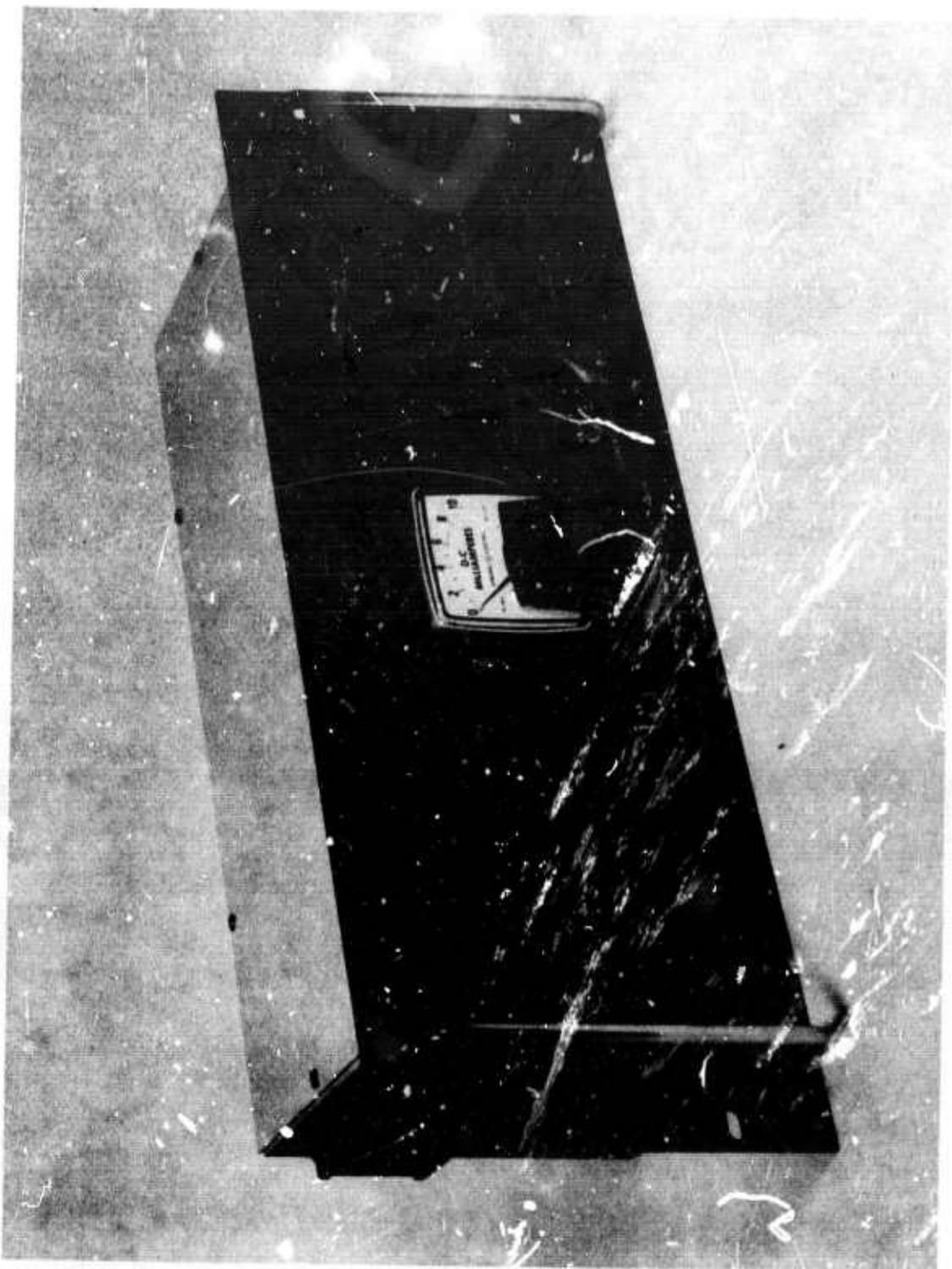
Figure 5. Array Controller, Model 22500
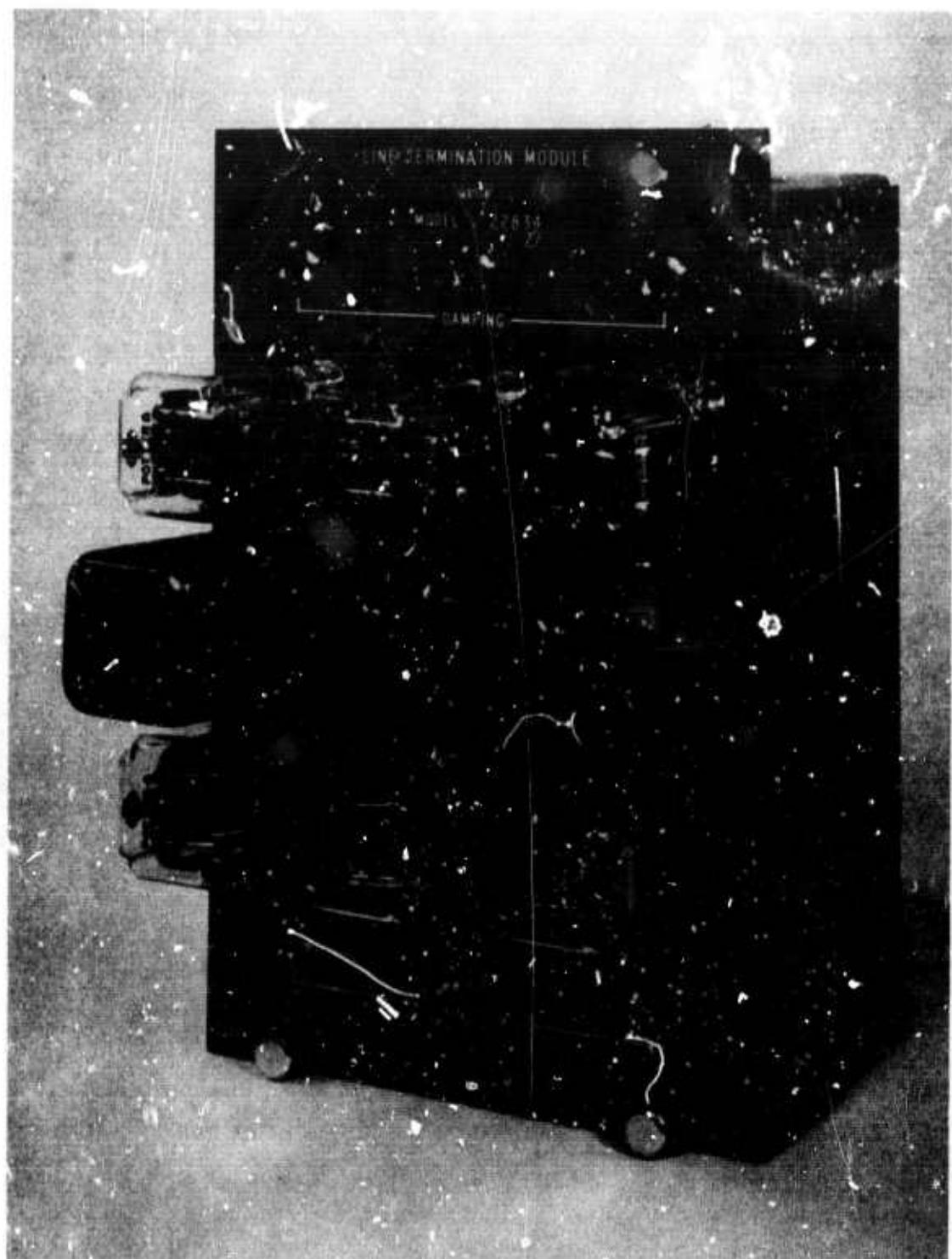
Figure 6.   Line Termination Module, Model 22834

4. INSTALLATION AND OPERATION OF THE VERTICAL ARRAY AT GRAPEVINE, TEXAS, TEST SITE

4.1 OVER-THE-HOLE EQUIPMENT

The hole at the Grapevine test site (GV TX) was used to test the vertical array. Because of the time schedule, only limited laboratory tests were performed on the individual components prior to the start of tests at GV TX.

The available facilities at GV TX included a 3040-m deep hole, two skid-mounted winches and cables, a standard oil-field derrick over the hole, and a building for maintenance and test work. A recording van from the Long-Range Seismic Measurement Program, Project VT/4051, and surface instrumentation from that project were available.

The winches were used in previous measurements at GV TX. The cable conductors are connected to the surface equipment through slip rings. The slip rings do not contribute measurable noise to the system.

The derrick at the site was used for installation and operation of the vertical array. In future installations, it would be possible to use some other over-the-hole device, such as the Heavy Duty Tripod, Model 18770. Because the work described in this report was largely experimental, the derrick was left in place and used in preference to a tripod.

As shown in figure 7, the derrick was modified to include a stand to hold seven seismometers and a catwalk around the top of the rack. The details of the stand are shown in appendix 5. If the derrick were not used, the stand would be either attached to the tripod, if one were used, or would be free standing on the ground and guyed as necessary.

4.2 LIGHTNING PROTECTION

Because of the large number of conductors required to connect between the PTA location and the recording van, a Station Protector, Model 7148, was used at each end of the cables rather than individual protectors. Figure 8 shows the protector installed at the PTA building. This protector, Model 7148, is the same as that used at the recording van in a normal LRSM installation.

Cook Electric Protectors, Model 09, were used at the winches.

Figure 7. Seismometer stand

Figure 8. Lightning protection at amplifier building

4.3 SURFACE ELECTRICAL CABLES

Spiral-four cable was used for all surface wiring exposed to the weather. Belden 8422 cable was used for all wiring within the recording van and amplifier building.

4.4 INSTALLATION IN THE RECORDING VAN

The rack-mounted equipment designed for use with the array was installed in the LRSM recording van wherever rack space was available. An additional tape recorder was installed to provide recording channels at multiple levels. In a routinely operated system, recording levels and/or summations would determine the number of channels required. In the experimental work at GV TX, extra channels were recorded to provide maximum flexibility.

The control modules in the recording van were modified as shown in appendix 4. The modification was made to allow tape recordings to be made at standard levels while operating at higher-than-normal amplitude on film.

4.5 OPERATION OF THE VERTICAL ARRAY

Preparations at GV TX for operation of the vertical array started in November 1964. All necessary equipment was moved to the site in December and operations started on 21 December 1964. Three seismometers were installed in the hole on 13 January 1965. Figures 9 and 10 show seismograms recorded with three seismometers in the hole.

The remaining three seismometers were prepared for installation the week of 11 January 1965 but were not in operation at the time of this report (15 January 1965).

5. CONCLUSIONS

The array, as designed, meets the requirements of the statement of work and includes the suggestions of the Project Officer (appendix 2). The installation of the array was accomplished at GV TX. No unexpected difficulties were encountered during the installation.
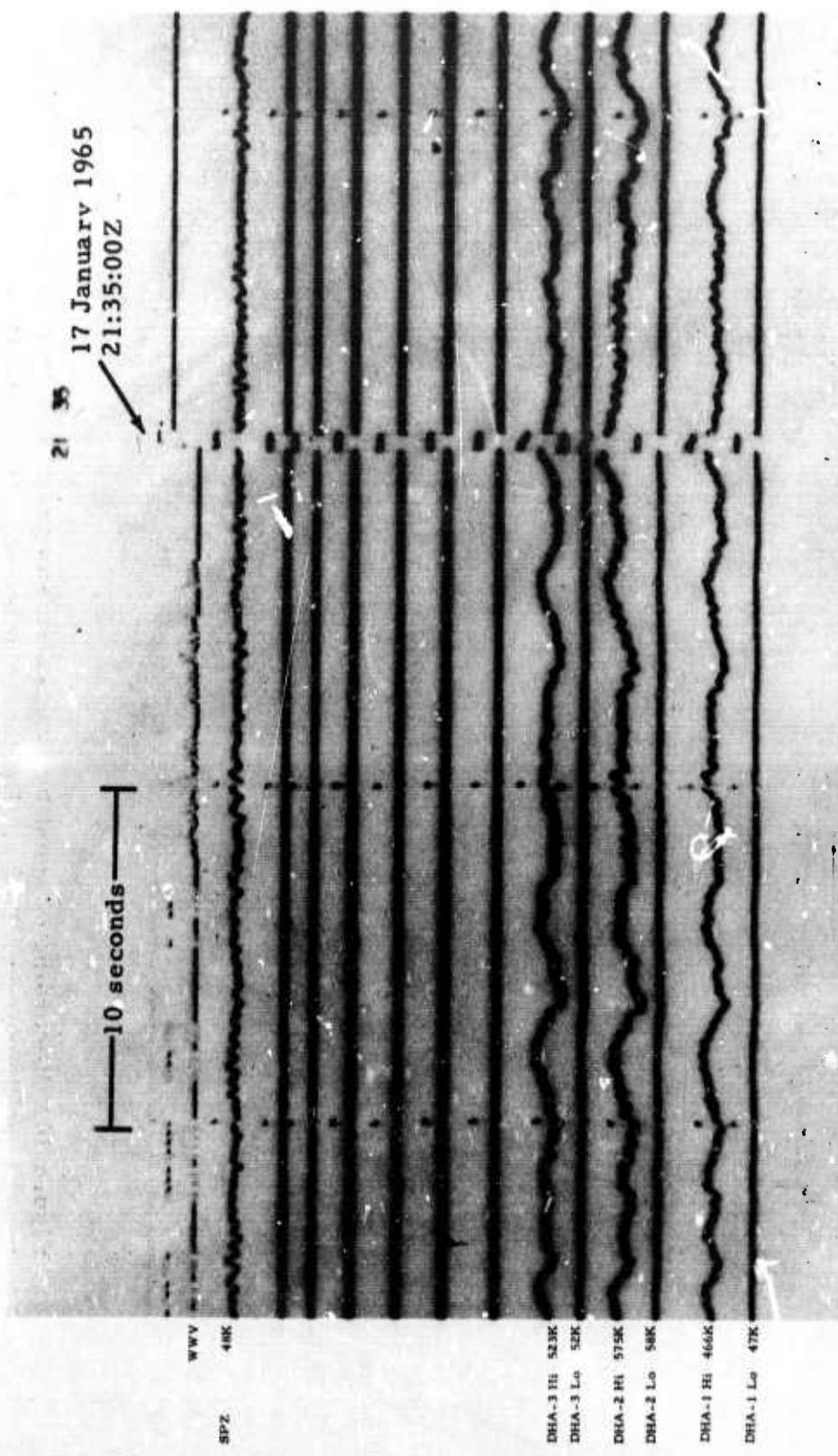
Figure 9. Recording of background noise by surface seismograph and deep-hole vertical array at Grapevine, Texas. Magnifications at 1 Hz (X10 enlargement of 16-mm film) DHA-1 at 2900 m; DHA-2 at 2600 m; DHA-3 at 2300 m

TR 65-3

-15-
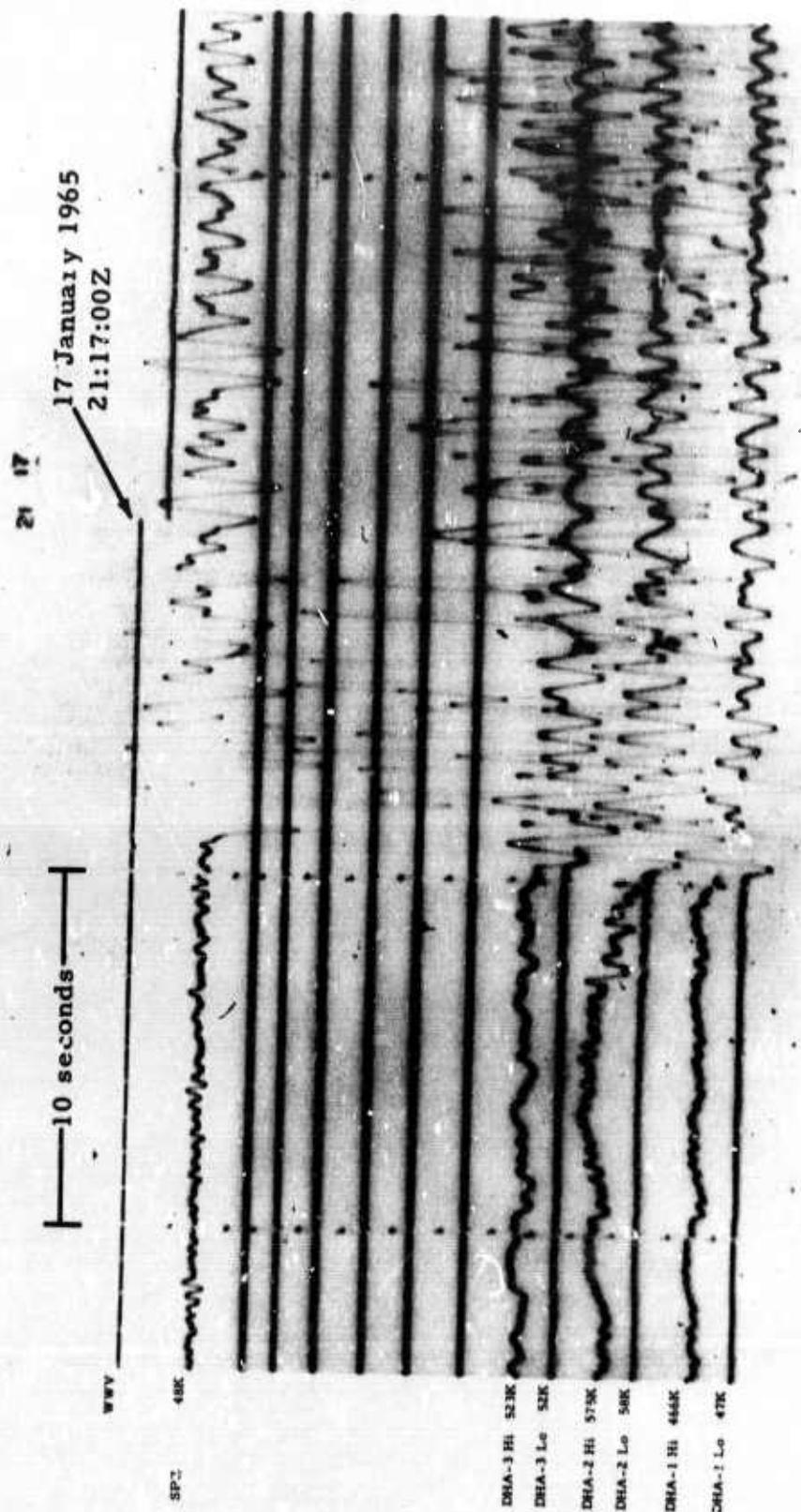
Figure 10. Recording of event by surface seismograph and deep-hole vertical array at Grapevine, Texas. Epicenter unknown. Magnifications at 1 Hz (X10 enlargement of 16-mm film) DHA-1 at 2900 m; DHA-2 at 2600 m; DHA-3 at 2300 m

6. RECOMMENDATIONS

The array should be operated at GV TX for a period of time sufficient to demonstrate its performance in a deep hole. After completion of work at GV TX, the array should be installed at a quiet site to determine its usefulness in improving signal-to-noise ratio.

APPENDIX 1 to TECHNICAL REPORT NO. 65-3

<u>LETTER, 17 AUGUST 1964</u>

HQ USAF (AFTAC/VELA Seismological Center)
Washington, D. C. 20333

Attention.   Major Robert A. Meek

Subject: Statement of Work, Project VT/5051
              Task la, Design Approval

Gentlemen:

The subject Statement of Work requires that AFTAC approval be
obtained for the design of a system to simultaneously operate six
deep-hole seismometers in a deep hole. We have started work on
this task and have reached certain conclusions as to a practical
method that should yield satisfactory results. It is important that
the fundamental concepts be acceptable to AFTAC before additional
work is undertaken. This is particularly important since we have
been asked to complete this work by 1 January 1965.

The approach we plan is substantially as outlined in our proposal, P-271,
dated 18 June 1964. That is, we propose to use one or more deep-hole
cables of the type used in our previous work and additional light-weight
cables. While special cables, with additional conductors could be used,
we do not believe this method is superior when all factors are considered.
Specific problems that would be created would include a need for a winch
with a much larger cable capacity than is presently available, redesign
of the seismometer to permit passage of conductors to other seismometers,
a method of handling short lengths of interconnecting cable and difficulty
in changing separation of instruments.

It should be pointed out that operation of six instruments increases the hazard of becoming stuck in the well, and that use of a single cable could reduce this hazard. However, this factor alone does not offer sufficient reason to use the single cable method.

We will undertake the development of the system at the Grapevine test site where, as you know, a standard pumping derrick is available. We plan to design our handling system around this derrick, and will plan to use a similar derrick at any other well where we may operate six instruments. These derricks are readily available and will in most instances be less expensive than a special purpose tripod.

We would appreciate your comments and approval concerning the preliminary design steps described above. We believe the described cable technique and the use of a derrick are justified and offer the greatest liklihood of success in this work. If you have questions concerning our plans or need further information, please contact the writer.

Very truly yours,

THE GEOTECHNICAL CORPORATION

Richard M. Shappee
Program Manager

RMS/map
CC: J. C. Cook

APPENDIX 2 to TECHNICAL REPORT NO. 65-3

LETTER, 21 SEPTEMBER 1964

REPLY TO
ATTN OF: AFTAC/VELA Seismological Center

SUBJECT: Design Approval of Task 1a, Project VELA T/5051   2 1 SEP 1964

TO: The Geotechnical Corporation
ATTN: Mr. Shappee
P. O. Box 28277
Dallas Texas 75228

1. Reference: ltr, Geotech, 17 Aug 64, Statement of Work, Project
VELA T/5051, Task 1a, Design Approval.

2. The design approach described in Proposal P-271 has again received
our review subsequent to your letter referenced above. Our approval is
given to proceed in the manner indicated.

3. While we agree with using the technique stated in your proposal, as
a practical matter we desire that several other approaches be considered.
We do not propose any new redesign if other possible techniques are
proven to be logistically unsound or impractical. In our opinion, however,
an expensive and complex winching and hoist system using large derricks
would not be desirable in the ultimate field applications of a vertical
array. Our considerations must take into account the technique when
placed in close proximity with other types of seismographs. Therefore,
we request your attention also be given to feasibility studies using
other methods considered to be practical.

4. This letter does not constitute authority to perform work which is not
covered by the contract. Any questions concerning allowability of costs
or contract interpretation should be referred to the administrative con-
tracting officer prior to incurring costs.

ROBERT A. MEEK   Copy to: DSCMD
Major, USAF
VELA Seismological Center
AF Technical Applications Center
DCS/Plans and Operations

Underwrite Your Country's Might - Buy U.S. Savings Bonds

TR 65-3, App 2

APPENDIX 3 to TECHNICAL REPORT NO. 65-3

EQUIPMENT LIST, DEEP-HOLE VERTICAL ARRAY

APPENDIX 3 to TECHNICAL REPORT NO. 65-3

EQUIPMENT LIST, DEEP-HOLE VERTICAL ARRAY

Table 1. Subsurface equipment

Item	Description	Mfr or supplier	Model	Qty
1	Deep-hole seismometer	Geotech	11167-1	6
2	Cable-head adapter kit	Geotech	22452	2
3	Adapter assembly	Geotech	22520	4
4	Holelock	Geotech	13900	2
5	Holelock	Geotech	13900-1	4
6	Control housing assembly	Geotech	22640	4
7	Connector	Geotech	22503	4
8	Connector	Geotech	22504	4
9	Connector	Schlumberger	CIS B	2
10	Union joint assembly	Geotech	22519	4
11	Cable	AS&W	7H4-TN	A/R

Table 2. Over-the-hole equipment

Item	Description	Mfr or supplier	Model	Qty
1	Sheave, 24 in. for 15/32-in. cable w/clearance for 1-1/4-in. connector	Any	-	4
2	Load cell 10,000 lb rating	Any	-	2
3	Goose neck	Any	-	1
4	Seismometer stand	Geotech	22081	1
5	Derrick	Any	-	1
6	Line wiper for 2-15/32-in. cables	Geotech	18894	1
7	T-clamp for 2-15/32-in. cables	Geotech	18898	1

Table 3. Recording and control

Item	Description	Mfr or supplier	Model	Qty
1	Array controller	Geotech	22500	2
2	Calibrator control	Geotech	18907	1
3	Motor and calibration control	Geotech	15956	1
4	Control module	Geotech	5792A (modified)	6

Additional equipment, such as recorders, and function generator, furnished as part of LRSM recording van.

Table 4. Amplifiers and line termination

Item	Description	Mfr or supplier	Model	Qty
1	Phototube amplifier w/5 cps galvo	Geotech	4300	6
2	Line termination module	Geotech	22834	2
3	Station protector	Geotech	7148	1
4	Lightning protectors	Cook	09	7
5	Filter	Geotech	6824-1	6
6	Power supply and cables	Geotech	4304	6

APPENDIX 4 to TECHNICAL REPORT NO. 65-3

SCHEMATICS OF CONTROL MODULE, MODEL 5792A AND
MODIFIED CONTROL MODULE, MODEL 5792A
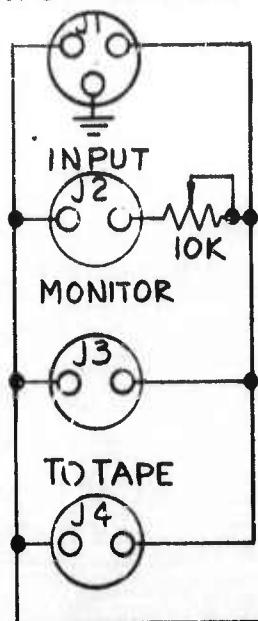
INPUT MONITOR

CONTROL MODULE MODEL 5792 A
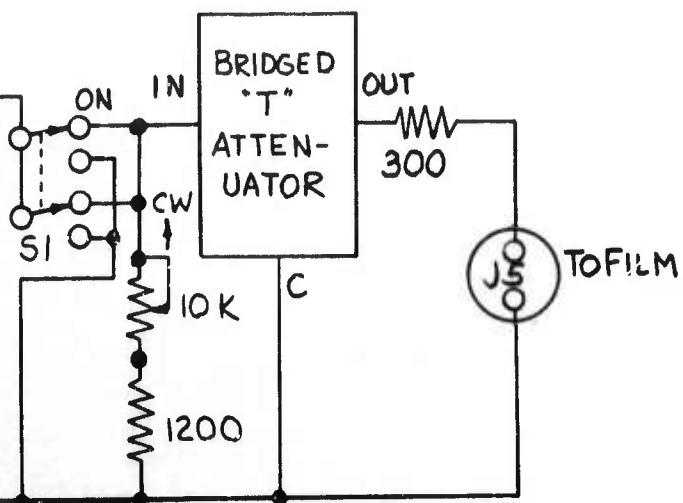
INPUT MONITOR
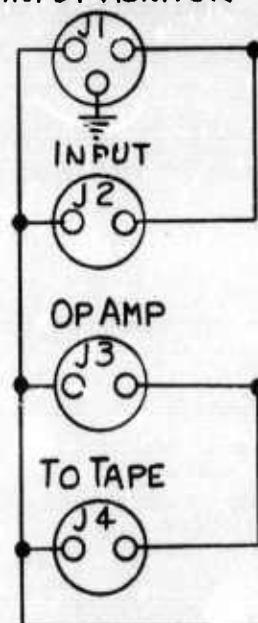
CONTROL MODULE MODEL 5792A
(MODIFIED)
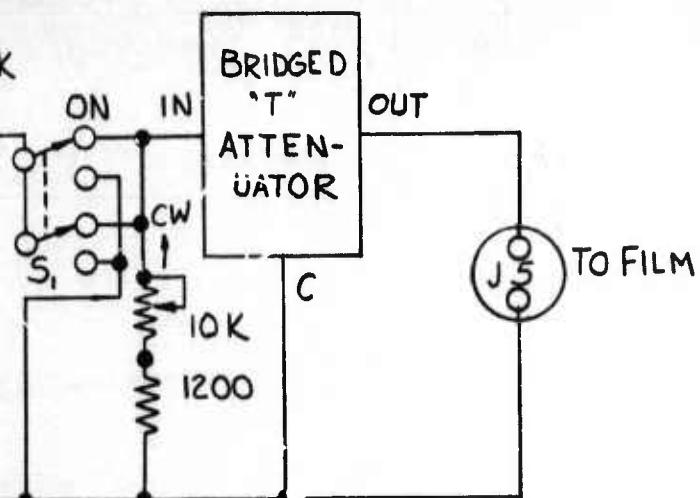
Schematics of Control Module, Model 5792A and
Modified Control Module, Model 5792A

APPENDIX 5 to TECHNICAL REPORT NO. 65-3

SEISMOMETER STAND
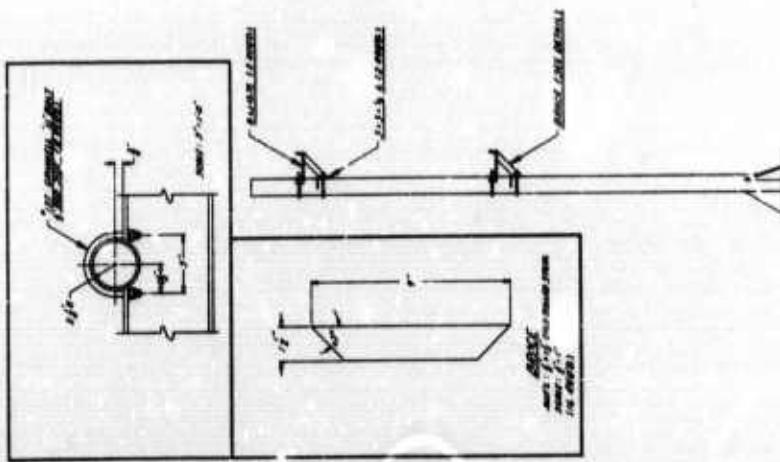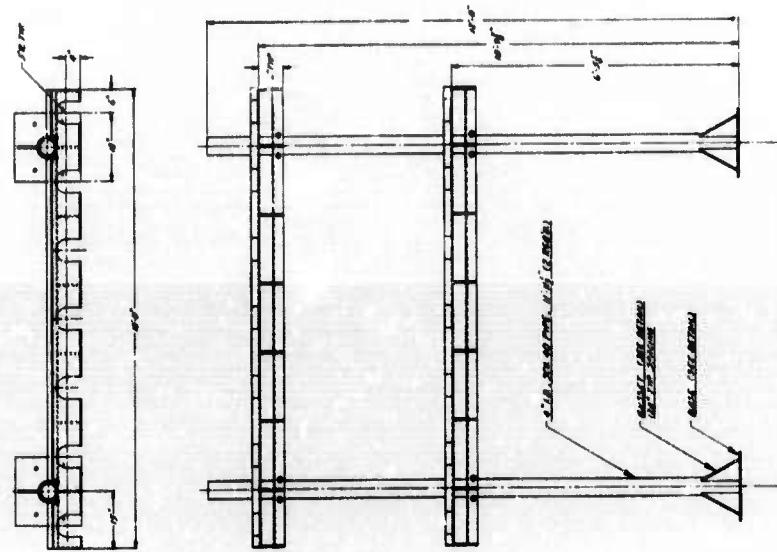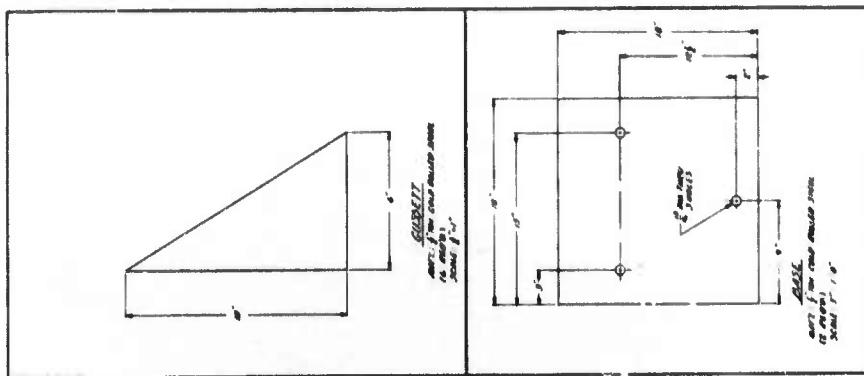
Seismometer stand

DOCUMENT CONTROL DATA - R&D

(Security classification of title, body of abstract and indexing annotation must be entered when the overall report is classified)

1. ORIGINATING ACTIVITY (Corporate author)	2a. REPORT SECURITY CLASSIFICATION
Teledyne Industries, Geotech Division 3401 Shiloh Road, Garland, Texas	Unclassified 2b. GROUP

3. REPORT TITLE

DEEP-WELL RESEARCH

4. DESCRIPTIVE NOTES (Type of report and inclusive dates)

Final, Report, 16 July 1964 - 28 February 1967

5. AUTHOR(S) (Last name, first name, initial)

Shappee, Richard M.
Douze, Eduard J.

6. REPORT DATE	7a. TOTAL NO. OF PAGES	7b. NO. OF REFS
28 February 1967	170	

8a. CONTRACT OR GRANT NO.	9a. ORIGINATOR'S REPORT NUMBER(S)
AF 33(657)-13668 b. PROJECT NO. VELA T/5051 c. d.	Technical Report No. 67-3 9b. OTHER REPORT NO(S) (Any other numbers that may be assigned this report) ---

10. AVAILABILITY/LIMITATION NOTICES

Qualified requesters may obtain copies of this report from DDC.

11. SUPPLEMENTARY NOTES	12. SPONSORING MILITARY ACTIVITY HQ USAF (AFTAC/VELA Seismological Center) Washington, D. C. 20333

13. ABSTRACT

A deep-hole array of six short-period seismometers was tested at the test site near Grapevine, Texas (GV-TX). After a brief period of successful operation, half the array was moved to the site near Apache, Oklahoma (AP-OK), and the other half was moved to the site near Franklin, West Virginia (FN-WV). Various techniques were employed to process the output of these arrays. The deep-hole test site (GV-TX) was maintained for testing applications requiring the use of a deep hole, including testing the triaxial seismometer and testing to determine if a useful long-period response could be obtained from the Model 11167 deep-hole seismometer. The results indicated it would require a complex and unstable system to provide a long-period response.

During the 29-month duration of this program, measurements were made in deep holes in West Virginia, Texas, Utah, Oklahoma, and Pennsylvania. Additionally, an off-shore measurement program was undertaken.

The information from wells and surface arrays was used to study short-period (6.0-0.3 sec period) noise and signals. An attempt was made to show that higher mode Rayleigh waves and body waves are present in the noise by comparing theoretical curves with experimental results. It was shown that surface waves generally predominate at the longer periods while body waves appear at the shorter periods at quiet sites. Not all data could be interpreted to define the wave types present. The short-period signals were analyzed both visually and digitally. Signal amplitudes at the surface were shown to be at least twice as large as at depth. The impulse response of layered media was used to compute inverse filters which changed the waveform characteristics of the deep-hole signals into those of the surface signals. Some preliminary work was done with the horizontal data obtained from the triaxial seismographs.

A complete system, composed of four triaxial seismometers, a digital processor, and associated equipment, was installed and operated at AP-CK. Data obtained from this array were processed using optimum filtering techniques. These techniques required the use of the inverse filters mentioned above and filters derived from the Wiener least mean-square technique. Both single-channel and multichannel processes were employed; however, the results obtained to date indicated that a one-sided single-channel optimum filter was the most effective processor.

DD FORM 1473
1 JAN 64

14	KEY WORDS	LINK A		LINK B		LINK C	
		ROLE	WT	ROLE	WT	ROLE	WT
	Vertical array Triaxial seismographs Optimum filtering VT/5051 Signal processor						

INSTRUCTIONS

1. ORIGINATING ACTIVITY: Enter the name and address of the contractor, subcontractor, grantee, Department of Defense activity or other organization (corporate author) issuing the report.

2a. REPORT SECURITY CLASSIFICATION: Enter the overall security classification of the report. Indicate whether "Restricted Data" is included. Marking is to be in accordance with appropriate security regulations.

2b. GROUP: Automatic downgrading is specified in DoD Directive 5200.10 and Armed Forces Industrial Manual. Enter the group number. Also, when applicable, show that optional markings have been used for Group 3 and Group 4 as authorized.

3. REPORT TITLE: Enter the complete report title in all capital letters. Titles in all cases should be unclassified. If a meaningful title cannot be selected without classification, show title classification in all capitals in parenthesis immediately following the title.

4. DESCRIPTIVE NOTES: If appropriate, enter the type of report, e.g., interim, progress, summary, annual, or final. Give the inclusive dates when a specific reporting period is covered.

5. AUTHOR(S): Enter the name(s) of author(s) as shown on or in the report. Enter last name, first name, middle initial. If military, show rank and branch of service. The name of the principal author is an absolute minimum requirement.

6. REPORT DATE: Enter the date of the report as day, month, year; or month, year. If more than one date appears on the report, use date of publication.

7a. TOTAL NUMBER OF PAGES: The total page count should follow normal pagination procedures, i.e., enter the number of pages containing information.

7b. NUMBER OF REFERENCES: Enter the total number of references cited in the report.

8a. CONTRACT OR GRANT NUMBER: If appropriate, enter the applicable number of the contract or grant under which the report was written.

8b, 8c, & 8d. PROJECT NUMBER: Enter the appropriate military department identification, such as project number, subproject number, system numbers, task number, etc.

9a. ORIGINATOR'S REPORT NUMBER(S): Enter the official report number by which the document will be identified and controlled by the originating activity. This number must be unique to this report.

9b. OTHER REPORT NUMBER(S): If the report has been assigned any other report numbers (either by the originator or by the sponsor), also enter this number(s).

10. AVAILABILITY/LIMITATION NOTICES: Enter any limitations on further dissemination of the report, other than those imposed by security classification, using standard statements such as:

(1) "Qualified requesters may obtain copies of this report from DDC."

(2) "Foreign announcement and dissemination of this report by DDC is not authorized."

(3) "U. S. Government agencies may obtain copies of this report directly from DDC. Other qualified DDC users shall request through

_____."

(4) "U. S. military agencies may obtain copies of this report directly from DDC. Other qualified users shall request through

_____."

(5) "All distribution of this report is controlled. Qualified DDC users shall request through

_____."

If the report has been furnished to the Office of Technical Services, Department of Commerce, for sale to the public, indicate this fact and enter the price, if known.

11. SUPPLEMENTARY NOTES: Use for additional explanatory notes.

12. SPONSORING MILITARY ACTIVITY: Enter the name of the departmental project office or laboratory sponsoring (paying for) the research and development. Include address.

13. ABSTRACT: Enter an abstract giving a brief and factual summary of the document indicative of the report, even though it may also appear elsewhere in the body of the technical report. If additional space is required, a continuation sheet shall be attached.

It is highly desirable that the abstract of classified reports be unclassified. Each paragraph of the abstract shall end with an indication of the military security classification of the information in the paragraph, represented as (TS), (S), (C), or (U).

There is no limitation on the length of the abstract. However, the suggested length is from 150 to 225 words.

14. KEY WORDS: Key words are technically meaningful terms or short phrases that characterize a report and may be used as index entries for cataloging the report. Key words must be selected so that no security classification is required. Identifiers, such as equipment model designation, trade name, military project code name, geographic location, may be used as key words but will be followed by an indication of technical context. The assignment of links, rules, and weights is optional.